Low-cost Zinc Oxide Nanorods Modified Paper Substrate for Biodiagnostics

Submitted in partial fulfillment of the requirements

of the degree of

Doctor of Philosophy

of the
Indian Institute of Technology, Bombay, India
and
Monash University, Australia

by

Sadhana Tiwari

Supervisors:

Prof. V Ramgopal Rao (IIT Bombay)

Prof. Gil Garnier (Monash University)

The course of study for this award was developed jointly by
Monash University, Australia and the Indian Institute of Technology, Bombay
and was given academic recognition by each of them.
The programme was administrated by The IITB-Monash Research Academy

(Year 2018)

Approval Sheet

The thesis entitled "*Low-cost Zinc Oxide Nanorods Modified Paper Substrate for Biodiagnostics*" by *Ms. Sadhana Tiwari* is approved for the degree of **Doctor of Philosophy**

Prof. Suman Chakraborty
[redacted]
External Examiner

Prof. Soumyo Mukherji
[redacted]
Internal Examiner

Prof. V. Ramgopal Rao
[redacted]
IITB Supervisor

[redacted]

Prof. M. Ravikanth
[redacted]
Chairman

Date: 27 April 2018
Place: IIT Bombay, Mumbai

Declaration

I declare that this written submission represents my ideas in my own words and where others' ideas or words have been included, I have adequately cited and referenced the original sources. I also declare that I have adhered to all principles of academic honesty and integrity and have not misrepresented or fabricated or falsified any idea/data/fact/source in my submission. I understand that any violation of the above will be cause for disciplinary action by the Institute and can also evoke penal action from the sources which have thus not been properly cited or from whom proper permission has not been taken when needed.

Notice 1
Under the Copyright Act 1968, this thesis must be used only under the normal conditions of scholarly fair dealing. In particular no results or conclusions should be extracted from it, nor should it be copied or closely paraphrased in whole or in part without the written consent of the author. Proper written acknowledgement should be made for any assistance obtained from this thesis.

Notice 2
I certify that I have made all reasonable efforts to secure copyright permissions for third-party content included in this thesis and have not knowingly added copyright content to my work without the owner's permission.

Student Name: Sadhana Tiwari

Acknowledgements

This thesis came up to completion with very kind and constant support from several individuals and institutions. Even if for reasons of space it is not possible to mention all of them here, I would like to take this opportunity to explicitly express my gratitude to at least some of them.

Firstly, I am grateful to my thesis advisors, Prof. V. Ramgopal Rao (IIT Bombay) and Prof. Gil Garnier (Monash University), for providing a gratifying experience in working with them and for their continuous guidance through-out my research work. I would like to thank the both examiner of my thesis, Prof. Suman Chakraborty and Prof. Sushanta Mitra as well as the other members of the Research Progress Committee, i.e. Prof. Soumyo Mukherji (IIT Bombay) and Prof. Wenlong Cheng (Monash University) for critical inputs and valuable suggestions.

I would also like to express my gratefulness to Prof. B. G. Fernandes, Head of Dept. of Electrical Engineering at IIT Bombay, who took over as Administrative Supervisor of my thesis when Prof. Rao took over the responsibility of the Director of IIT Delhi. Prof. Fernandes has supported my research and helped in speedily resolving any outstanding administrative issues as and when needed. I would also like to thank the administrative staff at the EE dept. for their friendly and competent support throughout this research.

I am sincerely grateful to Dr. Madhuri Vinchurkar for her continuous guidance and moral support during the course of the entire research.

Special thanks are due to IITB-Monash Research Academy for providing me financial and institutional support and a platform to conduct overseas collaborative research in Australia. I would like to convey my privileged thanks to all the staff of the academy for their valuable help and assistance throughout my work.

I am sincerely thankful to all colleagues and friends from my research group, such as Dilip Agarwal, Dr. Manoj Kandpal, Dr. Rajul Patkar, Mamta Ashwin, Whui Lyn, Heather McLiesh and, Dr. Vikram Raghuvanshi, for their continuous support and helpful discussions. Special thanks go to, Janette Anthony, for helping me out in every issue while doing overseas research at Monash University in Melbourne.

I gratefully acknowledge the support provided by MCEM (Melbourne Centre for Electron Microscopy) at Monash University, Melbourne and SAIF (Sophisticated Analytical

Instrumentation Facility), IRCC (Industrial Research and Consultancy Centre) at IIT Bombay in characterization techniques.

My special thanks go to all dear friends, such as Nikita, Geetanjali, Nayanika and Hanuman for their constant support, suggestions and encouragement and for being always there by my side at difficult moments.

At last, but not the least I feel immensely blessed and grateful to my parents, in-laws and siblings for their unconditional love, constant support and affection throughout this long journey. This section could not be completed without mention of a special person; my husband Rajnish. A big thank you for being constant source of inspiration, a great companion and bearing with me in tough situations.

Finally, a very grateful and sincere thanks goes to those special people both from professional and personal spheres whose immensely valuable and much-appreciated support in and during this research has to remain anonymous here for the lack of space but not for want of gratefulness.

Sadhana Tiwari

Abstract

Many of the point-of-care hand-held devices are based on the detection of very low concentrations of some specific protein biomarker in a blood or biofluid sample. There is an often need to preconcentrate by a few orders of magnitudes the analyte prior to measurement on the sensing area of the test to enhance the detection sensitivity for these miniaturized devices. Protein preconcentration is one of the major challenges in biosensing with miniaturized devices as enhancement of detection sensitivity for highly diluted analytes is critical and required for its better performance. Besides preconcentration, blood-plasma separation is another major challenge in biodiagnostics. The conventional blood-plasma separation involves centrifugation, which generally enables very efficient and fast results. But in case of point-of-care miniature devices it is necessary to have an integrated miniature blood-plasma separation system to reduce the number of sample preparation steps and quick diagnosis. Substantially-reduced total cost of ownership and usage are being seen as increasingly necessary to ensure affordable healthcare for a growing world population. In this context paper-based devices are gaining popularity as they are inexpensive, easy to fabricate and to modify, and once used, easy to dispose as they easily burn and are biodegradable. Paper has inherent capillary force created by the network of cellulose therefore, no external driving force or systems are required for fluid transport. Paper also provides a good support for growing nanostructures by providing a template for orientation and nucleation sites.

The work presented in this thesis involves, modification of paper with ZnO nanostructures to increase the available surface area for protein capture, biofunctionalization of nanostructures-modified paper. Emphasis is given on developing a protocol for protein preconcentration using the nanorods modified paper as a substrate and its confirmation by surface plasmon resonance, which also provided an opportunity to explore SPR studies on the ZnO nanorods modified gold chip. In addition to this passive separation of blood cells from plasma with the 1-D ZnO nanostructures modified paper as a substrate is also explored. There is no previous report on ZnO-nanorods modified paper as substrate for protein preconcentration and blood-plasma separation as well.

Key Abbreviations

AMI	Acute Myocardial Infraction
ZnO	Zinc Oxide
ZnO-NRs	Zinc Oxide Nanorods
WFP	Whatman Filter Paper
SEM	Scanning Electron Microscopy
AFM	Atomic Force Microscopy
XRD	X-Ray diffraction
XPS	X-ray Photon Spectroscopy
EDS	Energy Dispersive Spectroscopy
ELISA	Enzyme linked immunosorbent assay
P-ELISA	Paper based-ELISA
HRP	Horse Radish Peroxidase
TMB	Tetra Methyl Benzidine
SPR	Surface Plasmon Resonance
Au	Gold
CM5	Carboxy Methyl dextran chip -5
APTES	Amino-Propyl-Triethoxy-Silane
FITC	Fluorescein isothiocyanate
PBS	Phosphate Buffer Saline
RFU	Relative Fluorescence Unit
RU	Resonance Unit
EDC	1-Ethyl-3-(3-dimethylaminopropyl) carbodiimide
NHS	N-hydroxysuccinimide

ICP	Ion-Concentration Polarization
ITP	Isotachophoresis
µPAD	Microfluidic Paper-based Analytical Device
MEMS	Microelectromechanical Systems
BioMEMS	Biomedical Microelectromechanical Systems

TABLE OF CONTENTS

LIST OF FIGURES

LIST OF TABLES

Chapter 1

1. Introduction

World Health Organization (WHO) reported an estimate of global deaths occurred in year 2015 and stated that, 31% of all global deaths were due to cardiovascular diseases (CVDs). However, out of 17.7 million, 7.4 million were due to coronary also known as ischaemic heart disease which leads it to acquire top position among top ten causes of global deaths. As per WHO fact sheet published online in May 2017, “at least three quarters of the world's deaths from CVDs occur in low- and middle-income countries. People in low- and middle-income countries often do not have the benefit of integrated primary health care programmes for early detection and treatment of people with risk factors compared to people in high-income countries” [1]. Therefore, there is a need of affordable, early and quick diagnosis of cardiovascular diseases. Although, ECG is an important and most popular technique for the diagnosis but early accurate diagnosis is difficult with this as in many cases it is not able to produce diagnostic signals at early stage and provides false negative results. For the risk evaluation, use of biomarkers that can be identified in blood is one of the active research interest of healthcare community [2]. By definition, biomarker is a characteristic that is objectively measured and evaluated as an indicator of normal biological processes, pathogenic processes, or pharmacologic responses to a therapeutic intervention. Not only for CVDs, diagnostic and prognostic biomarkers can be identified for detection of various diseases biomarker may not always be a bio-molecule, for example; rubidium chloride is used as a radioactive isotope to evaluate perfusion of heart muscle [3]. Accurate detection of elevated levels of cardiac biomarkers such as troponin, myoglobin, FABP and CK-MB etc. becomes crucial for diagnosis.

Biodiagnostics is an area for the diagnosis and prognostics of a wide range of diseases and is mainly based on the detection of biomarkers in complex sample solutions and is of huge scientific and clinical research interest [4], [5]. Amongst the methods adopted for biomarkers detection, biosensors are gaining enormous popularity. Biosensors are devices used to sense biological analytes such as proteins, nucleic acid, cells, microorganisms, lipids and many other biomarkers [3]. Biosensors consist of three main parts: a biorecognition interface that enables the selective detection of an analyte, a transducer, which converts the recognition event into an electronic signal and a read out system with the associated electronics or signal processors to display of the results in a user-friendly way. The specificity of the biosensor depends on the selection of the biomaterial for the biorecognition interface. A wide range of biosensors based on different sensing mechanisms have been developed for cardiovascular diseases including, optical biosensors, fluorescence based sensor, electrochemical, luminescence and colorimetric, ELISA based methods, SPR based sensors and acoustic wave based biosensors [3].

Traditional practices of use of bioanalytical devices or biosensors involve sample analysis in centralized laboratories which require separate equipment for sample processing and involves multiple steps, expensive analytical instruments and well skilled manpower for analysis. Beside this, the other major drawbacks of these techniques are that they are time consuming due to multistep sample processing and are expensive for low income population. Therefore, need of simple, portable, affordable, rapid and sensitive bioanalytical devices or biosensors has emerged. Recent advances in miniaturization or microfabrication technologies provide a vast scope of designing portable point-of-care devices which could meet the need of majority of population. These lead researchers to explore more in this area. After developments in microfabrication technology in early 2000's, bioMEMS (biomedical microelectromechanical systems) emerged as an interdisciplinary domain where advances in macro, micro and nanoscales sciences are used for the development of new technologies for molecular analysis and biomedical research. With exponential raise in the research of nanoscience and technology, new devices are being developed to address current and future needs. Likewise, bioMEMS as a science is aimed at revolutionizing treatment and diagnosis of diseases through the development of devices and systems with unprecedented performance characteristics, such as sensitivity, specificity, resolution, throughput and multiplexing. MEMS (microelectromechanical systems) devices offer various advantages over traditional devices. Some of the most important advantages are; flexibility to use low amount of expensive biological agents, various module could be integrated on a single substrate (lab-on-chip) and ability to control fluid flow in the device [6].

Apart from miniaturization of bioanalytical devices, preconcentration of target analyte before sensing and making the whole device cost-effective is one other area where active research is going on. When it comes to cost, the very first step should be to select a low-cost substrate for the device fabrication. Paper-based devices are gaining popularity in diagnostics and environmental monitoring as they are inexpensive, easy to fabricate and to modify, and once used, easy to dispose as they easily burn and are biodegradable. Paper tests rely on the inherent capillary force created by the network of paper hydrophilic pores in which aqueous fluids naturally wick; no external driving force or systems are required for fluid transport. Paper also provides a good support for growing nanostructures by providing a template for orientation and nucleation sites. Nanostructures of a wide range of metallic and non-metallic elements have been potentially used and proven excellent efficacy for biosensing in various applications. Nanomaterials of gold, silver, zinc oxide, magnetic nanoparticles and carbon nanostructures

are widely accepted for fabrication of biorecognition interface in biosensors. 1-D and 2-D nanostructures such as nanowires, nanorods and nanofilms possess highly diverse mechanical, chemical, electrical and optical properties. These nanomaterials also have a large range of variations in their morphological properties such as; shape, size, surface to volume ratio, biocompatibility and biodegradability. The miscellaneous properties of 1-D and 2-D nanomaterials make them appropriate for a wide range of applications, including drug delivery, imaging, tissue engineering and biosensors [7].

1.1. Motivation

Many of the point-of-care hand-held devices are based on the detection of very low concentrations of some specific protein biomarker in a blood or biofluid sample. Blood is a complex colloidal system containing large numbers of small and large biological components like proteins, carbohydrates and minerals along with blood cells, it contains approximately more than 10,000 different proteins, with varying concentrations. This multiplicity of proteins and their enormous concentration ranges, creates a big challenge for researcher in sample preparation and its handling. The challenge of distinguishing a specific biomarker protein from the mixture of large variety of proteins requires approaches for selective preconcentration of that particular biomarker protein. Therefore, there is an often need to preconcentrate analytes by a few orders of magnitudes prior to measurement on the sensing area. This approach could significantly enhance the detection sensitivity for these miniaturized devices. Preconcentrators form the next generation single molecule purifiers. Miniaturization of these devices and integration with detection system is a challenging task where microfabrication and surface functionalization of materials has to be done to achieve the purpose.

In addition to preconcentration, another important and highly desirable aspect in biodiagnostics is to reduce the avoidable complexity of blood sampling by separating blood cells and to use plasma or serum sampling to achieve better results. Figure 1-1 shows a schematic layout of the device design of a low cost paper based all-in-one device, which can separate plasma from blood, preconcentrate the target analyte and sense as well. There could be three possibilities of using the nanostructures modified paper substrate; (i) it could be used as blood plasma separation module (ii) preconcentration module; the biofunctionalized paper substrate firstly treated with plasma which leads to specifically target protein capture followed by elution of

the protein. The concentrated protein could directly pass to the sensor or could be collected in a reservoir and later on pass to the sensor if preconcentrator and sensor are not integrated and (iii) both the module could be combined by creating channel between them in this way single substrate could be used for plasma separation, preconcentration - and subsequent detection of target analytes.

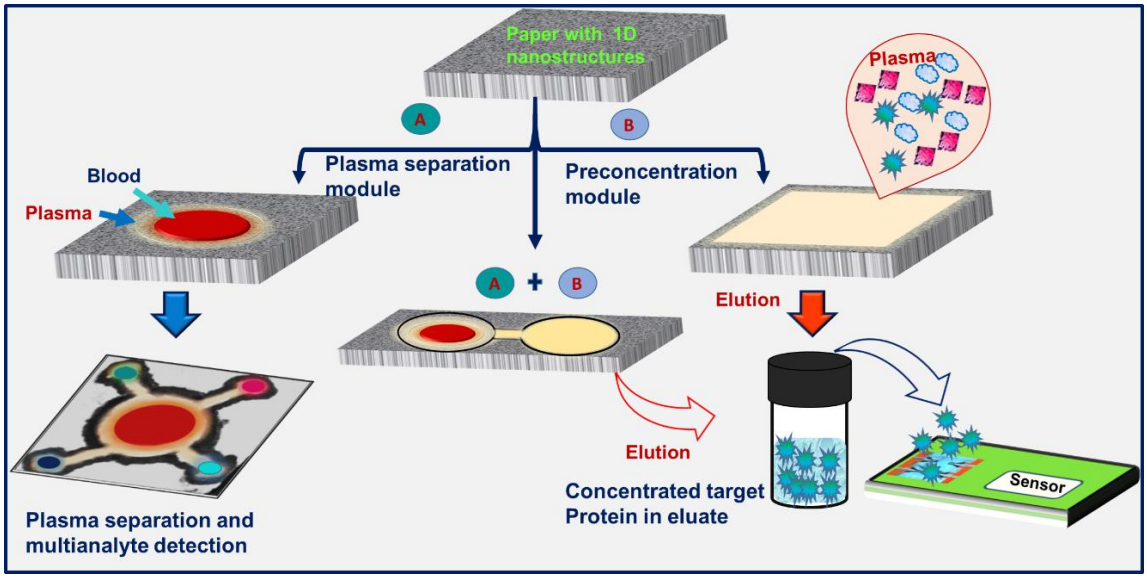

Figure 1-1: Schematic of different module of low cost nanostructure modified paper based all-in-one device which could be able to separate blood cell and plasma followed by preconcentration of target analyte and its sensing.

This approach could provide a promising strategy to capture and thus improve detection of very low concentration marker proteins in biosamples along-with separation of plasma from whole blood. Before moving further with the above mentioned approach, it is important to address certain very critical aspects. This leads to following research questions:

- Can the excellent properties of the paper and nanomaterials together be helpful to develop an efficient preconcentrator?
- How the paper could be biofunctionalized and used to concentrate the target protein followed by efficient elution of bound target protein from the substrate without any external power supply?
- What are the possibilities to develop low cost substrate which can separate blood cells from plasma and preconcentrate the target biomarker?

1.2. Objectives and scope of the work

This dissertation intends to propose a new approach to solve above questions and develop a new low-cost approach to preconcentrate an analyte using paper as substrate, which represents a limiting and crucial step for sample preparation in many paper based biosensors applications. There are many studies in regard to development of nanomaterial modified paper based substrate for biomedical and environmental applications [8], [9]. The efficient capture of a low abundance target protein requires a preconcentrator combining a high specificity for the targeted protein and a very large surface area; this can be achieved by growing 1-D nanostructures on paper and functionalizing the modified paper for high adsorption specificity for the marker of interest. In a second step, the adsorbed protein is to be desorbed from the nanostructured paper into the solution by providing a step change in its pH, ionic strength or even temperature without losing its characteristics. These possibilities in regard to development of a frugal paper based substrate for biodiagnostics, leads to following hypothesis:

Hypothesis 1: Modification of paper with nanostructures could increase the available surface area for protein capture followed by elution

The efficient capture of a low abundance target protein requires a preconcentrator combining either a high specificity for the targeted protein or a very large surface area; this can be achieved by growing 1-D nanostructures on paper and functionalizing those for high adsorption specificity for the marker of interest. In a second step, the adsorbed protein is desorbed from the nanostructured paper into the solution by providing a step change in its pH, ionic strength or even temperature. This approach could provide a promising strategy to capture and detect very low concentration marker protein in biosamples.

After successful modification of paper with nanostructures the next requisite and essential aspect is to test the utility of the substrate to fulfil the objectives. This leads to formulation of the next hypothesis:

Hypothesis 2: A protocol and SPR chip could be developed for preconcentration and elution of target protein on the modified substrate

Biomolecules immobilization on the nanostructures-modified paper using suitable immobilization chemistry for biofunctionalization of the paper. The covalent immobilization of biomolecules on the nanorods modified paper to be confirmed by surface plasmon resonance, which also provides an opportunity to explore SPR studies on the nanorods

modified gold chip. The modified paper is to be further tested for use as a protein preconcentrator. Preconcentration studies on the modified paper involve binding of desired protein to antibody and its release, followed by collection and quantification of released protein. Validation of enhanced protein capture efficiency and preconcentration on the nanostructures modified substrate with paper based ELISA and surface plasmon resonance techniques. As reported in literature researchers have also explored utility of paper substrate for blood-plasma separation, which is an important aspect in biodiagnostics. This provided scope to investigate ability of the nanostructures modified paper to separate blood cells from plasma.

Hypothesis 3: The 1-D nanostructures modified paper could serve as a substrate for passive separation of blood cells from plasma

In most of the biodiagnostics where blood is used as sample for diagnosis, there is need to separate red blood cells from the plasma. This minimizes crowding due to undesirable biomolecules at the sensing substrate which could cause hindrance in sensing process. Paper could be used as potential substrate for blood-plasma separation after some modification, as mentioned in existing literature. 1-D nanostructures could make paper less porous and with extremely dense surface coverage, the modified paper possibly could efficiently trap the red blood cells which leads to separation of plasma with maximum red blood cell capture.

To test all the above formulated hypotheses and investigate 1-D nanostructures modified paper as potential efficient substrate, Zinc Oxide nanorods have been chosen as ideal 1-D nanomaterial for modification of paper as they are easy to grow on paper. Cellulose fibres act as template for efficient growth of ZnO nanorods in a simple process. The scope of work is distributed in following subsections:

- Define a simple, low-cost, robust and efficient protocol for growth of zinc oxide nanorods on Whatman filter paper and its characterization.
- Biofunctionalization of the ZnO-NRs/Paper surface using silanization chemistry followed by antibodies immobilization on the modified paper.
- Develop and validate ZnO-NRs/Paper based protein preconcentration protocol.
- Explore use of the nanorods modified paper for blood-plasma separation.

1.3. Structure of the thesis

The report is structured on the lines described as flowchart shown in Figure 1-2.

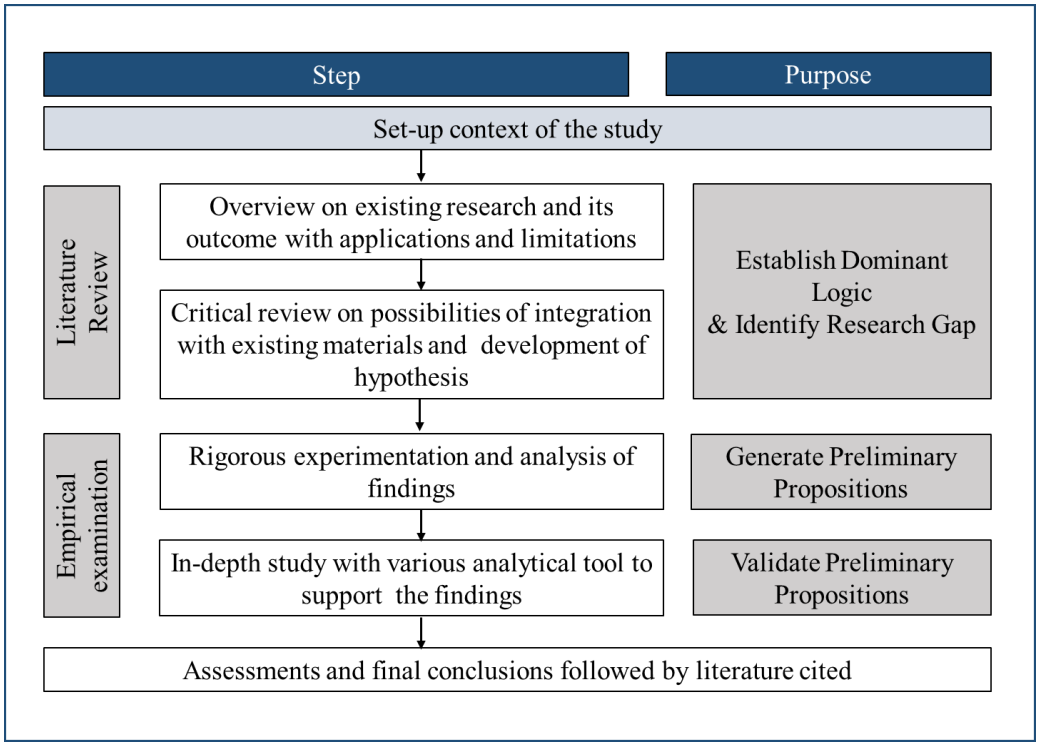

Figure 1-2: Flowchart showing thesis structure layout.

Chapter 2 - Literature review: This chapter will include the in-depth survey of existing literature related to biosensors, protein pre-concentrator, paper based devices, various nanostructures with their applications in various fields and limitations. This chapter will also focus on possibilities of integration of existing materials so that it can give some insight towards development of low-cost sensing devices.

Chapter 3- Growth of zinc oxide nanorods on paper and their characterization: This chapter will be completely dedicated to modification of Whatman filter paper with Zinc oxide nanorods. It will include the detailed process of Hydrothermal growth of nanorods on paper, optimization of growth conditions in terms of pH and growth time, for preconcentration purpose, hydrophobization and study their various characteristics with different characterization techniques including SEM, XRD, XPS, EDS and AFM, contact angle measurement and electrical characterization.

Chapter 4- Biofunctionalization and validation through Surface Plasmon Resonance studies: The chapter will be on biofunctionalization of the nanorods modified paper and its validation with more precise analytical tool i.e. SPR, which gives qualitative as well as quantitative information

about the ongoing phenomenon on the surface. For this a new chip has been developed for the study which was modified with Zinc oxide nanorods and named as ZnO-NRs/Au chip in the study. Morphology of the chip was studied with SEM imaging and then it was optimized for the maximum binding of cardiac-myoglobin using anti-myoglobin antibodies. Binding and concentration analysis will be discussed in detail. Also, to check compatibility of the chip with real blood/plasma/serum sample experimentation with real samples also be examines in this chapter. Some critical parameters like; stability, reproducibility and specificity will be addressed.

Chapter 5- Protein preconcentration studies: This chapter will be focused on examining the ZnO-nanorods modified paper based platform as a suitable and efficient substrate for protein pre-concentration (which include specifically capture of target protein and its elution). It includes antibody immobilization on modified paper and confirmation of binding. In this the techniques used for the study will be Fluorescence spectroscopy, Confocal microscopy, and paper based ELISA(p-ELISA). The findings from all these studies will also be critically analyzed and discussed in detail in this section.

Chapter 6- Blood-plasma separation studies: This chapter will provide some insight of paper based blood-plasma separation. Separation by using different blood-group antigens and comparative study on different types of paper will be explained. How the modification of paper with ZnO-nanorods affects blood-plasma separation with their morphological characterization will be explained.

The thesis will be concluded in chapter seven with brief discussion about the findings and future perspective of the work. Also a brief discussion about how the thesis contributes to existing knowledge and add new insights towards development of low-cost platform for protein pre-concentration and sensing will be part of this chapter. This chapter will be followed by list of literature cited and referred in the research carried out and in preparation of dissertation.

Chapter 2

2. Literature Review

2.1. Introduction

Myocardial infraction or Acute myocardial infarction (AMI) is a condition where blockage of circulation to heart tissue leads to necrosis of heart tissues. Following ischemic injury to cells, cell membrane integrity is damaged allowing intracellular constituents to leak into the blood stream. Biomolecules which are released into the blood from the striated heart muscles, are called 'cardiac markers'. They peak and reach their detectable range within a few hours after the onset of infarction. Myoglobin, Creatine Kinase(CK-MB), Troponin, Fatty Acid Binding Protein (FABP) are most preferred markers for diagnostic purpose. Troponin is a complex of three regulatory proteins (troponin C, troponin I and troponin T) that is integral to muscle contraction in skeletal and cardiac muscle, but not smooth muscle. Cardiac troponins T and I are the preferred markers for myocardial injury as they have the highest sensitivities and specificities for the diagnosis of acute myocardial infarction. Reference ranges of different cardiac biomarkers are shown in Table 2-1 as defined in literature. Whereas Figure 2-1 shows the activity curves for different cardiac markers with their release time and elevation in serum after myocardial infraction.

Markers	Reference Range	1st Elevation (hours)	Peak Elevation (hours)	Duration of Elevation (days)
Cardiac troponin I (cTnI)	<0.07 ng/mL	4-6	24-36	depends on extent of damage
Cardiac troponin T (cTnT)	< 0.1 ng/mL	As troponin I (cTnI)		
Creatine kinase MB isoenzyme (CKMB)	<10 ng/mL	4-6	18-36	3 (~2-3x normal)
Myoglobin	<170 ng/mL	2-3	6-9	1

Table 2-1: Cardiac markers with reference range and their critical diagnostic duration [10].

Detection of these biomarkers within the range of their risk limit, requires a rapid, handheld, simple device. MEMS based biosensors could offer a pronounced solution for this. These are the devices which utilize the microfabrication techniques for the fabrication and their dimensions are not more than few microns. Microfluidics is also involved in these devices as the channels for the flow of analyte and other reactants should be in micron level. One of the

most important challenges of BioMEMS device is to deal with complex biological samples, such as blood serum or cell extracts.

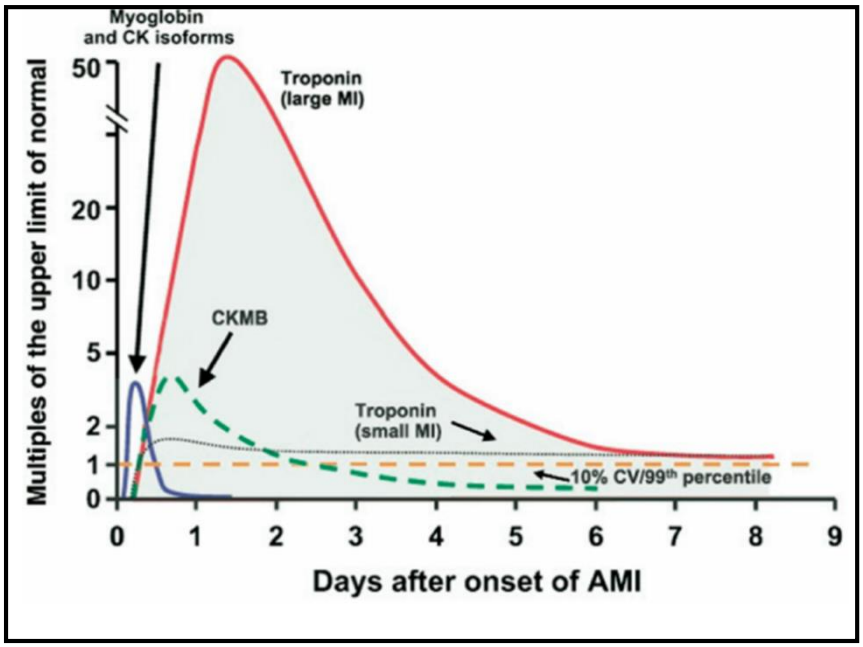

Figure 2-1: Activity curves for with release timing of different cardiac biomarkers after acute myocardial infarction; adapted from ref. [10].

Blood is a stable colloidal system consists of two major components red blood cells and plasma [11]. Whereas, red blood cells play major role in oxygen transport to the whole body, plasma serves as a fluid that is the blood's liquid medium, which by itself is straw-yellow in color. The blood plasma volume totals of 2.7–3.0 liters in an average human. It is essentially an aqueous solution containing 92% water, 8% blood plasma proteins, and trace amount of other materials. Plasma circulates dissolved nutrients, such as glucose, amino acids, and fatty acids (dissolved in the blood or bound to plasma proteins), and removes waste products, such as carbon dioxide, urea, and lactic acid. In blood some biomolecules could generate immune response and hence act as antigen that is non-self molecules for body. Some glycoproteins and carbohydrates are responsible for this immune response and called as immunogens. These biomolecules decide the blood type in humans (A, B, AB and O), and are displayed onto the surface of the blood cells [11]. Blood analysis have been done by variety of assays and tests include, glucose content, cholesterol, salts and metabolites like sodium, potassium, bicarbonate, blood urea nitrogen, magnesium, creatinine, calcium, triglycerides, microbial markers and various disease markers. In biodiagnostics where blood samples are used for analysis, it is actually a suspension of approximately more than 10,000 different proteins with varying concentrations. Due to this

multiplicity of proteins and their enormous concentration ranges and low abundance of certain biomarkers, creates big challenge for researcher in sample preparation and its handling. The challenge of distinguishing a specific biomarker protein from the mixture of large variety of proteins requires approaches for selective preconcentration of that particular biomarker protein. Various types of techniques have been developed for preconcentration which can accomplish high concentration factors up to 10^4, in small time duration [12]. This chapter is a detailed overview of various existing techniques, including low cost approaches, used materials and devices for protein preconcentration. A small section is dedicated to 0-D, 1-D and 2-D nanostructures used for paper modification and resulting enhancement of paper properties towards making it suitable for efficient use in biodiagnostics.

2.2. Materials used for preconcentration

2.2.1. Ion- selective and Ion-permselective membranes

For the purpose of preconcentration of analytes, methods based on selectively separating ions of interest from mixture have been most popular. Nafion membrane is commonly used for selective separation of ions, it is a synthetic hydrolyzed copolymer of perfluoro- olefins. The ionic properties of nafion are due to sulfonate ion present on its structure. It shows some physical and chemical properties same as Teflon base material and is extremely chemical resistant so it does not easily degrade in the surrounding medium. It functions as strong proton donor and highly permeable to water. These membranes with fixed negative charges and pore size are used as a cation-permselective membrane, which selectively allow cations to pass through it. On inserting nafion membrane between two electrodes in an electrolyte, cations can drift through the membrane towards cathode while anions get restricted to pass through the membrane in this way it serves as a mean of ion concentration polarization. Due to these unique properties of nafion it is used in various applications including, as separation membrane in fabrication of protein preconcentrator [13]. In preconcentrator it serves as cation exchange membrane which selectively allow to pass positively charged species through it and bind negatively charged proteins [14]. Shen et al [12] used these membranes in their design of microfluidic protein preconcentrator for negatively charged fluorescent protein and reported that using low voltage the device was able to preconcentrate the protein up to a concentration factor of 10^4. Figure 2-2 shows chemical formula of nafion and a preconcentration phenomenon

using nanoporous nafion membrane for fluorescent protein. Later Sarkar and Han used same concept for preconcentration of enzyme inside nanofluidic chip [15]. Beside ion-selective separations, Nafion membrane has also been used in fabrication of preconcentrator where the separation was based on ion-concentration polarization. Kwak et al [16] fabricated a continuous- flow cell concentrator using the membrane as a nanojunction at an angle to ensure continuous flow as well as separation, and achieved 100 fold increase in concentration. The obtained results were validated by using various target analytes including red blood cells. Cheow and Han patterned nafion membrane on glass slide for using it as integrated preconcentrator for IgE (immunoglobulin E) [17].

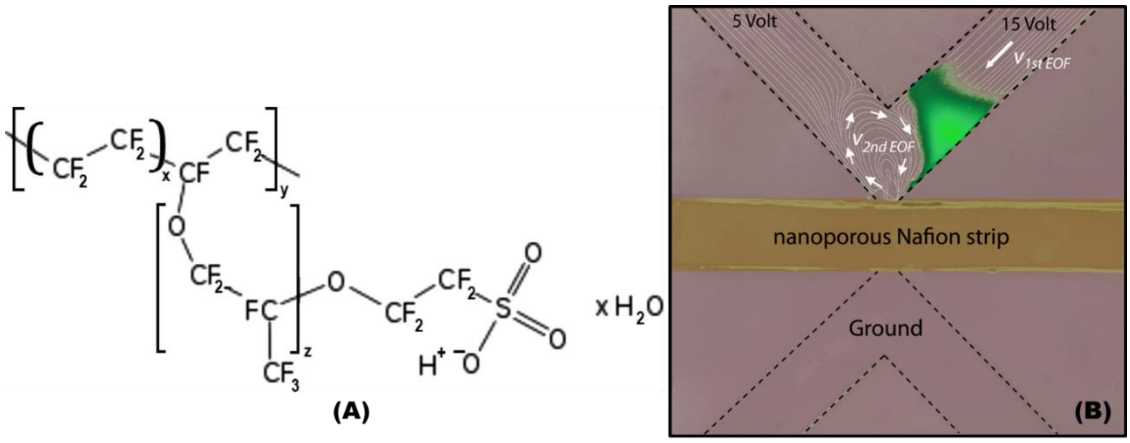

Figure 2-2: (A) Chemical formula of Nafion and (B) a preconcentrator design based on integrated nanoporous Nafion between two electrodes. Electrokinetic movement of proteins due to potential difference between electrodes(V_{1st}-V_{2nd}) and membrane led to preconcentration. Reproduced with permission from [12], [18], Copyrights (2014,2010) American Chemical Society.

Although nafion is widely used and very much popular among researcher as ion-selective membrane yet it has certain limitations and drawbacks. One of the major issues with nafion is its poor chemical and mechanical stability at higher temperature. Multicharged ions may act as contaminants which could leads to degradation of membrane conductivity [18].

However, Hlushkou et al [19] created charged hydrogel membrane and presented a theoretical model and simulation for the hydrogel membrane as ion-permselective membrane for cations which leads to concentration polarization. In their investigation they have compared the results with neutral hydrogel membrane and found that under the influence of electric field neutral/uncharged hydrogel acts as size-exclusion filter rather than preconcentrator. Whereas with charged hydrogel the concentration factor was found to be >100. Figure 2-3 represents two different types of hydrogel based preconcentration mechanisms, one is negatively charged

hydrogel based preconcentration (A) and second is neutral hydrogel based mechanism (B). An on-chip ion-permselective membrane for preconcentration of cancer biomarkers was fabricated by photopolymerization of acrylamide containing monomers.

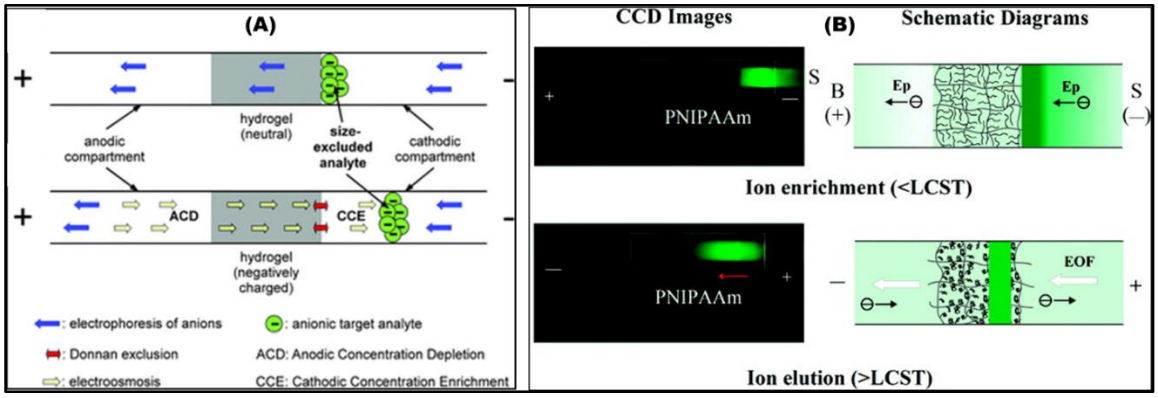

Figure 2-3: Two types of hydrogel based preconcentration (A) negatively charged and neutral hydrogel; charged hydrogel slows down electrokinetic movement of anionic target proteins, while with neutral hydrogel the preconcentration is due to size exclusion of target protein. (B) thermomodulated preconcentration and separation of charged species based upon a thermoswitchable swelling−shrinking property of hydrogel; poly(N-isopropylacrylamide). Reproduced with permission from [19], [20]. Copyrights (2008) Royal Society of Chemistry and (2010) American Chemical Society.

As the membrane consist of negative charge, anionic proteins were not allowed to pass through the membrane, which leads to concentration of target protein. For two cancer biomarkers, α-fetoprotein (AFP) and heat shock protein 90 (HSP90), the enrichment factor was found >10 fold [21]. Limitation of this material is if there could be other biomarkers in the mixture having same size and counter charge as membrane, could also pass through the membrane and could affect the specificity.

2.2.2. Nanoporous membrane

Nanoporous materials are such nanomaterials having pore size in range of 1nm-1000 nm and classified in three categories; microporous (0-2 nm), mesoporous (2-50 nm) and macroporous (> 50 nm) [22]. These porous materials possess a unique set of properties such as high surface area, fluid permeability and molecular sieving and shape-selective effects. The pore size and surface properties of these nanoporous materials changes with change in pore size, porosity, pore size distribution and composition. This variation in properties decides there use in various applications. According to need and criteria of the application one can choose suitable nanoporous material for their use [23], [24]. One of the most common uses of these materials

is in fabrication of nanoporous membrane. Nanoporous membrane is a thin film like structure fabricated by using nanoporous material. These membranes have potential application in biomedical field. Figure 2-4 shows some potentially used nanoporous materials for fabrication of preconcentration membranes. In biomedical systems these membranes are used in implantable devices, biosensing devices [25], drug delivery systems and in immunoisolation devices and protein separation [23].

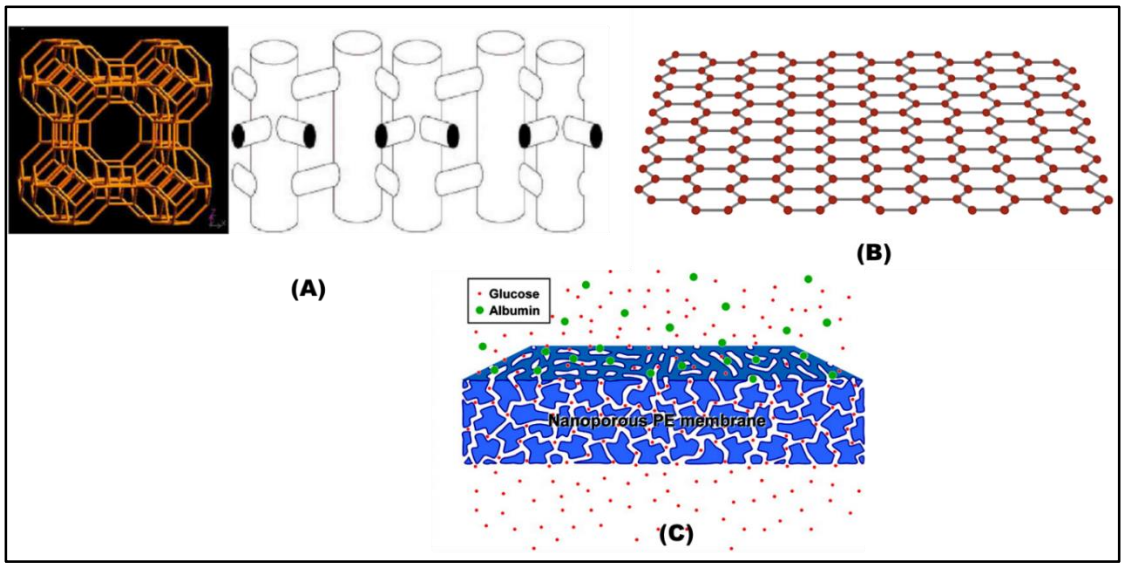

Figure 2-4: Nanoporous materials used as preconcentration membranes; (A) microporous Zeolite [22] (B) mesoporous graphene and (C) nanoporous polyethylene membrane [26].

In all these systems the membrane work as selectively permeable section which traps molecules larger to its pore size and allow passing desired molecules. In the past decade, researchers are putting efforts to fabricate automated point of care devices and µTAS (micro- total analysis systems) with high selectivity, reduced cost and sample requirement. The most exciting example on this track is lab-on-a chip devices which are able to perform various process; preconcentration, separation, reaction and detection on a single chip. In these systems nanoporous membrane serve as integral part of separation and preconcentrator component [27], [28]. Surface modified nanoporous opal membrane showed chiral permselectivity for cations and used as a potential separation for large range of chiral analyte molecules concentration [29] though there is no report on separation of bioanalytes with these membrane. Nanoporous alumina membrane has been proven a biocompatible potential surface for biodiagnostics. Having excellent ability of sensing, concentration and signal amplification, as showed in electrochemical biosensor for histamine detection in seafood by immobilizing antibodies against target analyte on the nanoporous membrane [30]. However, the major limitation with

nanoporous alumina membrane is its thickness. Membranes having thickness less than 70 µm found to be having less mechanical strength [31]. Gong et al [32] demonstrated low-cost paper based assay for diagnostics using nanoporous Nafion membrane for concentration and transport of analyte and achieved 40 fold concentration of analyte with 96% transport efficiency. Uehara et al [26] developed nanoporous membranes from polyethylene-block-polystyrene(PE-b-PS) for separation of glucose and albumin using size-selective diffusion principle. The system was designed for its application in an implantable glucose sensor. The membrane has advantage over alumina membranes as it exhibits tremendous flexibility and toughness. Nanoporous silica membranes are another widely used category of nanoporous materials used in biomedical applications. These are ordered three dimensional porous structures of silicon dioxide. Due to their definite structure, pore size and easily modifiable surfaces these membranes have potential application in various field including targeted drug delivery [31], [33], [34], biomedical devices and biosensors [35].

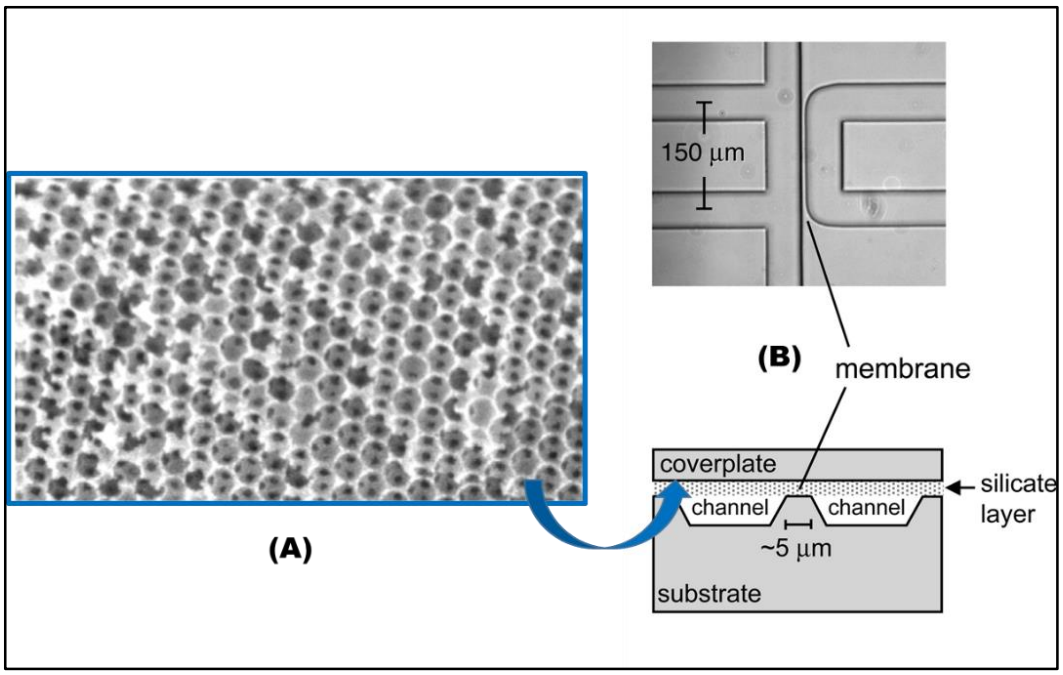

Figure 2-5: Nanoporous silica membrane: (A) scanning electron micrograph of nanoporous silica membrane [35] (B) a preconcentrator device design with integrated silicate layer which act as concentration membrane in a microfluidic preconcentrator device; microscopic image of the device (top) and design layout of the device (bottom) [36].

Recently various studies showed application of these ordered silica membranes for separation[29] as well as preconcentration of proteins and DNA.

Figure 2-5 is a representation of micron level structure of well-ordered porous silica membrane (A) and a device design based on the fabricated membrane (B). Separation of biomolecules like smaller proteins and even large DNA strand, on the basis of their size using these membranes, has been shown by Zeng and Harrison in their studies [37]. Foote et al [36] used the membrane for preconcentration of fluorescent labeled protein before analysis. The protein was preconcentrated by placing porous silica membrane adjacent to microfluidic channel. Using this strategy, they reported approximately 90-fold concentration of protein in 4 min subsequently 600-fold on-chip signal enhancement. Zheng et al [38] investigated a novel application of silica colloidal crystals for electrophoretic separation of charged analyte on the basis of differences in electrophoretic mobility and adsorptivity on the silica crystals. The two major drawback of porous silica membrane is that these membranes make surface hydrophobic up to some extent and second is associated with the morphology of the pores. The shape of pores of some membranes (e.g. rectangular) are such that it is difficult to diffusion of some proteins where 3D structure of the protein is not compatible with the pores like; immunoglobulins (Y-shape) [31]. Therefore, while selecting the membrane for preconcentration it become crucial to first investigate about the pores morphology.

2.2.3. Nanofluidic filters

With the advancement of nanofabrication techniques miniaturization of biomedical devices with higher precision is rapidly growing. Many investigations have been reported on various methods to integrate all the required component of a device on a single chip. Fabrication of nanofluidic filters is a very advance step in this direction. Nanofluidic filters serve as molecular sieve for separation of various biomolecules like DNA and proteins [39]. These nanofluidic filters have more chemical and mechanical strength than other membrane based separation system as they could be easily engineered according to requirement by slight modification in the fabrication step and could be integrated with device during microfabrication process. Han and Fu [40] fabricated nanofluidic filter for separation of smaller biomolecules like small DNA segments and proteins. The nanofluidic channels with larger gap than size of analyte were fabricate by photolithography on silicon substrate having. Biomolecules smaller than dimension of nanofluidic filter gap, get separated due to steric hindrance mechanism. As the sizes of DNA molecules are almost similar to filter channel gap, they get stuck before entering the channel due to comparable size whereas, smaller molecules can easily cross the channel and move faster as there is no steric hindrance, this way they get separated with large

molecules. Chung et al [41] proposed a new approach for non-lithographic creation of wrinkled nanofluidic channels on the PDMS substrate, by stretching PDMS sheet followed by oxygen plasma treatment subsequently formation of a rigid covering of Silicon oxide which upon releasing the stress generate wrinkled pattern of nanoscale dimensions. The underlying mechanism in protein preconcentration was electrokinetic trapping with support of electroosmotic flow through the wrinkled nanochannels resulted 100-fold concentration. Earlier, Wang et al [42] had developed a simple, robust and high performance integrable preconcentrator using lithographically patterned nanofluidic filters and achieved a very high concentration factor 10^6 -10^8. As an extension of preconcentrator application, Lee et al concentrated low abundant enzymes and substrate to increase rate of the biological reaction, achieving 100 fold enhancement in the sensitivity, using nanofluidic filters as preconcentrator [43]. Beside all the above mentioned advantages there are certain limitations associated with nanofluidic filters. These filter work mainly on sieving principle so there is very high probability of getting mixture of different small proteins i.e. co-concentration of other unwanted proteins rather one specific protein. Secondly, the separation of the proteins with these is much slower than the devices or substrate where capillary action plays major role in fluid flow [40].

2.3. Designs of protein preconcentrator

2.3.1. Preconcentration chip with integrated nafion

For a preconcentrator design nafion was material of choice for many researchers. Shen et al design a preconcentrator using integrated nafion strip inside PDMS channels. The PDMS with integrated nafion strip is then mechanically clamped on glass substrate. The basic theory behind this system is that being cation permiselective nafion act as ion selective membrane between two electrodes and separate microfluidic channels i.e. sample channel (anode) and buffer channel (cathode). By providing different potential they created electric field across the membrane and electrokinetic movement of ions started, due to this concentration polarization takes place near the membrane. The electrophoretic flow of negatively charged biomolecules along with electroosmotic flow concentrates the biomolecules. Using same concept Lee et al [43] developed a nanofluidic preconcentrator chip for both enzyme and substrate by patterning nafion on glass substrate and creating microchannels on PDMS. Scheme of the

preconcentration device was that patterned nafion membrane of 191nm thickness on glass goes across three microfluidic channels on PDMS. The enzyme and substrate preconcentration mechanism is same electrophoretic flow along with electroosmotic flow due to potential difference across membrane.

Liu et al [13], designed a preconcentrator based on capillary valve fabricated microchannels for nafion resin, to introduce accurate and controlled amount of nafion resin into the channel this design was used for preconcentration of protein R- phycoeryrthrin by capturing it on antibodies. In the device capillary valve based ion selective membrane junction was fabricated on chip. In the design to confine antibodies near the preconcentrator region they create differential fluid resistance in the path of flow by using hydrophobic microvalve and creating channels of different width. The sample channel consists of two parts one for introduction of only antibody and other for fluid containing target molecule. Immobilization of antibodies was done only at vicinity of preconcentrator. In this way area near to preconcentrator gets occupied by antibodies thus minimizes sample depletion. A preconcentration of protein by getting captured by immobilized antibodies and forms a concentration plug by creating the potential difference across different channels. Major advantage of this design is that it can be operate at higher buffer concentration without affecting the process. Cheow et al [44], Kwak et al [16], Sarkar and Han [15] proposed different designs of preconcentrator using integrated nafion membrane for preconcentration of various biomolecules. Kwak et al achieved 100 fold of concentration factor for different biomolecules including whole bacteria and RBC by using a bifurcated channel design with integrated nafion.

To enhance enzyme productivity, Chen et al [45] proposed a unique design which is a combination of preconcentrator and microfluidics based droplet generator in a chip. The preconcentrator was fabricated using PDMS bonded with glass substrate. Nafion was used as ion selective membrane as previous mentioned design the preconcentration was based on electrokinetic flow of biomolecule along with electroosmotic flow. Beside the preconcentrator part there the device consists an additional microfluidic drop generator system. After enzyme get concentrated it get mixed with substrate and form monodispersed microdroplets with the help of fluorocarbon oil which act as carrier fluid and the droplets further collected in analysis compartment. Using this design, they achieve 10 fold of increased productivity which is confirmed by fluorescence intensity measurement.

2.3.2. Multiplex preconcentration design

In biodiagnostics and clinical treatment it is extremely important to understand possible genetic abnormalities, variation and mutations which could be the potential cause of illness. For this state-of-the-art instrumentations are needed which includes simultaneous analysis of large number of analytes in less time. In this direction capillary-array based electrophoresis was the path breaking technique used for small scale DNA sequencing [46], [47]. Initially, the technique has been commonly used for DNA analysis, Emrich et al [48] fabricated 384-lane capillary array for high throughput genetic analysis. Nowadays, the design and principle is gaining popularity for fabrication of multiplexed protein preconcentration device. Lee et al developed surface patterned ion-selective membrane based protein preconcentrator on PDMS chip and achieved 10^4 fold concentration factor by combining ten individual preconcentrator [49]. By using multiplex electrokinetic system with the nafion based preconcentrator, Cheow et al [44] showed the increased sensitivity of enzyme-linked immunosorbent assay (ELISA) up to 65 fold.

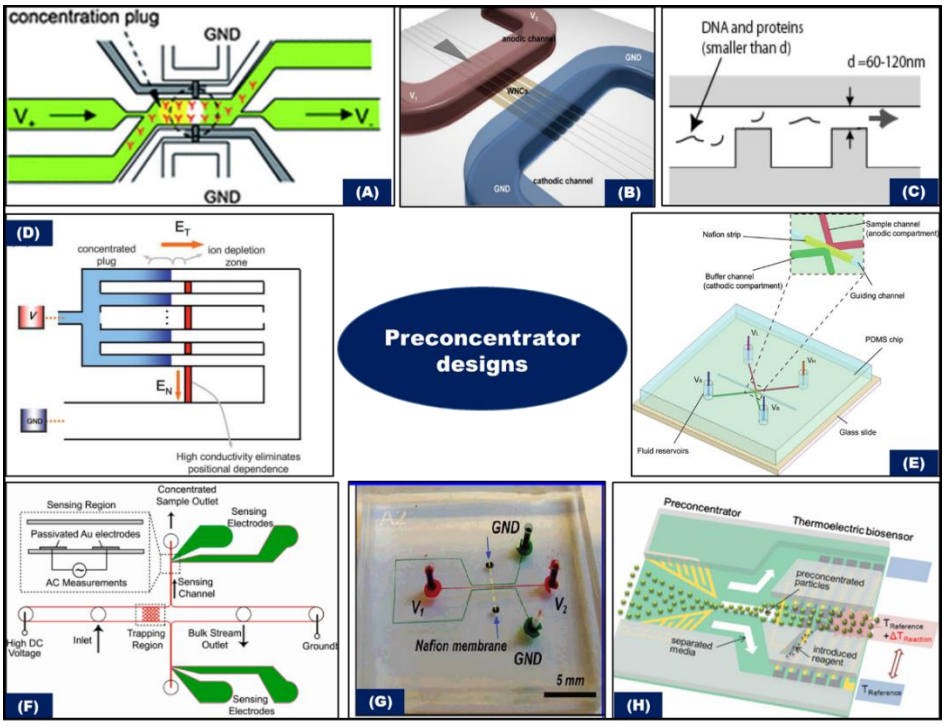

Figure 2-6: Various protein preconcentrator device designs (A) preconcentrator based on capillary valve fabricated microchannels [13] (B) protein preconcentration device consisting of the WNCs and microfluidic channels [41] (C) nanofluidic filter for preconcentration (D) parallel multiplexed preconcentration [50] (E) microfluidic microchannel integrated nafion based device [12] (F) insulator-

based dielectrophoresis [51] (G) integrated nafion based design [43] (H) multiplexed electrodynamic preconcentrator [52].

Later, Ko et al [50] proposed a design to overcome less volume output of preconcentrated molecules from previous designs by introducing multidimensional multiplex design. In this design to get high volume output the anodic microchannel is divided into 128 sub-microchannels. Unlike to other designs in this design there is no formation of ion enrichment zone instead of that enriched ion directly being pushed into reservoir by strong enhanced electrokinetic flow. In this design many channels could be placed parallel with a single common input and output reservoir. Major drawback of this design is that it requires expertise in handling thus not user friendly hence, not suitable for point of care devices. A brief overview of some of most popular designs for preconcentration devices is represented in Figure 2-6.

Besides previously mentioned designs there are few reports where 1-dimensional nanostructures (1-D) have been potentially used for protein preconcentration. Krivitsky et al developed Si nanowires forest based on chip bimolecular filtering, separation and preconcentration device which was able to perform all the three process on a single platform. By using the device150 fold more attachment of antibodies was achieved compares to flat surfaces [53]. Figure 2-7 is schematic representation of protein preconcentration on silicon nanowires forest using blood sample. Carbon nanotubes and other one dimensional nanostructure based preconcentrator are reported in the literature for heavy metal like; lead, but there are not many reports on 1D nanostructure based preconcentrator for biodiagnostics applications.

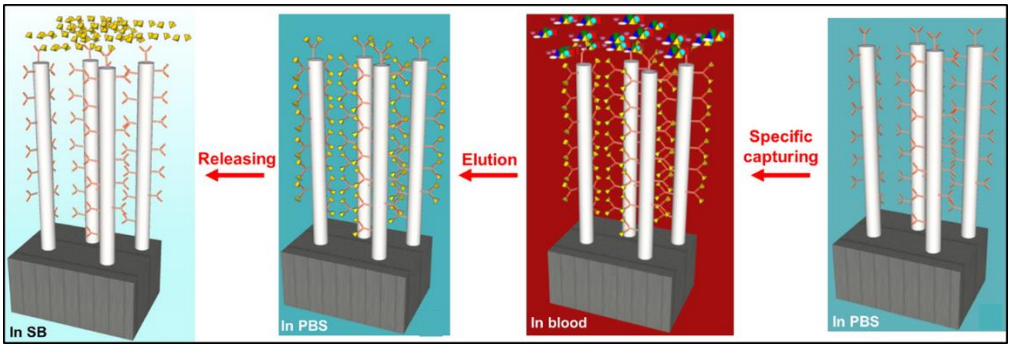

Figure 2-7: 1-D nanostructure (Silicon nanorods) based specific protein preconcentration in whole blood sample followed by elution and release of captured target protein. Reprinted with some modification with permission from [53], Copyright (2012) American Chemical Society.

The above mentioned preconcentration devices although offers very good preconcentration factors and are very efficient yet there are some drawbacks and limitations associated with them. Most of the devices require very much expertise in microfabrication techniques as lot of complex fabrication processes are involved in creation of micro/nanochannels. Secondly, working principle of most of the devices is based on ion concentration polarization and movement of particular type of ions. This requires integration of electrodes in the device and electrical energy source to create potential difference between electrodes. Due to involved complex design the overall cost of device could be high. Therefore, a low- cost approach is much needed in this context. Beside this specificity is another important issue with these. For example; ion selective membranes are specific to a particular type of ions but if there is a mixture of several proteins there could be high probability of co-concentration of unwanted proteins or contaminants. These limitations could be minimized by adopting low-cost substrate like; paper for device fabrication and there is also need to modification of the substrate for biomolecules immobilization and ensure specificity. The next sections of the chapter is an effort to provide an insight towards these aspects.

2.4. Paper based preconcentration devices

First use of paper for biological application was paper chromatography, by two biochemists Martin and Synge to determine numbers of amino acids in a particular protein and was awarded with Nobel Prize in chemistry for their work [54]. This invention created new magnitudes towards development of paper based devices for innumerable biological applications including dipstick assay, lateral flow assay and micro-paper-analytical devices (µPADs) for proteins, nucleic acids and whole cell detection [55]. First strip based assay was developed by Free et al. to identify Glucose in urine samples, by simply dipping the paper strips coated with enzymes in the samples and observe the blue colour due to reaction between the enzymes and glucose present in the sample [56]. Development of “Clearblue One step” three-minute, simple first home pregnancy test kit by Unipath Ltd, England in 1988, was one of the most successful paper based assays in the area of biodiagnostics. Since then paper based assays have been constantly gaining lot of popularity as a simple, efficient and affordable technique for a large range of analyte detection which has been elaborately reviewed by Nery et al and Marco et al [57], [58].

Frugal paper based diagnostics and preconcentration could serve as a striking substitute for analysis and separation of various blood components. The sensitivity and accuracy of the paper based system could be enhanced by some modification like colloids engineering, functionalization with nanoparticles, bioactive paper surface engineering and creating microfluidic patterns on paper. Hence the paper based preconcentration could be coupled with various applications including detection of health hazardous toxins and protein biomarkers present in trace amount in body fluids. Beside application in biomedical, the paper based preconcentration could detect hazardous chemical and pesticides present in extremely low quantity in drinking water [59]. In most of the cases, the concentration of analyte is too low that it cannot reach up to lower limit of detection of the device so there is a need of preconcentration of such samples. The paper based preconcentration concept used in chromatography from very early time but it was mainly used for solid phase extraction than protein preconcentration. Thus, the paper could serve as low cost, simple and a good platform for preconcentration of biomolecules and other trace compounds prior to detection. Paper is a polymer made up of cellulose fibers after its mechanical and chemical modification. Besides being light weight, cost-effective, abundant and recyclable, it also possesses some specific properties like ability to easily absorb fluid by capillary action and liquid can propagate on it without applying any external force up to some distance. These properties make it a novel platform for fabrication of low-cost biodegradable devices, mainly in developing country. From past few decade paper has been used in various devices including electronics, point of care diagnostic and for environmental monitoring. Biocompatibility and biodegradability makes it suitable for various low cost strip based assay.

Paper based preconcentration for biomolecules is now a rapidly emerging area of research interest for past 4-5 years, as there were very few reports on this concept till year 2013. Figure 2-8 summarizes different paper based device designs based on different operating mechanisms, which have been developed and reported since past decade. Cortez et al [60] applied ring oven based technique for preconcentration of analyte on paper. The ring-oven technique was first described by Weisz and this technique includes use of oven into which a filter paper disc has been incorporated. Sample in the liquid form are placed onto the filter paper drop wise manually. The sample diffuses toward periphery due to capillary force and due to heating solvent evaporates as sample propagates. Thus only non-volatile analytes remain on paper. Major drawbacks of this technique are, firstly it cannot be used for preconcentration of biomolecule due to high operating temperature of oven (more than 100°C), and at this much

high temperature biomolecule get denatured. Secondly, it cannot be incorporate with microdevices because of large dimensions and finally its limit of detection is poor. This technique is mainly used for preconcentration of chemical compounds like alkali metals and transition metals during their detection in water samples. A brief summary of various paper based preconcentration device along with their working mechanism is shown in Figure 2-8. Recently Abbas et al [61] developed a multifunctional platform on paper which could separate, preconcentrate and detect the analyte on using Whatman no. 1 filter paper having 10 µm cellulose fiber strand length. They choose a star like geometrical pattern to cut the paper for final device fabrication, this design avoids lithographic and pattering steps and provides simple sample handling system with rapid drying of solvent at the tip of each arm, based on flow of liquid through capillary force. Due to this the flow of sample enhances towards dry area from wetted surface and analyte get concentrate at the tip. For simultaneous separation and preconcentration they modify each arm of star shape µPAD with two different polyelectrolytes one is positively charged and other having negative charge in different concentration. Separation takes place due to surface charge gradient. Charge gradient is having been created by different concentrations of PAH and PSS polyelectrolytes.

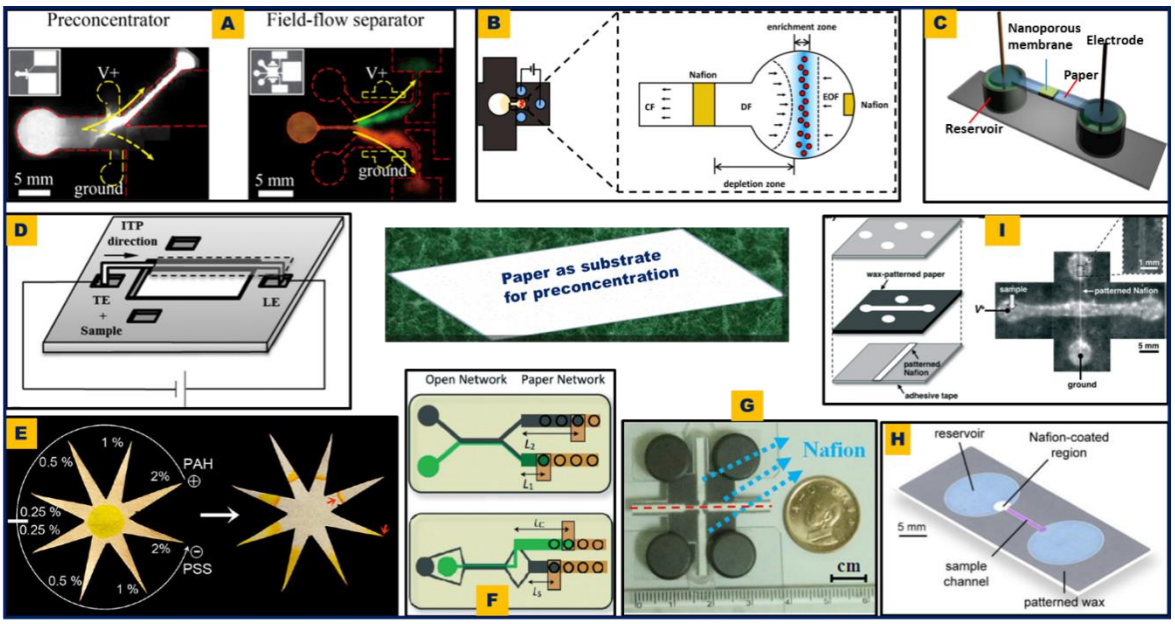

Figure 2-8: (A) continuous-flow preconcentrator on a paper platform, which can preconcentrate a field-flow separation system [62], (B) folding-paper-based ICP based preconcentrator with integrated nafion [63] (C) design of the paper-based ICP device with: paper (blue), nanoporous membrane (green) with reservoir [64], (D) schematic of paper based Isotachophoretic device [65], (E) multifunctional analytical platform on a paper strip for separation and preconcentration [61], (F) hybrid paper microfluidic devices

[65], (G) configurations of μPAD showing three convergent microchannel with Nafion coatings [66], (H) paper based ICP device schematic with reservoirs (blue), sample channel (purple), and Nafion-coated region (white) for analyte preconcentration [67] and (I) schematic of fabrication of the paper-based ICP preconcentrator [68].

In Figure 2-8E, there is schematic illustration of working of the paper based preconcentrator, after creating charge gradient, at the center a fluorescein droplet was deposited. Fluorescein migrated into different fingers, in the figure the red arrows indicate the concentration at which fluorescein forms either a band or concentrates at the tip. The absorption of the drop on paper is spontaneous and after that it rapidly spread along each polyelectrolyte coated arm of the star shaped platform. Depending on electrostatic interaction the migration of analyte takes place along the arms and concentrates near to tip in the form of band. In this way separation of different analyte takes place on a single platform.

Moghadam et al [69] used nitrocellulose for preconcentration using Alexa Fluor 488 (AF488) succinimidyl ester as sample to concentrate. The underlying principle was isotachophoresis (ITP) of sample ions between leading and trailing electrolytes. Heating and evaporation of electrolyte solutions are the major challenges in paper based ITP. To keep paper hydrated during experiment, cross shaped design was used by folding ends of paper strip and dipped them in water ITP on nitrocellulose has been proven capable of up to a 900-fold increase in initial sample concentration leads to increased sensitivity of paper based LFIA (lateral flow immunoassay) as reported. Hung et al [66] demonstrated a portable sample preconcentrator for paper based microfluidic device (μPAD) consisting different convergent microfluidic channels with integrated Nafion. The device performance was evaluated with fluorescein and a fluorescein isothiocyanate-labeled bovine serum albumin (FITC-BSA), 140 fold of concentration was achieved in 2 minutes Another report from the same group described similar studies and explained the advantage of convergent microfluidic channels in protein preconcentration over straight channels [70]. Most of the reports on paper based preconcentration has described the application of such concentrator for proteins whereas, Gong et al [67] established paper based platform for DNA analysis and its amplification on the same strip. The design of device consists a sample channel, reservoirs defined by wax printing and a small region coated with cation selective Nafion on nitrocellulose strip. As described in previous sections, Nafion creates an ion-concentration polarization (ICP) which eventually leads to concentration of ions having counter charge as Nafion. The device was used to amplify and detect HBV (Hepatitis B virus) DNA in human serum and assess sperm DNA integrity in

human semen. Required number of copies for early diagnosis of viral DNA were obtained and satisfactory results for sperm DNA were obtained too. The estimated cost of device was <1USD per test and claimed to be rapid as it takes about 10 min for DNA analysis. Later, Son et al [64] also demonstrated paper based ICP device for selective preconcentration of a human breast cancer marker (muc1 gene) fragment and a lamp-2 gene fragment which is associated with Danon disease and achieved up to 60 fold concentration of both the DNA. The two concentrated genes were claimed to get extracted easily though the extraction mechanism has not been explained.

In most of the ion concentration polarization (ICP) based preconcentration devices for biomolecules, a preconcentration plug is used for the delivery of the samples. The major and critical problem with this is dispersion of the plug. The driving force in ICP devices is electric field, on removal of the field the various force balance which is required to hold the sample in the plug get disturbed which leads to dispersion of preconcentration plug and loss of the sample. Recently, Lee et al [63] addressed this very important issue by investigating a 3D folding paper based preconcentrator for extraction of ICP preconcentrated plug with minimal dispersion effect. The design includes printed ICP preconcentrator on wax patterned Whatman filter paper 1. With 3D folded structure the dispersion effect was reported to minimized with efficient extraction. A preconcentration factor of 300-fold for 10 min was achieved with the device.

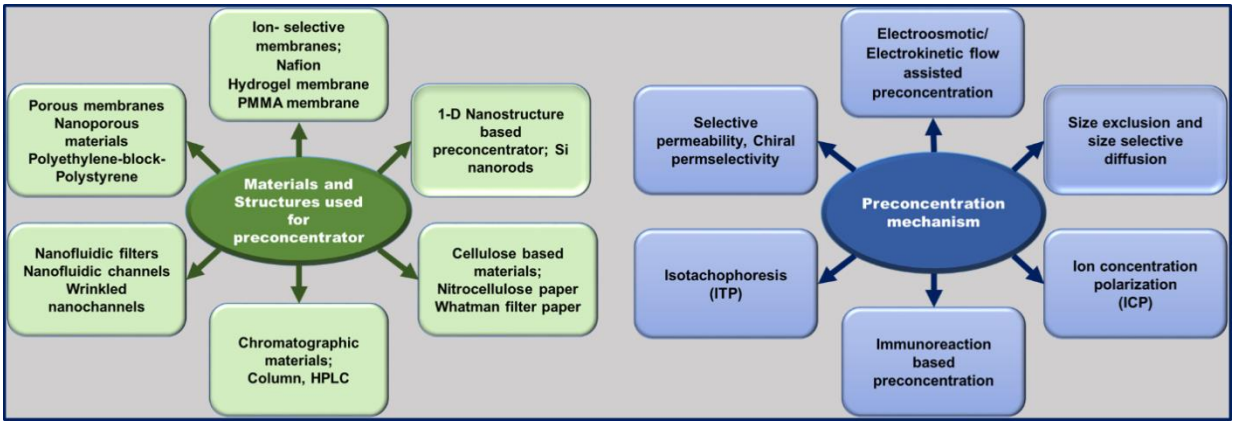

Figure 2-9: Charts showing different popular materials and structures for preconcentration and preconcentration mechanisms specifically used for proteins/biomolecules preconcentration.

Figure 2-9 represents two different charts, which give a brief overview of materials and mechanisms used and have been reported for protein or biomolecules preconcentration. It is clear from the charts that majority of the preconcentrator devices are based on movement of

ions which requires electrical energy to drag the fluid and concentration plug forward. Which is one of the big limitation of such devices and a challenge for researcher to develop such a device which could be operated without use of high voltage.

2.5. Modification of paper for biomolecules immobilization

One of the several advantages of using paper as potential substrate for biodiagnostics is the huge scope of modification of paper according to applications either at the time of manufacturing by altering physical, chemical and morphological properties of natural cellulose fibers [71]–[76] or post manufacturing by various methods including colloid engineering and filtration [77], using cationic polymer [78], [79], engineering of paper based surface using bioactive inkjet printing[80] and modifying paper with nanoparticles [9]. Most of the proteins have negative charge so binding of protein on the paper could be enhanced by pre-coating paper with cationic polymers that will stick to cellulose surface and offer a highly cationic charged surface. Many cationic polymers like Polyamide–epichlorohydrin (PAE) and Polyvinyl amine (PVA) imparts cationic coating to the paper surface. While using this method for modification of paper it should be keep in mind that the surface could bind most biomacromolecules, so it may be necessary to use blocking agents like Tween 20, bovine serum albumin, casein and protein-A to prevent nonspecific adsorption [79]. Coating nanoparticles on paper could also serve as a good platform for antibodies attachment. Being biocompatible and having excellent optical properties gold nanoparticles are being frequently used for this purpose. The effect of addition of gold nanoparticles (AuNPs) was studied by Ngo et al [81], and the ability of the resultant composite materials to amplify the surface enhanced Raman scattering (SERS) signal of a dye adsorbed was examined. It was found that on the addition of analyte, functionalized and well dispersed AuNPs are induced into aggregates which show a significant colour shift. This is due to interparticle plasmon coupling which occurs as the surface plasmon of the individual AuNPs combine when their interparticle distance is smaller than their diameter.

To improve the sensitivity of a paper-based colorimetric biosensor, Peng et al [77] applied colloids engineering in combination with filtration to lower the paper substrate backgrounds and optimize the immobilization of bio-molecules on paper. Their study aims at engineering controlled colloid flocs incorporating biomolecules (colloids engineering) to increase the sensitivity of paper-based biosensor (bioactive paper). Two hypotheses relying on controlled

colloid flocs were tested. The first was that the retention efficiency of biomolecules increases by retaining particle-biomolecule flocs through filtration; the second was that the activity of an immobilized biomolecule improves when incorporated within the biocompatible flocs. Alkaline phosphatase (ALP), was selected as ideal biomolecule as it produces a colour change from light yellow to dark blue, when in contact with the liquid substrate, 5-bromo-4-chloro-3-indolyl phosphate and nitro blue tetrazolium (BCIP/NBT). Thus enables to visualize and to quantify the bioactivity of the target biomolecule ALP. Two crucial requirements to engineer biosurfaces are the ability to produce accurate patterns of biomolecules on surfaces and to retain the functionality of the immobilized biomolecules. Recent studies have shown printing to be a favourable means to create biomolecular patterns on surfaces. Applications of particular interest are firstly, scaffolds for tissue engineering and secondly paper based diagnostics. Proteins can functionalize polymeric scaffolds for regulating cell growth, for instance, directed neuron outgrowth for neural regeneration applications. These applications require accurate printing of biomolecules in fine patterns, concentration gradients or within fluidic channels. Digital inkjet printing is an attractive choice for the manufacturing process because of its precision, speed and flexibility [80]. Beside these there are many other reports from various research groups for the modification of paper to make it suitable for microfluidics based biosensing devices.

2.6. ZnO nanostructures as potential material

ZnO nanostructures exhibit relevant properties including high catalytic efficiency and strong adsorption ability. Recently, interest has been focused towards applications of ZnO in biosensors due to its high isoelectric point (IEP) of ~9.5, biocompatibility, and abundance in nature [82]. The high isoelectric point of ZnO results in a unique ability to immobilize an enzyme with a low isoelectric point through electrostatic interaction. Furthermore, nontoxicity, high chemical stability and high electron transfer capability make ZnO a promising material for immobilization of biomolecules without an electron mediator and can be employed for developing implantable biosensors [83]. One-dimensional single-crystalline ZnO nanostructures have been synthesized successfully in several groups. Such structures exhibit high surface to volume ratios and superior mechanical stability making them ideal candidates for sensors. Gas sensors based on ZnO nanorods and thin films have been reviewed in[84]. Pearton et al [85] reviewed the significance of wide band gap semiconductors, including ZnO,

in sensor applications. It is stated for example, that the use of enzymes or adsorbed antibody layers on the semiconductor surface leads to highly specific detection of a broad range of antigens of interest in the biomedical field. The biocompatibility and fast electron transfer ability allow the nanoparticles to function as a biomimic membrane material with the ability to fix and modify proteins. The advantages of ZnO nanoparticles may also be applied to develop enzymatic detection devices [86]. Costa et al [87] proposed a methodology to grow zinc oxide nanorods on paper by simple, cheap and effective hydrothermal synthesis. This methodology does not require any surface modification. Using Zn^{+} ion as seed layer they demonstrated a detailed strategy to grow nanorods of height few micron or nanometres.

To test the hypothesis formulated in previous chapter and on the basis of literature survey, the work presented in the subsequent chapters is dedicated to investigate opportunity of modification of paper with ZnO nanostructures to increase the available surface area for protein capture, biofunctionalization of nanostructures-modified paper. Emphasis is given on developing a protocol for protein preconcentration using the nanorods modified paper as a substrate. Effort has also been made to explore scope of thus nanostructure modified paper for separation of plasma from whole blood.

Chapter 3

3. Growth and Characterization of Zinc Oxide Nanorods on Paper

3.1. Introduction

ZnO nanomaterials have achieved an extensive acceptance due to their distinguished performance in various research areas including electronics, optics and photonics. These nanostructured materials can provide a suitable platform for development of high performance biosensors due to their unique fundamental material properties [88] like, high isoelectric point (IEP), a wide gap semiconductor, biocompatibility, and richness in nature [82]. Most proteins have a lower IEP than the ZnO, hence the electrostatic interactions between the two surfaces gives this oxide an exceptional capability to immobilize proteins. In addition to this, biocompatibility or nontoxicity, high chemical stability and high electron transfer capability make ZnO a promising material for immobilization of biomolecules without the need of an electron mediator. These characteristics make it a potential material to be used in the development of sensors for various applications including implantable biosensors [83]. Earlier, amongst a range of ZnO nanomaterials, ZnO thin films have received a lot of attention from researchers because of their applications as sensors, transducers, catalysts and solar cell. However, in the last few decades, one dimensional (1D) nanomaterials have become a prominent threshold in nanoscience and nanotechnology research. One-dimensional single-crystalline ZnO nanostructures like; nanorods, nanowires and nanobelts possess high surface to volume ratios and superior mechanical stability with excellent electrical and optical properties, making them ideal platforms for sensors [89].

Zinc oxide nanostructures can be synthesized by either solution phase or vapor phase synthesis methods. In solution phase synthesis, growth of nanomaterials takes place in a liquid medium. If the growth process is carried out in aqueous solutions, then the process is referred as hydrothermal growth process. Solution phase synthesis processes majorly include: Zinc Acetate Hydrate derived nano-colloidal sol-gel route [90], Zinc Acetate Hydrate in alcoholic solutions with sodium hydroxide (NaOH) or tetra methyl ammonium hydroxide (TMAH) [91], [92], template assisted growth [93], [94], spray pyrolysis for growth of thin films [95], [96], and electrophoresis [97]. Whereas, vapor or gas phase growth methods consist of: vapor solid (VS) and vapor liquid solid (VLS) growth [98]–[100], physical vapor deposition [101], [102], chemical vapor deposition [103], metal organic chemical vapor deposition (MOCVD) [104] and thermal oxidation of pure Zn and condensation [105], [106]. Gas phase synthesis takes place in gaseous environment and in closed chambers. Usually the gas phase synthesis is carried out at high temperatures from 500 °C to 1500 °C. The gas phase synthesis methods are

expensive and complicated. Among all the above-mentioned processes, the hydrothermal process of growing ZnO nanostructures has gained immense popularity due to its simplicity and endurable growth conditions. Since, the synthesis is carried out in aqueous solution, the growth temperatures are less than the boiling point of water [107]. Recently, 1-D ZnO nanorods modified paper substrate has been widely used for nanodevices fabrication for various applications including biodiagnostics. For ZnO nanorods modified paper based devices, hydrothermal route for synthesis is most simple, rapid and low cost method for growing nanorods on paper substrate [108], [109]. In this chapter, a detailed description has been given for growth of nanorods on paper along with characterization techniques used for the modified paper.

3.2. Material and methods

3.2.1. Material

All chemicals were analytical grade reagents and used without further purification. Zinc acetate dehydrate (98%), Zinc nitrate hexahydrate (98%) and hexamethylenetetramine (HMTA) (99%) were purchased from Sigma-Aldrich. Whatman filter paper no.1 with basis weight; 87 gm/m^2, pore size; 11 µm was used as the substrate for growing the nanostructures and was procured from Sigma-Aldrich. All the precursor solutions were prepared in deionized water (DI water). A customized mini-autoclave vessel with inner Teflon chamber with lid and outer stainless steel jacket, was used for hydrothermal growth of the nanorods.

3.2.2. Hydrothermal growth of ZnO nanorods on paper

Standard hydrothermal process was used to grow ZnO nanorods on Whatman filter paper no.1 (WFP) as a substrate. For hydrothermal synthesis a seed layer is required on the substrate to initiate the growth process. Seed layer characteristics put high impact on the structures to be grown/synthesized. Hence it is important to create seed layer with desired crystallinity and uniformity. In most of the adopted hydrothermal route for the nanorods growth, zinc acetate has been widely used as precursor for seed layer. For this, 1.1 gm of zinc acetate dihydrate $Zn(CH_3COO)_2.2H_2O$ salt was dissolved in 50 mL of deionized water to prepare 100 mM solution at pH 6.0. The clean paper (WFP) was then cut into strips of desired dimensions (2 cm x 6 cm) and soaked in this solution for 60 seconds followed by annealing at 100°C inside oven

for 1 hour to create a seed layer. WFP strips with the seed layer was then subjected to further growth process. For the growth of the ZnO nanostructures (nanorods), the paper strips with the seed layer were transferred to a mini hydrothermal reaction vessel containing equimolar mixture of two precursors. Precursor solutions were prepared as: (i) 0.7 gm of hexamethylenetetramine (HMTA) salt was dissolved in 50 mL of DI water to form 100 mM solution at pH- 7.8 likewise, (ii) 1.45 gm of zinc nitrate $Zn(NO_3)_2.6H_2O$) salt was dissolved in 50 mL of DI water to form 100 mM solution at pH-3.5. The reaction vessel was filled with equal volume (20 mL each) of the two solution after the pH was set to 6.5. The ZnO nanorods synthesis was carried out for 5hrs. at 90°C. Upon completion of 5 hours. all the strips were taken out from the vessel followed by washing with DI water thrice to remove excess of salt and afterward, annealing at 100°C for 30 minutes inside oven.

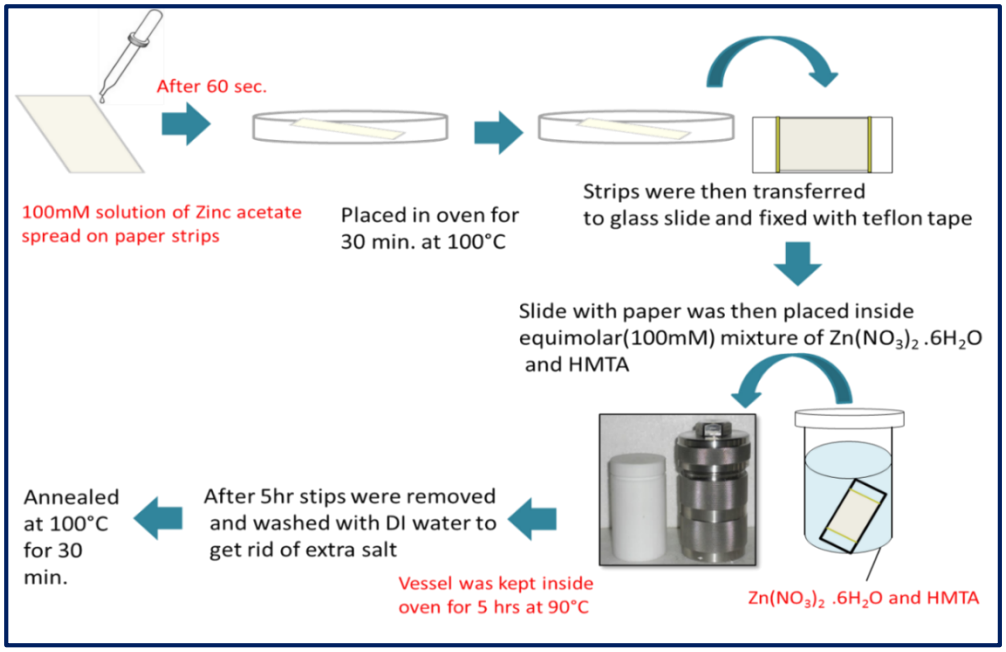

Figure 3-1: Schematic of steps involved in hydrothermal route of growth of nanorods on Whatman filter paper.

A schematic of the procedure and steps followed for modification of paper with zinc oxide nanorods by adopting hydrothermal route for the nanorods growth on Whatman filter paper is given in Figure 3-1. The final growth conditions were optimized after repeated experiments. All the optimization experiments have been done in triplicates.

3.2.3. Morphological and structural investigations of modified paper

Structural and surface characterization of the ZnO nanorods modified paper was performed using a combination of techniques consisting of scanning electron microscopy (SEM), atomic force microscopy (AFM), X- ray diffraction analysis (XRD), X-ray photon spectroscopy (XPS) and Energy Dispersive X-ray spectroscopy (EDS).

Scanning Electron Microscopy: For morphological investigation of the nanorods modified paper, samples were observed under scanning electron microscopy (SEM) (RAITH-150 scanning electron microscope). Both, the nanorods modified and unmodified paper, initially showed high charging effect that hindered the imaging. To overcome this problem all the samples were coated with 5 nm thin layer of gold with Nordiko 3-target metal sputter system.

X-Ray Diffraction: The X-ray diffraction data from nanorods modified (Zn-NRs/WFP) and unmodified paper (control) were collected on high resolution RigakuSmartLab X-ray diffractometer using CuKα1; λ= 0.154056 nm (high-resolution) at 40 kV/30mA, over a range of $10^{o}< \theta<60^{o}$. Sample size for each measurement was 5 mm x 5 mm.

X-ray Photon Spectroscopy: Development of nanorods growth on paper was observed and an increase in atomic concentration of Zinc and Oxygen elements as well as their chemical bonding was determined by XPS (X-ray photon spectroscopy) with PHI 5000 Versa Probe-II (USA). The scan area was kept at 10 µm x 10 µm with analysis in triplicates and the angle of X-ray beam relative to paper (substrate) was 45° for all the measurements.

Energy Dispersive X-ray Spectroscopy: EDS is a technique for quantitative estimation of different elemental concentration in a particular spot of the material. 5 mm x 5 mm sample size was used for the study and a spot on the ZnO-NRs/WFP was defined for the measurements.

3.3. Results and Discussion

3.3.1. Optimization of growth of ZnO-NRs on paper

The characteristics of any synthesized materials/structures largely depends on the reaction conditions. The growth conditions for the nanorods on paper were optimized by several sets of the experiment using different conditions. The reactions were carried out by changing growth time while maintaining constant pH of 6.5 for the precursor solution (consist of HMTA and zinc nitrate hexahydrate). Formation of the $Zn(OH)_2$ in a controlled manner is an essential requirement for the growth of the ZnO nanorods. Hexamethylenetetramine (HMTA) supplies

additional OH^- while zinc nitrate is the source of Zn^{2+} ions for the reaction. Also, the formation of $Zn(OH)_2$ in a controlled manner is an essential requirement for the uniform growth of the ZnO nanorods. Thus a precursor is usually used that can supply additional OH^- ions in the solution, thereby increasing the pH of the solution. HMTA is a very good choice for such purpose. HMTA decomposes into formaldehyde and ammonia and the decomposition depends on the pH of the buffer solution resulting in a controlled supply of OH^- ions in the solution ion due to the slow decomposition of HMTA [89], [110]. Thus it acts as a poor ligand for zinc in the growth of ZnO nanostructures. The detailed reaction mechanism of hydrothermal growth of nanorods can be represented as below:

$$ZnO(NO_3)_2 \longrightarrow Zn^{+2} + 2NO^-_3 \quad (1)$$

$$(C_6H_{12}N_4) + 6H_2O \longrightarrow 6HCHO + 4NH_3 \quad (2)$$

$$2NH_4OH \longleftrightarrow 2NH_3 + 2H_2O \quad (3)$$

$$Zn^{+2} + 2OH^- \longrightarrow Zn[(NH_3)_4]^{+2} \quad (4)$$

$$2H_2O \longleftrightarrow H_3O^+ + OH^- \quad (5)$$

$$Zn^{+2} + 2OH^- \longrightarrow Zn(OH)_2 \quad (6)$$

$$Zn(OH)_2 \longrightarrow Zn\text{-}NRs + H_2O \quad (7)$$

The nanorods growth on paper strips was analyzed by observing the modified strips under scanning electron microscope. Figure 3-2 shows scanning electron micrographs of paper subjected for zinc oxide nanorods growth experiment using different parameters to optimize the growth conditions. The observations from SEM images are summarized in Table 3-1. It is clear from the images that as the duration of growth experiments increased, length and density of the nanorods also increased. There was also an increase in the surface coverage of paper by nanorods as the reaction time increased. It was observed that after 5 hours, very high aspect ratio structures with good surface coverage were obtained, which was desired to meet our objectives. Thus the optimum condition for modification of paper with ZnO nanorods was found to be; reaction time 5 hour at pH- 6.5. Obtained results were further confirmed with X-ray photon spectroscopy by difference in peak intensity at different growth conditions. The obtained results from XPS will be discussed in details in next section.

S. No.	Time	pH	Observations
1.	30 min.	6.5	No growth
2.	1 hr.	6.5	Very less growth
3.	3 hrs.	6.5	Low aspect ratio with low surface coverage
4.	5 hrs.	6.5	High aspect ratio with good surface coverage

Table 3-1: Effect of growth time and pH on growth pattern of nanorods.

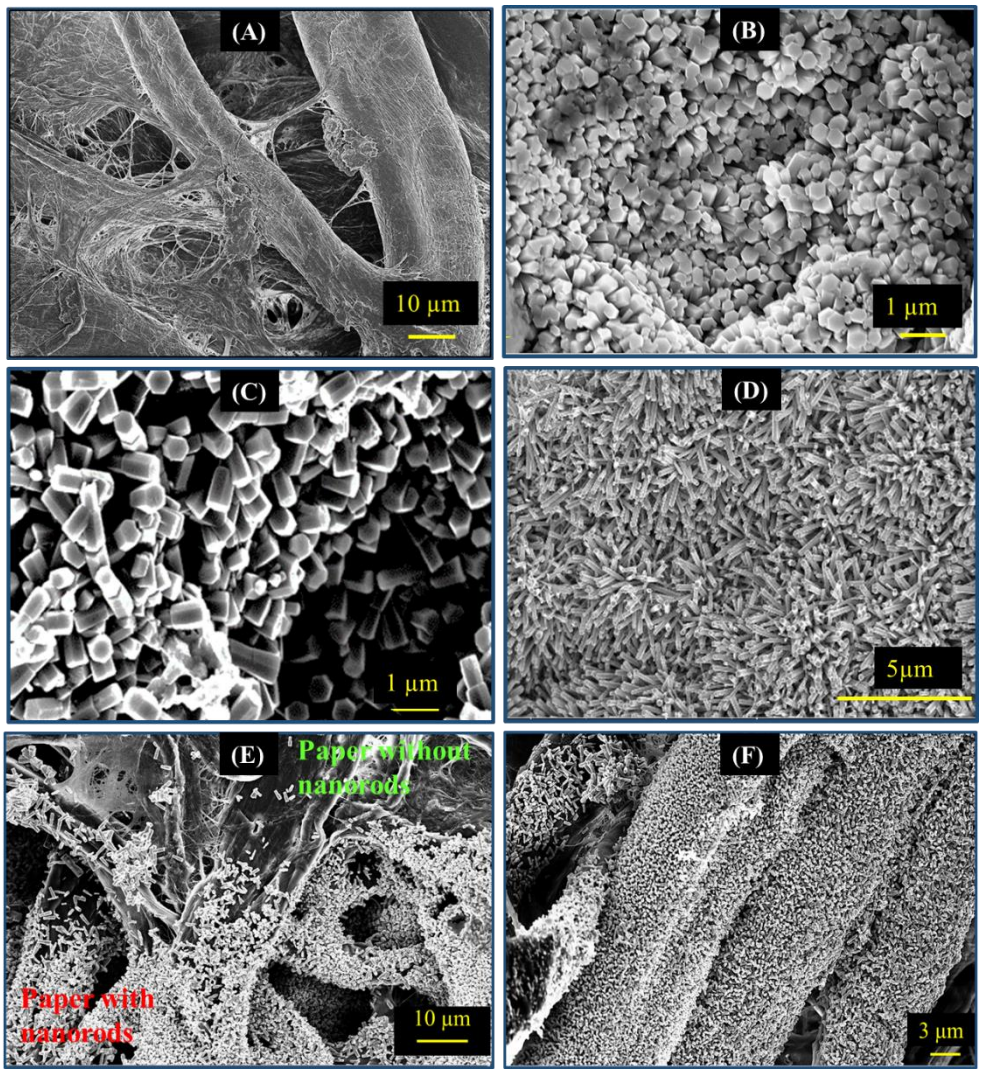

Figure 3-2: SEM images of paper after different growth time: (A) Whatman filter paper (B) after 1 hour (C) after 3 hours and (D) after 5 hours in reaction vessel respectively, (E) micrograph taken at interface showing two regions of the filter paper; with and without nanorods (F) dense vertical growth of nanorods on cellulose fibers.

3.3.1. Morphological characterization of ZnO-NRs/ Paper

Hydrothermally grown Zinc Oxide nanorods (ZnO-NRs) on Whatman filter paper were characterized by a series of complementary techniques. The very first technique used to investigate surface morphology of the substrate with nanorods was SEM. SEM was also used to calculate surface coverage by the grown nanorods on WFP. For this samples were observed under scanning electron microscope (SEM). Figure 3-3 shows scanning electron micrographs of zinc oxide nanorods functionalized paper, representing the growth pattern of the nanorods on paper fibers (Figure 3-3A) and the cross-sectional SEM micrograph indicating that the nanorods grew all through the paper with very good surface coverage (Figure 3-3B). The average length of the nanorods on the paper was found to be 1µm as observed from the represented histogram (Figure 3-3D) with an average diameter of 200 nm. Figure 3-3C shows the length distribution of nanorods (calculated from 400 nanorods).

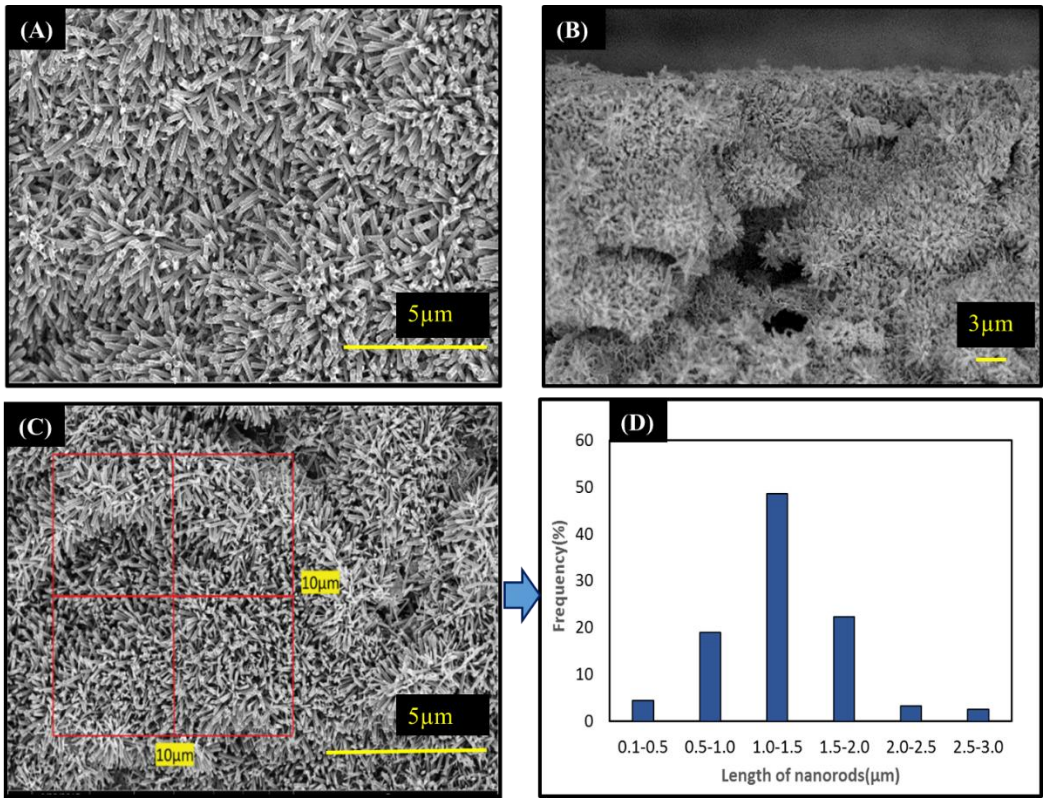

Figure 3-3: SEM images of ZnO-NRs/WFP:(A) Top view of the modified paper showing surface coverage by the nanorods, (B) cross section of the ZnO-NRs/WFP, (C) SEM image of area of paper with nanorods selected for histogram (D) histogram showing average length of nanorods grown on paper.

The morphology of the ZnO nanorods reveals growth of hexagonal ZnO nanorods of diameter ~300 nm and length up to 1-3 µm (Fig 3.3C), which varies according to growth parameters. In preliminary experiments the rods were randomly distributed on the paper substrate but after optimization of parameters they are well aligned and more uniform having good surface coverage with high aspect ratio of ~10 as listed in Table 3-2. The contribution of ZnO-nanorods to increase the surface area available for biomolecules immobilization was calculated with the help of obtained SEM micrographs. They showed a high surface coverage on paper and enhanced the area by a factor of 6.5, which will significantly enhance the target protein capture.

Sample name	Growth time	Length of nanorods (from SEM)	Diameter of nanorods (from SEM)	Aspect ratio
ZnO-NRs/WFP-1	30 min.	-	-	-
ZnO-NRs/WFP-2	1 hr.	650 nm	300 nm	2.1
ZnO-NRs/WFP-3	3 hrs.	1000 nm	300 nm	3.3
ZnO-NRs/WFP-4	5 hrs.	3220 nm	300 nm	10.7

Table 3-2: Different properties of ZnO nanorods at varying growth time.

Image analysis combined with basic calculations show that a 100 μm^2 (10 µm x 10 µm) section of paper, once treated, has an approximately 90% surface coverage of hexagonal ZnO rods, consisting of 1000 rods, 1 µm high and with a diagonal of 200 nm; this forest of rods provides an additional surface area of 650 μm^2 (Appendix A). Therefore, with high aspect ratio and high surface coverage by the nanorods, the modified paper could provide very large surface area for binding of biomolecules. The surface properties of the modified paper (ZnO-NRs/WFP) and its performance as protein preconcentration platform were further analyzed and characterized by other methods.

3.3.2. Structural characterization

To characterize the crystallinity of the nanorods modified paper, we used X-ray diffraction. The XRD diffractogram of a ZnO-NRs/WFP is presented in Figure 3-4. The obtained diffractogram exhibits characteristic peaks of hexagonal ZnO and indicated polycrystalline phase of the nanorods. Peaks positioned at $2\theta = 31.7°$, 34.4°, 36.2° and 56.6°corresponded to miller indices (100), (002), (101) and (110) crystallographic planes. This was found to be consistent with results previously reported on ZnO films and ZnO nanostructures[111], [112].

The (002) diffraction peak indicates film with crystal growth with a preferred orientation along the c-axis and perpendicular to the surface. Whereas, diffraction peaks at 2θ =14.7°, 16.8° and 22.7° correspond to the characteristic crystallographic planes of crystalline cellulose which was the major constituent of Whatman filter paper fibers.

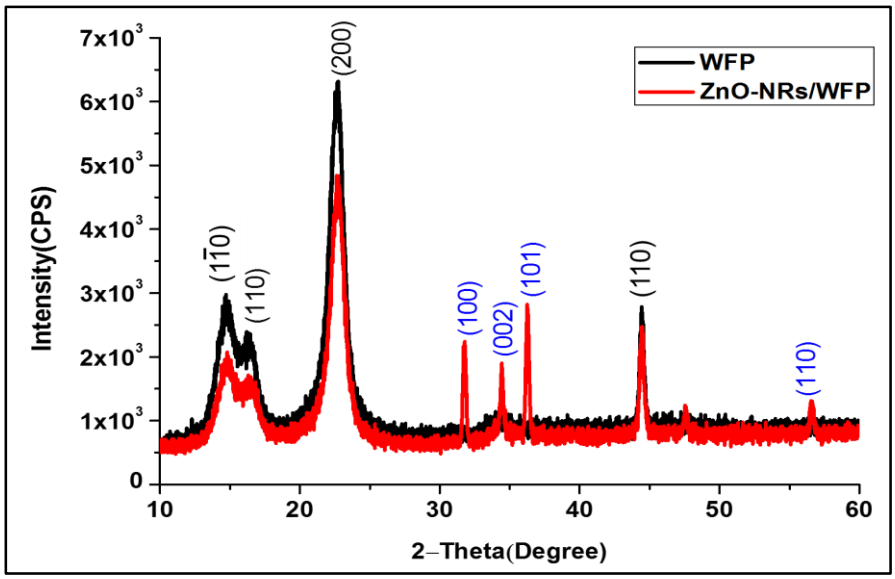

Figure 3-4: XRD spectra of WFP; without ZnO-NRs (black) and with ZnO-NRs (red) displaying various characteristic peaks of both cellulose and hexagonal zinc oxide nanorods.

3.3.3. Elemental analysis of ZnO-NRs/Paper

Elemental heterogeneity of the modified paper was quantified using EDS. The EDS spectra of ZnO-NRs/WFP provide a detailed picture of elemental composition and their contribution to the surface (Figure 3-5A). Quantitative analysis of the spectra indicated approximately equal molar ratio of zinc and oxygen i.e. 25% and 37% respectively, in the final product. This shows formation of ZnO on the paper. Beside these two elements, a significant amount of carbon atomic concentration was also observed which could be due to lot of carbon content present in paper.

Figure 3-5B, shows the full XPS spectra of WFP functionalized with zinc oxide nanorods at different growth time. The spectral peak intensities reveal that the formation of ZnO linearly increases with growth time. The graph in inset shows the specific peak enhancement of Zinc as a function of growth time. The penetration depth of the X-ray used was 7nm. XPS spectra also show the effect of process time on the atomic concentration of zinc. For zinc, primary XPS

region used to be Zn2p with overlapping O KLL and V LMM. The characteristic doublet peaks of ZnO formation corresponded to $Zn2p_{3/2}$ and $Zn2p_{1/2}$ were observed at 1023 eV and 1045 eV binding energies. Zn2p peak exhibits split spin-orbit components (Δ_{metal}=23 eV). We also observed the same and the two peaks showed a difference of 22 eV which lies within the standard range. and no metallic Zn peak was observed.

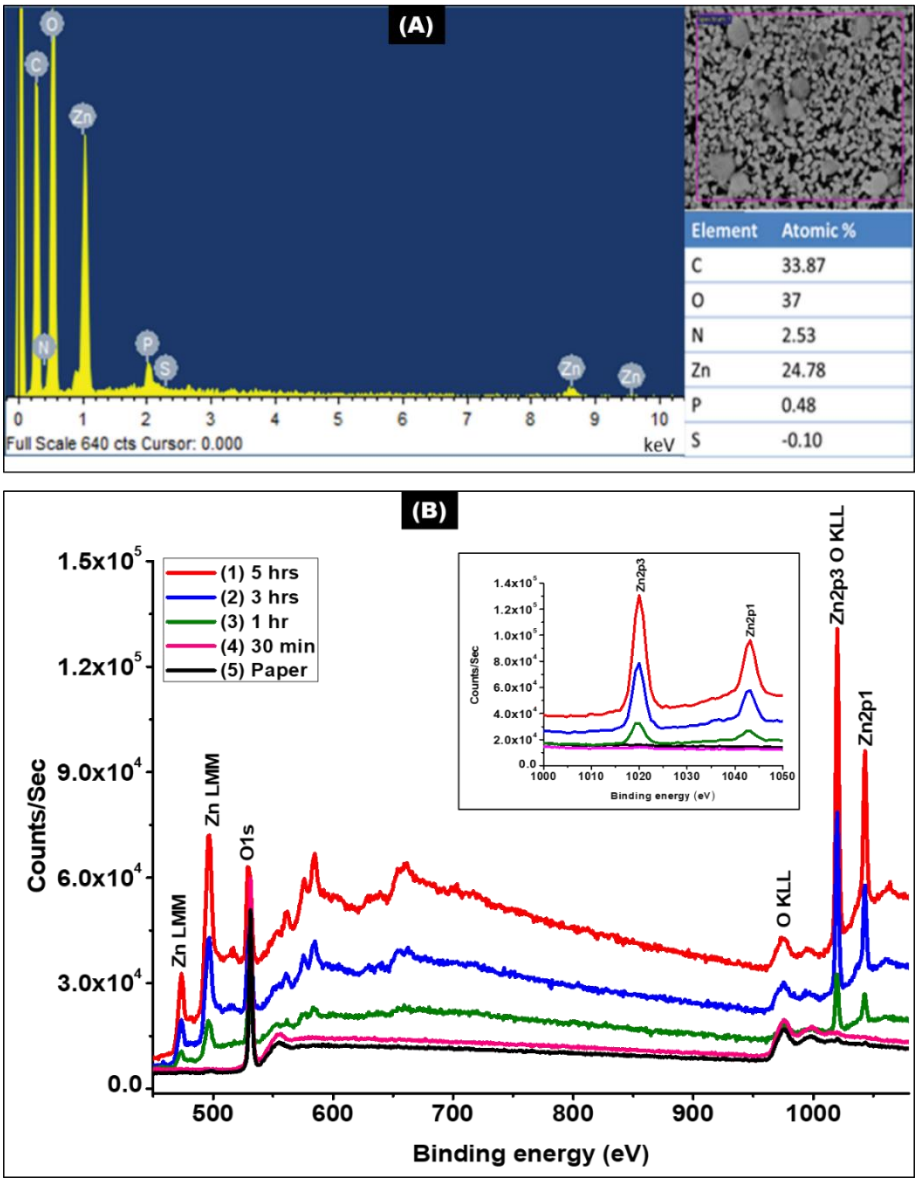

Figure 3-5: EDS spectra (A) showing different elemental atomic concentration and (B) XPS survey spectra showing the growth dynamics of ZnO-nanorods on paper at different time and highlight of the peaks specific to ZnO formation (inset).

After 5 hours of growth, the spectral intensity (~$14x10^4$ counts/second) is much higher than at 1 hour and 3 hours. Spectral analysis shows no significance growth after 30 minutes (Figure 3-5B). The characteristic Zn2p peaks were completely absent in case of unmodified Whatman

paper (control) and after 30 minutes of paper subjected to growth. The peaks advanced with time. In the spectra we have also observed an O 1s spectrum with two peaks which were also observed in previous investigations. These peaks possibly were due to presence of either $Zn(OH)_2$, or oxygen vacancies. Whereas, Zn LMM were X-ray induced Auger peaks.

3.3.4. Roughness determination via atomic force microscopy (AFM)

Roughness analysis and surface topography was studied by atomic force microscopy. We observed that average roughness of paper is much higher than paper with ZnO nanorods. The average roughness (Ra) of paper without ZnO was found to be ~ 30 nm whereas, paper with ZnO-NRs showed an average roughness value of ~18 nm (Figure 3-6). Decreased roughness of ZnO-nanorods modified paper in compare to normal filter paper is due to conversion or coverage of pores by formation of nanostructures i.e. nanorods.

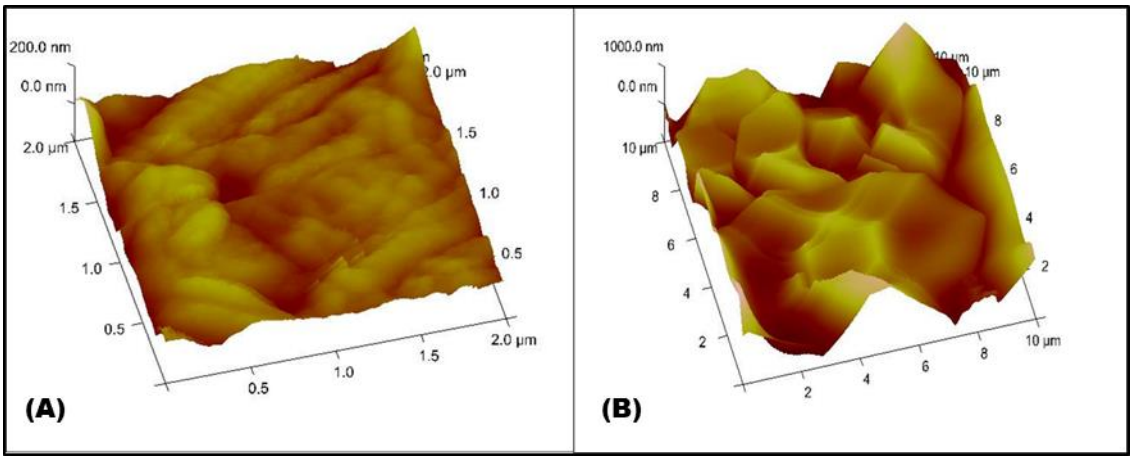

Figure 3-6: AFM images of normal Whatman paper (A) and ZnO-NRs/WFP (B).

Thus the nanorods have not only contributed to surface area but are also responsible for decrease in surface roughness of the paper. Surface roughness plays a significant role in surface-protein interactions. Surface roughness contributes to protein and other biomolecules adsorption on the surface, adsorption enhances with the increase in roughness. However, it also induces a decrease in binding affinity of surface towards proteins [113]. Therefore, decreased roughness promotes specific binding of proteins to the surface and minimizes non-specific adsorption. This phenomenon would be highly desirable where specific binding of proteins to the surface is needed. ZnO nanorods increased surface smoothness of the WFP and hence created a favourable conditions for protein binding.

3.3.5. Electrical characterization

To measure electrical properties of ZnO nanorods/ WFP, there was a need of some surface modification as unmodified surface did not show any electrical response. For this purpose, three sets of gold electrodes of thickness 50 nm were patterned on the nanorods modified paper at different areas of the paper. Distance between two electrodes was kept 1 mm. The electrical measurements were taken using four probe Proxima setup. On observing the obtained results, it was found that there was no proper electrical conduction shown by the nanorods modified paper. As ZnO nanorods have some gap between them, it is necessary to ensure a proper mode of conduction between them. Hence, Whatman filter paper was coated with a conducting polymer PDOT:PSS (Poly(2,3-dihydrothieno-1,4-dioxin)-poly(styrenesulfonate). It is highly conducting and widely used polymer in sensors and organic optoelectronic devices. The reason behind choosing the polymer was that being water soluble it can be coated on paper by simply soaking or spin coating of the paper in the aqueous solution of the polymer. The paper was coated with the polymer by spinning 1 mL solution at 3000 rpm for 30 seconds, followed by dehydration at 60ºC for 10 minutes inside an oven.

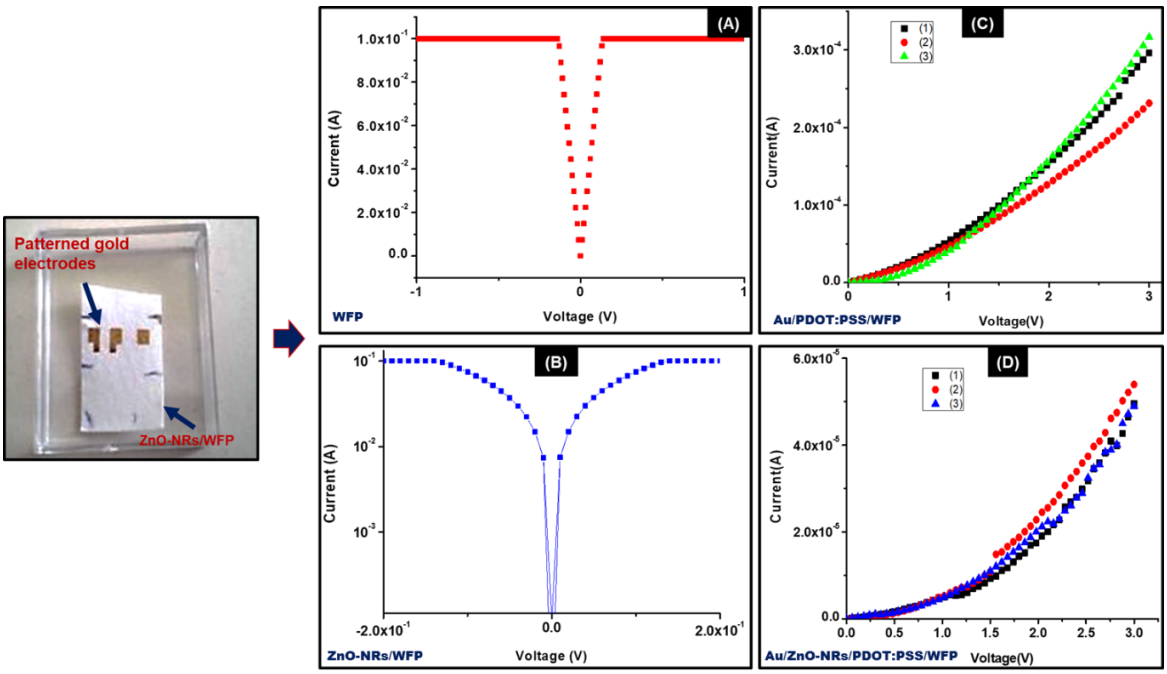

Figure 3-7: I-V characteristics of ZnO-NRs/WFP measured after patterning gold electrode on the modified paper: (A) unmodified WFP (B) ZnO-NRs/WFP and after coating PDOT:PSS (C) Au//PDOTPSS/WFP and (D) Au/ZnO-NRs/PDOT:PSS /WFP.

The modified paper was then subjected for hydrothermal growth of zinc oxide nanorods on its surface, using pre-optimized protocol. As the rods were aligned vertically it was necessary to make two contacts for the I-V characteristics measurement. Hence, 50 nm of gold layer was deposited on one surface of PDOT:PSS coated paper with zinc oxide nanorods. I-V characteristics measurements were done in Proxima setup at 3V.

Figure 3-7 shows the plots of different I-V characteristics of the nanorods modified paper. Figure 3-7A, B are the plots of Whatman filter paper with and without ZnO nanorods whereas, Figure 3-7C and D are the plots after coating with PDOT:PSS with and without nanorods. From the figure it is clear that without polymer coating there is no conclusive observation. A clear increase in current was observed with the nanorods modified PDOT:PSS coated paper. Therefore, thus modified paper could be also used for fabrication of paper based sensors. However, these results were not consistent and we could not get desired reproducibility with the substrate. The work will be further carried forward in this direction by our research group in future.

3.4. Summary and Conclusion

The phenomenal properties of paper and ZnO nanorods combination have been exploited to design a paper based protein preconcentrator. Zinc oxide nanorods were hydrothermally grown on Whatman filter paper.1 and growth of nanorods on paper was characterized in the laboratory to achieve repeatability and structure optimization. SEM, XRD, XPS, EDS and AFM techniques were used for the nanorods structural and elemental characterization. These techniques showed that the cellulose fibers of the paper provide an excellent platform for nanorods to grow on it. SEM and XRD analysis provided all the morphological and crystallographic information about the nanorods modified paper including its surface coverage. Whereas, the chemical bonding and elemental composition with their percent atomic concentration was investigated with XPS and EDS. Decreased roughness with the nanorods modified paper (as observed from AFM analysis) will support specific binding of proteins on paper while minimizes physical adsorption. Efforts have also been put to make the modified paper electrically conducting though we could not get the desired outcomes from electrical characterization of it. All these observations led to conclusion that the nanorods having very high aspect ratio and high packing density on paper could provide plenty of binding sites to the capture antibodies which could led to efficient capture of target protein over the nanorods forest.

Chapter 4

4. Biofunctionalization and Validation through Surface Plasmon Resonance

4.1. Introduction

Paper has high absorbing tendency towards liquids, due to which it is difficult to ensure if the antibodies are actually immobilized on ZnO-NRs surface or physically adsorbed on paper fibers. Physical adsorption of biomolecules take place through various weak interactions like; van der Waals forces, hydrogen bonding, and hydrophobic interactions. Therefore, biomolecules attached through physical adsorption are likely to slowly leach from the surface. Another issue with physical adsorption is that the adsorbed molecules form a randomly oriented, heterogeneous surface, which may reduce their activity, and surface density. These issues can be resolved by immobilizing antibodies on the substrate by adopting covalent methods for biofunctionalization of the substrate. Covalent immobilization of biomolecules is the most stable and uniform immobilization technique on a paper and other substrates as well., Both the biomolecule and the substrate should contain functional groups to covalently link them. Homobifunctional or heterobifunctional chemical linkers are used for covalent biofunctionalization, that acts as a bridge between the substrate and the biomolecules [114]. Two most commonly used biofunctionalization strategies are; amine modification and thiol modification and the selection of the method depends on the surface to be modified. Variety of chemicals (organosilanes) are used for these two types of surface modifications and creating amine-terminal and/or thiol-terminal surfaces. Among the organosilanes 3-aminopropyltriethoxysilane (APTES) is the most popular chemical for creation of amine-terminal biofunctional surface, due to its three hydrolysable ethoxy groups which ensure a strong anchoring of the silane to the surface whereas, the amine function of the aminopropyl group remains available for further reaction. Terminal amine groups are widely used for surface functionalization because they easily form covalent bond with various reagents including acid, aldehyde, or thiocyanates [115]. APTES, silanizes oxide surfaces by reacting with the hydroxyl groups on the oxide surfaces. The oxygen terminated ends of ZnO after forming hydroxyl groups allow for condensation reactions to occur between the APTES molecules and the ZnO surface and thus creating free amine group on the surface for further reaction with incoming linker and later on biomolecules [116]. Although the covalently biofunctionalized nanorods modified paper surface tends to be stable as reported in literature, there is a need to ensure that the antibodies are being immobilized specifically on the nanorods surface.

Therefore, to study the interaction of antibodies specifically with zinc oxide nanorods, grafting density and quantification of bound protein, Surface Plasmon Resonance (SPR) can be used as

a potential investigating tool for protein-surface and protein-protein interactions as reported in several studies [117]–[119]. Biacore system is the most widely used tool for SPR studies. It relies on microfluidic system to deliver molecules on surface and exploit the phenomenon of surface plasmon resonance (SPR) to monitor the interaction between molecules in real time. The approach involves attaching one interacting partner on the surface of a sensor chip, followed by passing sample containing other interaction partner over the surface. Binding of molecules to the sensor surface generates a response due to change in refractive index of the medium where reaction is taking place. The generated response is directly proportional to the bound mass, and can be detected at a level of a few picograms or less. The detected amount of bound mass per square millimeter on the sensor surface, corresponds to concentrations in the picomolar to nanomolar range in the bulk sample solution. Binding events are followed in real time and a range of interaction characteristics like; binding kinetics, surface affinity or binding affinity, ligand affinity etc. can be determined. Response due to change in refractive index, is measured in resonance units (RU). The response is directly proportional to the concentration of biomolecules on the surface [120]. Wei et al [121] reviewed many reports on ZnO nanostructure based sensors including chemical sensors, gas sensors, pH sensors UV sensors and biosensors for various biomolecules including carbohydrate antigens, DNA, cholesterol and urea. Thin film of ZnO based gas sensors have been reported and their performance has been analyzed by SPR [122]–[125]. Although there are many studies on ZnO nanostructure based sensors, there are very few reports on sensors based on the principle of SPR especially nanorods based SPR sensors [123]. This chapter deals with biofunctionalization of the nanorods modified paper and validation of strong binding with SPR technique. Also, in this an effort has been made to explore scope of ZnO nanorods as potential nanomaterial for surface plasmon resonance based biosensors beside other ZnO nanostructures.

4.2. Materials and Methods

4.2.1. Materials

ZnO-NRs/WFP, HIgG, FITC tagged goat-antiHIgG, 3-Aminopropyl tetraethylene silane (3-APTES) for creating amine group on nanorods surface, anhydrous Toluene as solvent for 3-APTES, Bovine Serum Albumin (BSA) as blocking agent for unbound site and Zinc acetate dehydrate, Zinc Nitrate, Hexamethylenetetramine (HMTA) were used as the nanorods

synthesis precursors. All chemical reagents required for nanorods synthesis were procured from Sigma-Aldrich.

For SPR studies, cardiac myoglobin was used as target antigen, anti-Myoglobin antibodies were used as ligand for antigen capture. PBS for sample preparation, HBS-EP buffer (0.01 M HEPES pH 7.4, 0.15 M NaCl, 3 mM EDTA, 0.005% v/v Surfactant P20) for all the sample preparation and as running buffer in Biacore experiments, Magnesium Chloride (3M $MgCl_2$) as regeneration buffer, EDC (1-Ethyl-3-(3-dimethylaminopropyl) carbodiimide), NHS (N-hydroxysuccinimide). Buffers and other solutions for SPR experiments were provided in kit by GE healthcare. Biacore X (GE Healthcare, Uppsala, Sweden) was used for all the experiments and the software for analysis was Biacore X Control Software. Hot air Oven and customized mini-autoclave was used for hydrothermal synthesis of nanorods.

4.2.2. Biofunctonalization of ZnO-NRs/WFP

The nanorods modified paper was functionalized using APTES silanization followed by glutaraldehyde chemistry to get free –CHO group on the surface which acts as a linker and facilitate binding of antibodies to the surface. Whatman filter paper with ZnO nanorods was subjected to silanization using wet method. The strips of Whatman filter paper no.1 with ZnO nanorods were firstly cleaned using ethanol and DI water followed by drying them using N2 gun. Paper strips were placed on a heating plate (100°C for 15 minutes under vacuum) covered by a beljar for dehydration. The entire setup was sealed and an inert gas ambience was being created (Ar in our case). 1% solution of 3-aminopropyltriethoxysilane (APTES) was prepared using the ethanol and acetic acid (5 mL + 2 mL) and the paper strips were dipped in the solution for 5 minutes. Then strips were taken out and thoroughly washed with ethanol and DI water three times followed by heat drying at 100°C for 15 minutes.

For immobilization, glutaraldehyde chemistry was used. 1% aqueous solution of the homobifunctional agent, glutaraldehyde (OHC-CH2-CH2- CH2-CHO) was prepared and the silanized paper strips were dipped for 30 minutes followed by rinsing with PBS (pH 7.4) and blow drying with nitrogen. Fresh antibody solution was applied on the surface by drop casting method. For immobilization, working solution of HIgG (20 µg/mL) was prepared from stock solution of both HIgG (10 mg/mL) and FITC- antiHIgG (1 mg/mL) using 0.1 M PBS (pH-7.4). The free aldehyde sites of glutaraldehyde functionalized ZnO-NRs/WFP were allowed to react with the amine group of HIgG (20 µg/ mL in PBS) by incubating the sample surface for 1 hour. In order to remove loosely adsorbed biomolecules; the surfaces were washed with a detergent

solution (0.1 % aqueous solution of Tween-20) and rinsed with PBS. The unsaturated aldehyde sites and non-specific adsorption sites on the antibody immobilized sample surfaces were blocked by dipping the samples for one hour at room temperature in 1 mg/mL solution of BSA in PBS followed by three rinsing cycles with PBS. To identify immobilized/ grafted antibodies the paper strips were put in solution of FITC tagged goat-antiHIgG (20 µg/mL) and allowed to react for 1hour followed by giving a thorough washing with PBS. Paper strips were then stored at 4ºC.

To confirm that antibodies are firmly anchored on the nanorods surface and will sustain their binding with the surface in harsh conditions (high pH), an elution experiment was also carried out. For this 10 µL of FITC-Ab (20 µg/mL) was immobilized on 5 mm x 5mm strips (in triplicates) of the ZnO-NRs/WFP as above mentioned immobilization protocol. After 30 min. all the strips were washed with PBS thrice followed by DI water. 200 µL elution buffer (PB, pH-8.5) was flowed through all the strips and eluate were collected in separate microcentrifuge tubes and subjected to fluorescence spectroscopic measurements.

4.2.3. Preparation of ZnO-NRs/Au chip

Preparation of chip for the study involved three major steps (i) Synthesis of nanorods of required dimension (ii) Drop casting and spin coating of the synthesized rods on bare gold chip (iii) Annealing of the rods over the gold chip. For ZnO nanorods synthesis glass cover slip (thickness = 0.17 mm) was used as growth platform. Prior to use the cover slip was cleaned with DI water followed by acetone rinse and dried at room temperature. A seed layer for growth was created using Zn-acetate dihydrate by using 100 mM aqueous solution of the same to create required nucleation sites for the growth by spinning the solution at 3000 rpm for 60 seconds followed by annealing of the film at 100°C for 1hour. Further, the standard hydrothermal process was followed for nanorods growth using equimolar mixture of 100 mM of Zinc nitrate and Hexamethylenetetramine solution as precursors at pH-6.5 and temperature 90°C for 5 hours. The nanorods were then scratched from the glass slip and collected as powder. The nanorods were characterized using SEM, XRD, EDS and XPS, discussed in Chapter 3. Figure 4-1 shows schematic of the chip preparation. An aqueous solution of nanorods with concentration of 0.1 mg/mL was prepared and 30 µL of this solution was pipetted over the exposed top surface of bare-gold sensor chip followed by baking it for 2 hours at 80°C for proper adhesion of nanorods over the gold surface.

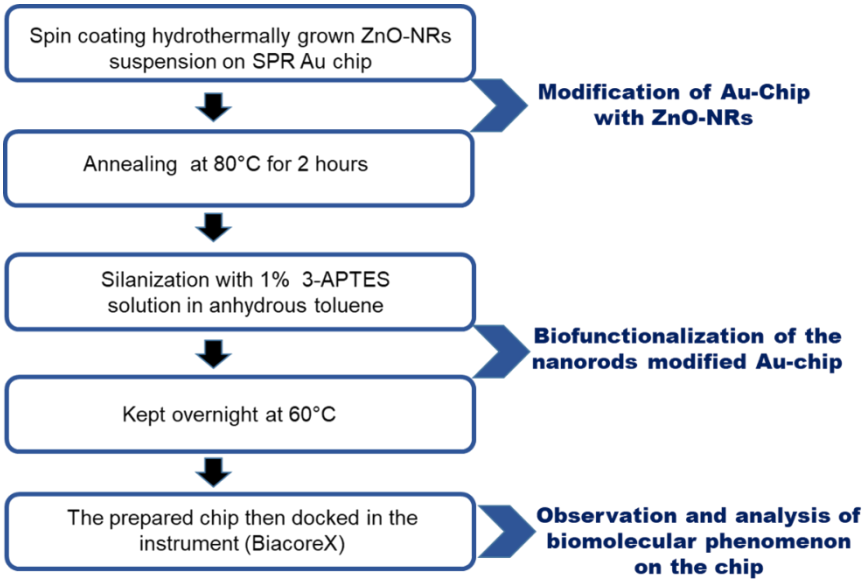

Figure 4-1: Schematic of process followed for ZnO-NRs/Au chip preparation for the study.

4.2.4. Biofunctionalization of ZnO-NRs/Au chip

For favorable antibody immobilization the prepared ZnO-NRs/Au chip was amine functionalized by using 1% solution of 3-APTES (3-aminopropyltetraethoxysilane) in anhydrous toluene. Maintaining anhydrous condition is very crucial for surface functionalization using APTES.

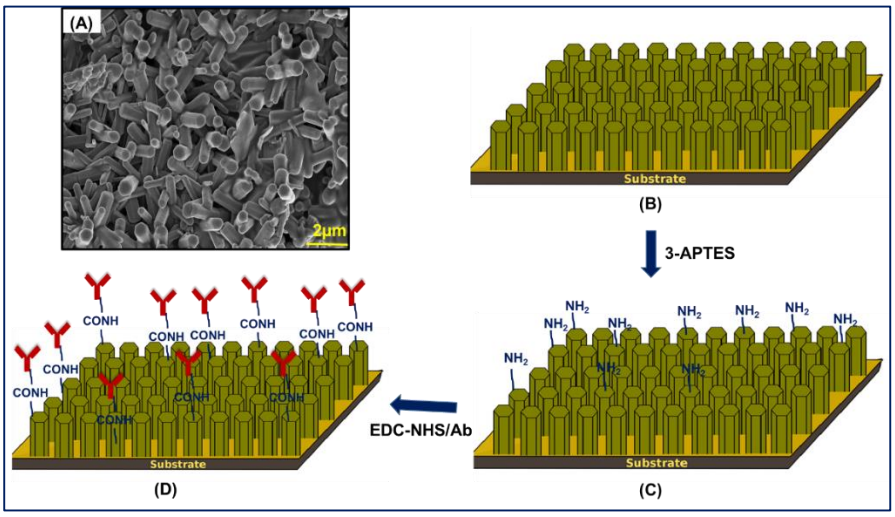

Figure 4-2: Schematic of the modified chip and scanning electron micrograph of the modified chip: (A) SEM image of ZnO-NRs/Au chip (B) diagrammatic representation of the chip (C) creation of amine group by APTES modification (D) antibodies binding with free amine group on the surface of ZnO-NRs/Au chip.

For this 1 µL of 3-APTES was dissolved in 99 µL of anhydrous toluene to make final volume 100 µL. 5 µL of this solution was pipetted from a corner of the chip which led to uniform spreading of the solution over the chip followed by ethanol washing to remove any unreacted 3-APTES. To avoid any moisture and impurity the chip was kept overnight in vacuum oven for drying at 60°C. A detailed schematic of biofunctionalization of chip is given in Figure 4-2. Silane group of silanization agent i.e. 3-APTES bind with surface –OH group of zinc oxide and created free amine group on the surface. EDC-NHS activation of surface followed an efficient ligand immobilization.

4.2.5. Optimization of maximum immobilized concentration and myoglobin binding

For the optimization of maximum antibodies immobilization on the newly developed chip a set of experiment have been performed. The running buffer for Biacore assay used during all measurements was HBS-EP pH-7.4. The modified chip (ZNO-NRs/Au) was docked into the instrument (Biacore X) and the baseline was allowed to stabilize for 1hour by passing HBS-EP buffer. The flowrate was maintained 5 µL/min and temperature was kept 25°C throughout the experiment. Prior to measurement the chip was activated by using a mixture of 55 µL of EDC and NHS each and 50 µL of the mixture was injected. To evaluate maximum Mab (anti-myoglobin antibodies) immobilization on modified chip surface, a series of measurements were done with different concentration from 1% to 10% of stock of Mab (9 mg/mL) (rather than saying what % of stock, just write what concentration gradient was used). All the dilutions were prepared in HBS (pH-7.4) and Sodium acetate (pH-5) was used as immobilization buffer.

The binding assays were performed on two types of SPR chips (i) CM5 sensor chip with short carboxymethylated dextran matrix (ii) Gold (Au) sensor chip modified with ZnO-nanorods (ZnO-NRs/Au). The covalent immobilization of anti-myoglobin (Mab) on ZnO-NRs/Au chip surface was done by silanization chemistry using 3-APTES (3-aminopropyltetraethoxysilane) followed by EDC/NHS activation. For CM5 chip EDC/NHS chemistry was used for covalent immobilization of antibodies. After each measurement the SPR chip surface was regenerated using 3M $MgCl_2$ for 60 seconds at flow rate 5 µL/min. Pure cardiac-myoglobin protein samples of different concentration ranging from 0.0001 µM (100 pM) -1 µM, were prepared from stock concentration of 2 mg/mL, in HBS-EP buffer at pH-7.4 with interval of factor of 10.

4.2.6. Preparation of plasma samples

To check the compatibility of the modified chip with real blood or plasma sample, it was subjected to ten binding and regeneration cycles. Plasma from three of each four blood groups was used for the study and was separated via centrifugation from the blood samples procured from Red Cross Society Melbourne. All the plasma samples were diluted in DI water at 100x and 50 µL of each sample was injected on the modified chip for binding analysis. In another experiment, separated and diluted plasma sample was spiked with 200 ng/mL of Myoglobin to check the specificity of the modified chip. The ratio of each in injected mixture was Plasma: Myoglobin; 1:1. The final injected volume was 50 µL.

4.3. Results and Discussion

4.3.1. Antibodies immobilization on WFP

The ZnO-NRs/WFP modified paper was biofunctionalized with antibodies. The antibodies were covalently immobilized using silanization chemistry with 3-APTES, which provides sites for amide ($–CONH_2$) bond formation. Silanization of ZnO-NRs/WFP with 3-APTES was confirmed by FTIR (Figure 4-3). The peak at about 3410cm^{-1} corresponds to the stretching vibration of N–H and O–H. The peaks at about 1578 and 1517cm^{-1} are attributed to the bending vibration of N–H which is absent for paper without silanization. The peak at 1016cm^{-1} refers to the Si–O bond stretching vibration, while at 493cm^{-1} there is clear peak in modified paper which belongs to the Zn–O bond stretching vibration. Silanized ZnO-NRs/WFP paper was then biofunctionalized with the antibodies. The structures of about 50-100 nm were observed from SEM image of the biofunctionalized ZnO-NRs/WFP (Figure 4-3B). These could be immobilized antibodies on nanorods as no such structure were observed on normal unmodified filter paper.

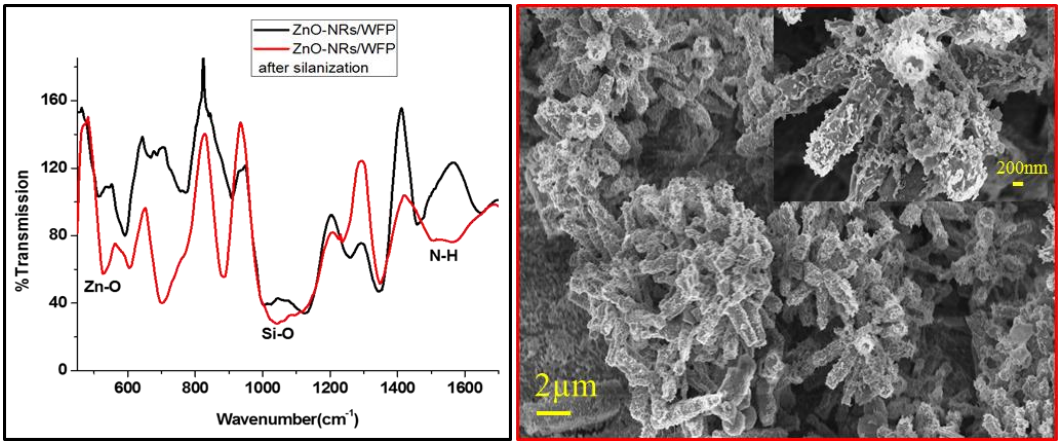

Figure 4-3: Confirmation of surface biofunctionalization: FTIR-spectra (A) and SEM image (B) of ZnO-NRs/WFP after APTES modification. The inset shows the magnified micrograph of ZnO-nanorods after antibodies immobilization.

The immobilization was further confirmed with elution experiment. Figure 4-4, shows schematic of the followed strategy for the confirmation and the other part of figure shows obtained fluorescence spectra of collected eluate. Though the covalent binding method for biofunctionalization was followed by immobilization, the results from fluorescence spectroscopy show some weak signal of fluorescence in two out of three eluate samples. It is possible that the fluorescence observed was a result of some remaining unbound or physically adsorbed antibodies, hence we cannot comment on the stability of antibody binding.

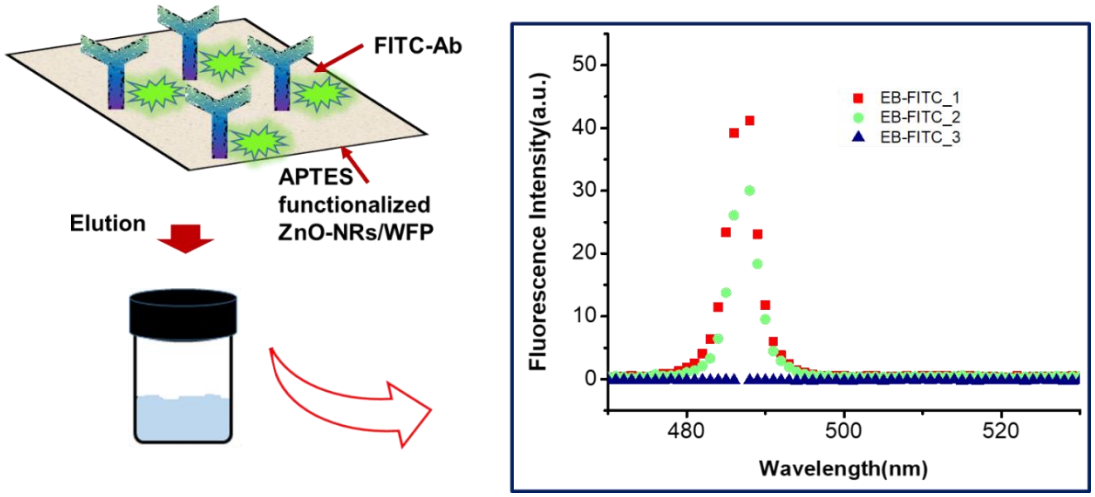

Figure 4-4: Schematic of confirmation of immobilization with elution buffer by immobilizing tagged Ab on the modified paper followed by passing elution buffer over it (left) and fluorescence spectroscopic measurement of the collected eluate(right).

We therefore proceeded with surface plasmon resonance to provide concrete proof and support for confirmation of the antibodies immobilization as well as efficient binding of target protein.

4.3.2. Optimization of immobilization on ZnO-NRs/Au chip

One of the most important studies on any new sensing surface where sensing is based on binding of ligand-target interaction, is to optimize the maximum level of ligand/antibodies immobilization on the sensing surface. In our study we have focused on anti-Myoglobin antibodies- cardiac Myoglobin interaction. The ZnO-NRs/Au chip has been analyzed by repeated experiments on the chip with different concentration of Mab. Fig 4-5A shows the plot between immobilized concentration and response (RU), drawn by collected data from Biacore X system using Biacore control software. There is a logarithmic increase in obtained response with increase in Mab concentration. After a certain concentration the response become constant. This could be due to saturation of the available surface for immobilization and there was no available space to accommodate molecules further. Here the trend became constant after 5% concentration of Mab and on further increase to 10% the obtained response is almost same as the response at 5% or even small dip in response has been observed at 10% concentration. We can conclude that the optimized immobilization concentration on ZnO-NRs/Au chip was 5%. Whereas, Figure 4-5B shows a comparison of level of immobilization on the two chip (Zn-NRs/Au and CM5 chip).

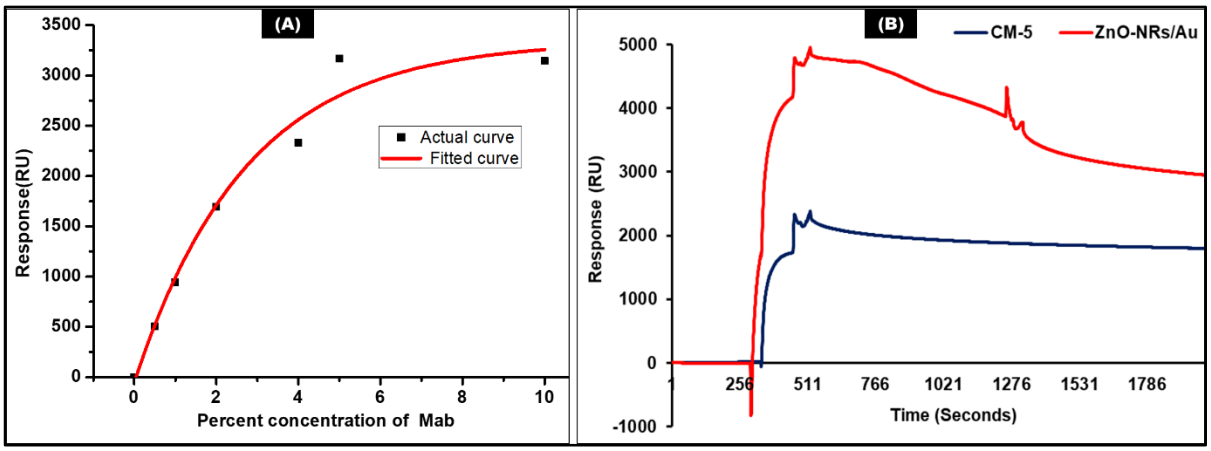

Figure 4-5: (A) Optimization of anti-Myoglobin immobilization concentration on ZnO-NRs/Au chip (B) comparison of antibodies immobilization level on both the chip ZnO-NRs/Au and CM5 chip. The optimized concentration (5%) of antibodies was used on both the chip.

A clear difference of about 1200 RU was observed in both the chip. These observations supported and confirmed our hypothesis that nanorods could enhance the level of ligand

(antibodies) immobilization thus the modification of substrate with nanorods eventually lead to efficient binding of proteins/biomolecules of interest. It was found that using same optimized concentration of antibodies i.e. 5%, the nanorods modified chip produced higher level of immobilization response. The obtained response with ZnO-NRs/Au chip was found to be approximately 3200 RU however, with CM5 chip the immobilization value in terms of RU was 2000 RU.

4.3.3. Binding analysis of myoglobin on ZnO-NRs/Au chip

To further test our hypothesis it was essential to investigate binding of target protein on the ligand immobilized newly developed chip. For this, standard solution of cardiac myoglobin of different concentrations from 1 nM to 100 nM, were prepared by diluting the stock in HBS-EP buffer pH-7.4. Figure 4-6A represents typical sensogram showing different events took place on the ZnO-NRs/Au chip; EDC-NHS activation, Mab immobilization, blocking with 1% BSA (2 mg/mL) followed by myoglobin binding. Myoglobin binding on ZnO-NRs/Au chip is found to be more efficient compared to CM5 chip. Mab bound concentration on the two chips was compared by injecting 30 µL of optimized 5% of Mab solution as ligand, at flow rate 5 µL/min. Figure 4-5B shows the difference in immobilized amount on two chip, ZnO-NRs/Au chip showed significant enhancement in response on Mab binding than CM5-chip. Corresponding enhancement could be seen on different myoglobin concentrations. Figure 4-6B shows the behaviour of the two chips towards different concentration of cardiac myoglobin.

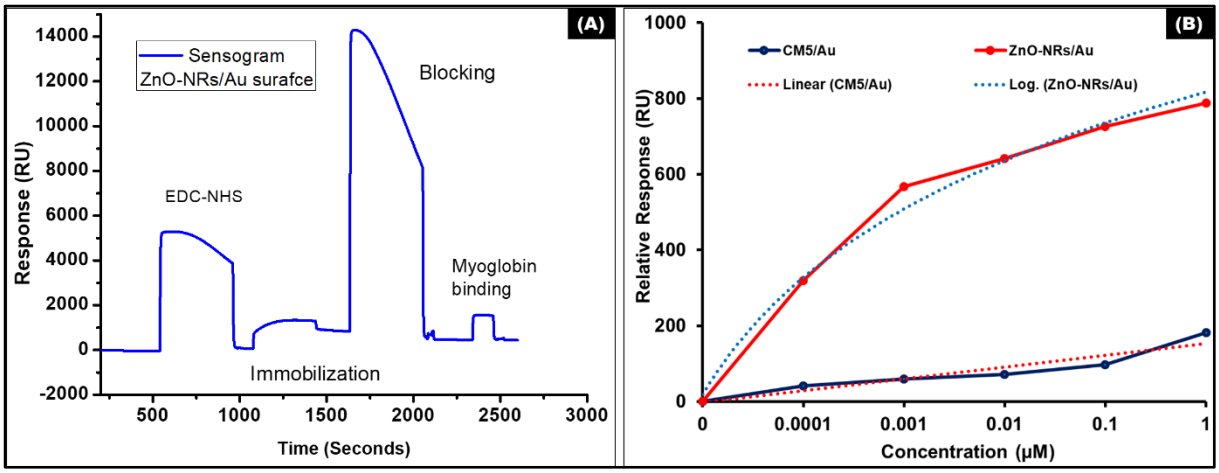

Figure 4-6: A typical SPR-sensogram showing EDC-NHS activation, immobilization, blocking and binding phenomenon of anti-Myoglobin immobilization on ZnO-NRs/Au surface followed by myoglobin binding (A) and myoglobin binding on the two chip at different concentration (B).

The protein capture trend for both the chip was also found to be quite different, for CM5 chip the response increased linearly whereas, for ZnO-NRs/Au chip it followed logarithmic trend which shows that the binding in this case proceeds slowly and after a certain time the chip with nanorods will be saturated for further binding. This could be due to stearic hindrance caused by structural configuration of nanorods on the chip surface. Furthermore, the amount of bound protein was found to be much higher with ZnO-NRs/Au chip and it showed a significantly higher response with each concentration of myoglobin as compared to traditional CM5 chip. This could be interpreted as high binding affinity of the nanorods modified gold chip towards protein. Binding capacity of the surface in terms of maximum response (RU) could be calculated using the expression:

$$R_{\max=} \frac{analyte\ MW}{ligand\ MW} ximmobilized\ amountx\ valency$$

In the above expression putting analyte molecular weight (MW for Myoglobin = 17 KD) and ligand molecular weight (MW for Mab = 150 KD), immobilised amount of anti-myoglobin in terms of response was found to be; 3200 RU for ZnO-NRs/Au and 2000 RU for CM5 (described in previous section), and valency of antibody (binding sites per antibody) = 2. Detailed calculation of maximum binding capacity (R_{max}) is given in Appendix B. The calculated maximum binding capacity from above expression for CM5 chip was R_{max}≈450 RU, whereas for ZnO-NRs/Au chip it was≈750 RU which is almost double (2x) of the value obtained from CM5 chip. This implies that the chip should show the highest value of response after analyte binding equal to value of R_{max}. The results showed that for lowest concentration (0.0001 nM) the response was found to be 320 RU (from plot shown in Figure 4-6B) for ZnO-NRs/Au chip, which is almost half of the R_{max} and remaining half was achieved by rest of the concentrations. At 0.1 nM concentration the chip showed value of response equal to R_{max}. However, it was observed and clear from the plot that the chip was responding for higher concentration even after achieving value of R_{max}. With CM5 chip at lowest concentration the obtained response was 40 RU, which is one eighth of the response from ZnO-NRs/Au chip. Therefore, the nanorods modified chip had shown a very efficient binding even at very low concentration than traditional chip. A SPR response of 1RU approximately corresponds to 1 picogram/mm^2 of protein ligand for standard SPR chip. Thus, the amount of protein captured on ZnO-NRs/Au chip was calculated using least concentrated myoglobin solution. The reason behind taking lowest concentration was to validate our hypothesis of enhanced preconcentration of diluted protein solution with the nanorods modified chip. Hence, the

amount of protein captured on the chip was found to be; 320 RU= 320 picogram/mm^2. Similarly, for CM5 chip it was found to be 40 picogram/mm^2 which is clearly eight times less than the amount captured on the ZnO-NRs/Au chip.

4.3.4. Stability and reproducibility of the chip

In order to check whether the modified chip is stable and the results are reproducible or not after repeated binding-regeneration cycle the ZNO-NRs/Au chip was subjected to 12 cycles and the data was recorded. The study was performed using 12 different blood samples of different blood groups. The reason behind using blood was to investigate the behaviour of the newly fabricated chip towards such a complex fluid. Table 4-1 presents various responses values for 12 different blood samples in RU; initial, final and binding values. Figure 4-7A and 4-7B shows the plots drawn by using the values of responses given in the Table. After each cycle the baseline was found to be stable even after twelve cycles. Each of them was found to be showing almost same response as there is no role of blood groups in binding as blood group antigens are found on RBCs.

Sample	Initial Response	Final Response	Binding
A1	21027.5	23580.7	2553.2
A2	21430.6	23563.7	2133.1
A3	21331.3	23430.7	2099.4
B1	21582.5	24107.5	2525.0
B2	21470.6	23642.6	2172.0
B3	21358.9	24253.8	2894.9
C1	21450.1	24011.0	2560.9
C2	21666.0	23694.1	2028.1
C3	21356.1	24332.6	2976.5
D1	21458.2	24023.8	2565.6
D2	21386.1	23762.7	2376.6
D3	21399.2	23598.6	2199.4

Table 4-1: The data obtained from different plasma samples of four different blood group showing initial, final and binding responses in RU.

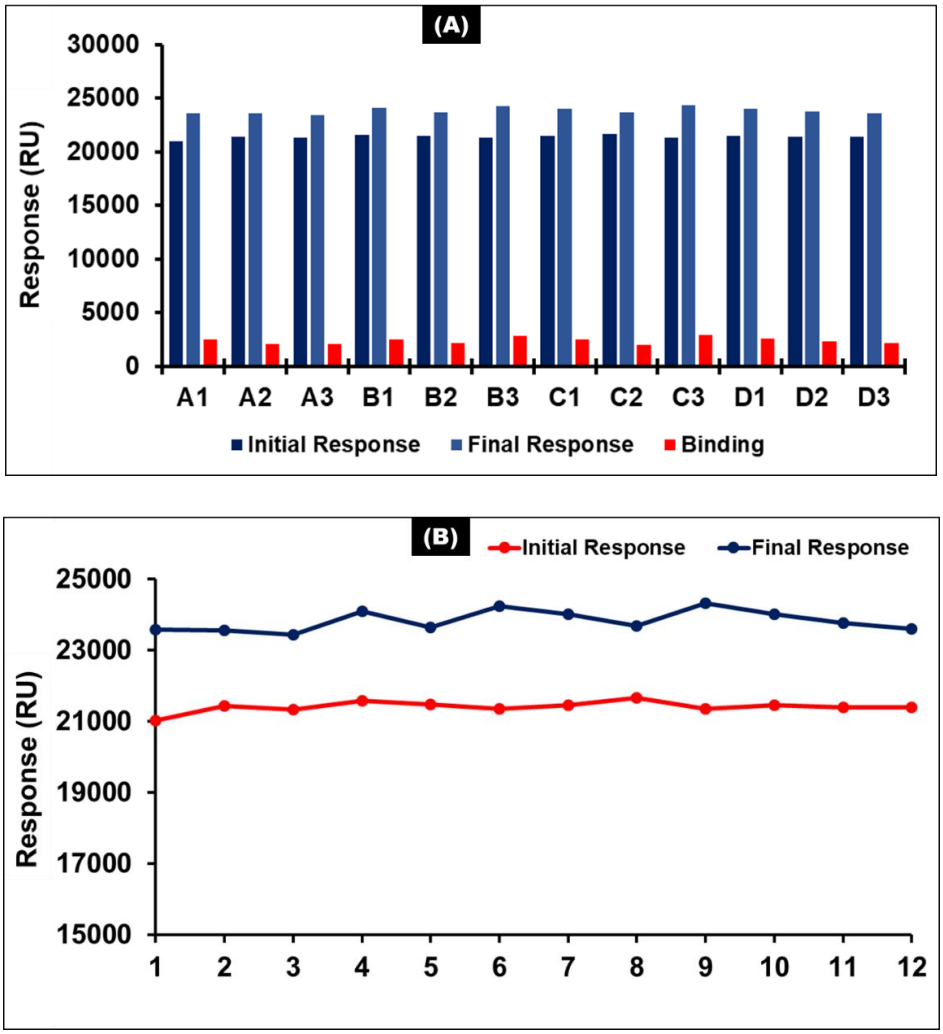

Figure 4-7: Reproducibility and stability of ZnO-NRs/Au chip:(A) plot showing reproducibility of the surface after twelve binding-regeneration cycles using different samples (B) stability plot after each binding cycle.

For any surface which could be potential surface for sensing, one of the most important and critical parameter to be investigate is; specificity. The surface should bear excellent specificity for a particular analyte to be detected. Hence, specificity of the ZnO-NRs/Au was also examined by using two samples (i) pure Myoglobin and (ii) mixture of plasma and Myoglobin. We compared the binding response obtained from cardiac myoglobin protein with myoglobin spiked plasma (Figure 4-8) and found a difference of about 500 RU between values of response with pure Myoglobin and plasma spiked with same concentration i.e. 200ng/mL of Myoglobin. This shows that the ZnO-NRs/Au surface is showing some specificity issues for Myoglobin.

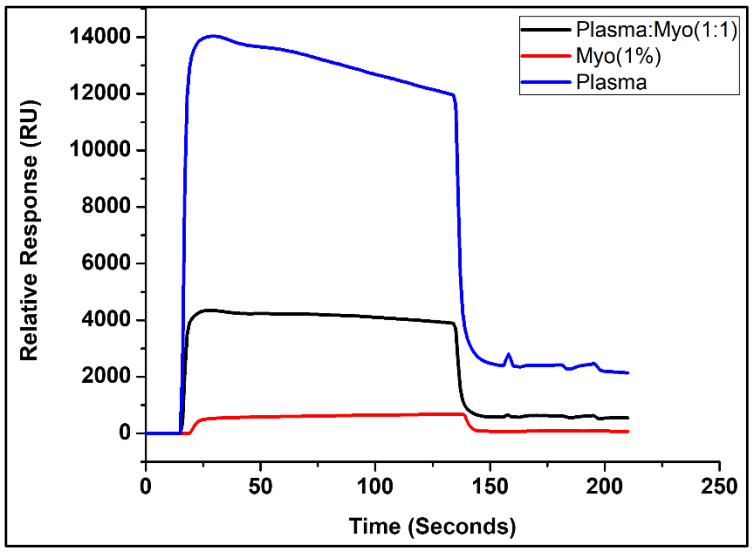

Figure 4-8: Comparison between binding of cardiac myoglobin protein and myoglobin spiked plasma sample.

Many factors could play a role in such processes; (i) presence of many different big and small proteins in plasma with high refractive index, which may lead to higher bulk response and binding response, (ii) the inherent property of ZnO to attract proteins towards it due to its isoelectric point ≈9, (iii) cross-reactivity of anti-Myoglobin antibodies. To confirm and assure the specificity studies are still going on and there is a need to conduct some more investigations with real samples with more different concentrations of Myoglobin as our preliminary results showed a very good response from the modified surface.

4.4. Summary and Conclusion

The ZnO-NRs/Paper has been successfully biofunctionalized with appropriate chemistry and antibodies were immobilized on the surface. Biofunctionalization and immobilization was confirmed with FTIR and other techniques. In the chapter, detailed description of a new SPR chip has been given. The need to use SPR technique as a tool for validation generated as non-conclusive and concrete results obtained by fluorescence method. As our paper substrate was modified with ZnO nanorods thus to mimic the same phenomenon the chip with ZnO nanorods became essential for the investigation. Zinc oxide nanorods modified chip (ZnO-NRs/Au chip) was successfully fabricated and tested with cardiac myoglobin as target antigen. The immobilization efficiency of the modified chip was optimized and found to be quite high as compared with traditional chip. Subsequently, the target protein i.e. cardiac myoglobin was

also found to be more efficiently bound on the chip. Reproducibility of the sensing surface was also analyzed by repeated cycles of experiments and the surface was found quite stable as well as remarkably reproducible. With real blood-plasma samples it was found very much stable even after many binding-regeneration cycles. Beside these advantages, there were certain limitations with the chip. The observed SPR phenomenon was restricted up to 300 nm of the chip surface whereas the height of nanorods was much more than this dimension and the real binding could be even much higher than the observed. Though the chip was found to be quite stable but specificity of the chip was not found to be up to mark. However, it deciphered our objective to validate biofunctionalization and preconcentration with the nanorods modified substrate.

Chapter 5[1]

5. Protein Preconcentration Studies on Nanorods Modified Paper

[1] This chapter draws on author's published work; Tiwari, S. et al. Zinc oxide nanorods functionalized paper for protein preconcentration in biodiagnostics. Sci. Rep. 7, 43905; doi: 10.1038/srep43905 (2017).

5.1. Introduction

Protein preconcentration is one of the major challenges in biosensing with miniaturized devices as enhancement of detection sensitivity for highly diluted analytes is critical and required for its better performance. Biomarker proteins related to various diseases and abnormalities like; cancer, myocardial infraction and many other are often present at very low concentrations. Such low concentrations are very challenging to detect with standard techniques such as ELISA and other immunoassay and non-immunoassay based methods. Since past decade several researchers around the globe has been working on this field and have developed methods for protein preconcentration, viz. chromatographic preconcentration techniques, membrane filter based preconcentration, field-amplified sample stacking, isotachophoresis, solid-phase extraction, temperature gradient focusing, electrofocusing techniques electrokinetic trapping and micellar electrokinetic sweeping [126], [127]. Although these methods are very efficient, yet bear certain limitations such as buffering requirements which can obstruct the downstream of the sample and could makes them difficult to integrate with detection module of the sensing device, electrokinetic based techniques show potential as an effective and efficient way to concentrate proteins, but stability along with linearity is the major concern with these methods [128], [129], whereas, chromatographic preconcentration techniques are based on hydrophobic interactions to capture proteins hence they are more sensitive towards large hydrophobic proteins and may not be as efficient for smaller hydrophilic proteins [130], [131]. This could be also valid for membrane filter based preconcentration as smaller biomolecules may pass through these filters [132], [133]. All these methods use a wide range of materials for protein capture and on the basis of used mechanism of preconcentration several preconcentration devices have been designed.

Adding to existing methods, we have conceptualised a new method for low-cost protein preconcentration, which will be described in detail in this chapter. The key hypothesis behind our protein preconcentrator substrate is that increase in available binding surface area will eventually lead to enhanced biomolecules immobilization and subsequently large amount of target protein capture. In this study we have modified paper with high aspect ratio ZnO nanorods which significantly increased surface area of the paper. A detailed description regarding this has been discussed in chapter 3. Figure 5-1 represents a schematic of protein preconcentration concept with nanorods modified paper. Confocal microscopy, fluorescence spectroscopy and paper-based ELISA are the main analytical techniques used for

preconcentration studies. Elution of captured target protein without losing its activity is also a critical phenomenon and this chapter also deals with the protein elution and its qualitative analysis.

5.2. Materials and Methods

5.2.1. Materials

Whatman filter paper no.1 (GE-healthcare) and WFP modified with zinc oxide nanostructures (nanorods). HIgG and FITC-Ab were purchased from Sigma-Aldrich. Bovine Serum Albumin (BSA), Aminopropyltriethoxysilane (APTES) and NaH_2PO_4 (sodium dihydrogen phosphate) and Na_2HPO_4 (disodium hydrogen phosphate) for phosphate buffer and elution buffer were purchased from Sigma Aldrich. Cardiac myoglobin and anti-myoglobin used in paper-ELISA and control experiments were procured from Abcam. For paper-ELISA we used Human Myoglobin ELISA kit (Abcam, US).

5.2.2. Fluorescence measurements

To observe protein capture directly on modified paper, the use of fluorescent tagged antibodies was investigated. Confocal microscopy was used to measure and locate the fluorescence of the immobilized antibodies on ZnO-NRs/WFP. Confocal laser scanning microscope IX 81 combined with FV-500 Olympus microscope was used for the study. This technique avoids the interference of the intrinsic fluorescence of Whatman filter paper. Six types of paper strips were used for the experiment. Two different sets of both modified and unmodified paper strips were made and 5 µL of 10 µg/mL of FITC-Ab was pipetted on the strips. Low concentrations; 50 ng/mL, 100 ng/mL and 200 ng/mL of FITC-Ab were also immobilized on ZnO-NRs/WFP and control paper. To observe the release of the bound antigen (FITC-antiHIgG), a separate experiment was performed using 200 µL of elution buffer (1 mM PB, pH-8.5) which was continuously passed through the paper strips with bound FITC-antiHIgG as antigen and HIgG as capture antibody. The experiment was carried out for 30 minutes and eluate was collected in six different micro-centrifuge tubes at 5 minutes' interval. The experiment was performed in duplicates; Fluorescence spectroscopy was used for quantitative analysis of FITC-antiHIgG in the eluate. The emission and excitation spectra were recorded using a Jasco 2000 spectrofluorometer. The schematic of the hypothesis is represented in Figure 5-1.

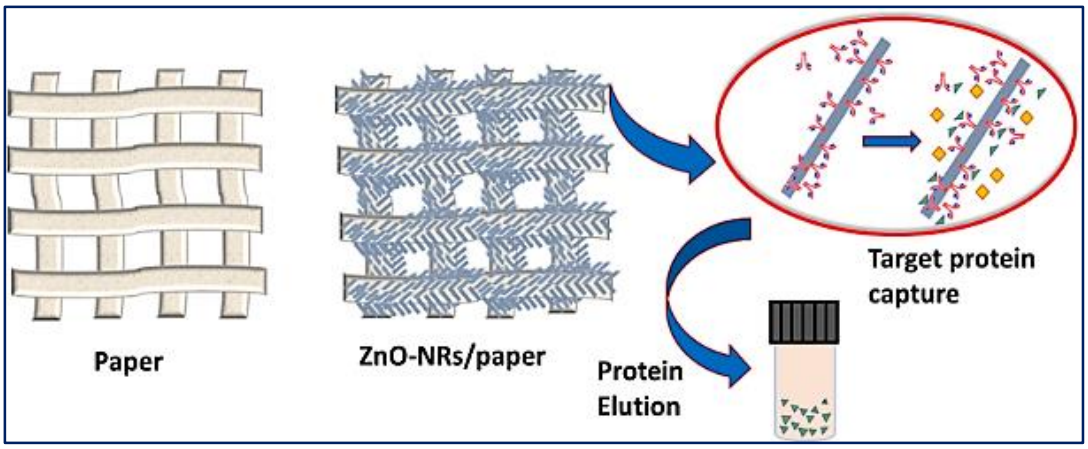

Figure 5-1: Schematic of the concept showing nanorods forest on paper fibers and zoomed portion showing antibodies immobilization on nanorods, target protein capture and elution of the target protein for further sensing.

5.2.3. Paper-based ELISA

To determine the performance of ZnO-NRs/WFP as protein pre-concentrator platform, ELISA was performed on both ZnO nanorods modified and unmodified Whatman filter paper #1. The two types of papers were cut into strips 1 cm x 4 cm and hydrophobic barriers were created using permanent black ink marker (water contact angle 97°). Four identical circular test regions of 5 mm diameter were created on both types of paper strips. For biofunctionalization of paper for paper based ELISA (P-ELISA) was performed with one step silanization protocol. For this strips of Whatman filter paper no.1 with ZnO nanorods were dipped into a 1% anhydrous toluene solution of aminopropyltriethoxysilane (APTES) for 5minutes. These strips were then heat dried at 100°C for 15 minutes.

Sandwich paper based ELISA (P-ELISA) was performed by immobilizing rabbit polyclonal Anti-myoglobin antibodies on the paper strips as primary antibodies. Biofunctionalization in the circularly marked regions of both the ZnO nanorods modified and unmodified papers was essentially the same as described above followed by blocking with 1 mg/mL BSA solution to avoid non-specific adsorption. The paper strips with the immobilized antibody were used for capture of various concentrations of the marker protein *viz*. Human cardiac Myoglobin. The Abcam ELISA kit with Human Cardiac Myoglobin solutions of 0 ng/mL (control), 50 ng/mL, 100 ng/mL, 250 ng/mL and 500 ng/mL were pipetted on the circular regions having immobilized antibodies on both type of strips. The pipetted volume for each concentration on

each circle was 5 µL. Binding of antigen-antibody was allowed for 10 minutes followed by washing with 10 µL, 1 M PBS three times to remove excess protein. Horse Radish Peroxidase (HRP)-conjugate polyclonal anti-myoglobin was used as secondary labeled antibody. 5 µL of secondary antibody solution was pipetted on each region in both strips and the binding was allowed for 1 minute. Then the strips were washed with PBS three times. Now 5 µL of TMB (tetra methyl benzidine) substrate for HRP provided in the kit was placed on each test region and the reaction was allowed to take place for 30 minutes at room temperature. After 30 minutes the colour change from colourless to blue was clearly visible. The strips were then scanned using a desktop scanner and analyzed by image J. All the images obtained after completion of ELISA were analyzed using Image J software version. The blue colour intensity for different myoglobin concentration on the nanorods modified and unmodified paper was observed. Firstly, a scale was set for all the colour intensity measurements and images were calibrated. Using circular area selection tool area on the different sets of images were selected for analysis and blue colour intensity was analyzed. To show pre-concentration, we prepared 1mL cardiac myoglobin solution from 250 ng/mL stock and final concentration of the protein solution was 0.5 ng/mL. The entire volume (1 mL) of protein was pipetted drop by drop on each type of strips treated with immobilized antibodies. Similar ELISA experiment was performed on the strips and the colour change was analyzed by image J.

5.3. Results and Discussion

5.3.1. Confocal microscopy of ZnO-NRs functionalized paper

Confocal microscopy can measure not only surface fluorescence but also in-depth fluorescence which is very crucial to accurate quantification of the adsorbed molecules in the substrate. Whatman filter paper and zinc oxide nanorods both exhibit fluorescence at wavelength used for tagged molecule i.e. at 488 nm which is termed as background fluorescence. This technique minimized the occurrence of background fluorescence up to remarkable extent. Figure 5-2 represents results obtained from the confocal microscopic data. A very much clear enhancement of fluorescence was observed in each sample of the nanorods modified paper as compared to unmodified one. The plot in Figure 5-2A shows that ZnO-NRs/WFP without any fluorescent molecule does lightly fluoresce because of the inherent photoluminescence of ZnO

at 488 nm [134]. To ensure that the observed fluorescence was due to binding of antibodies over the surface and not due to non-specific adsorption, fluorescence images for both ZnO-NRs-treated paper and filter paper strips were captured without and with APTES (indicated as AP in the plot and figures) coupling chemistry. Confocal microscopy analysis revealed that covalent coupling of antibodies is a more effective way of biofunctionalization than physical adsorption; this is valid for both types of paper (ZnO nanorods modified and unmodified). Increased fluorescence intensity with APTES chemistry interpreted as an indication of efficient covalent immobilization of the FITC-Ab for the surface. This was also observed with normal filter paper. Therefore, for further target protein binding on such surfaces efficient blocking of unbound sited becomes a very crucial. Integrated intensity density of fluorescence was calculated using the same area for each image with image J and plotted. The extreme right of Figure 5-2A is the plot of fluorescence intensity from various paper strips.

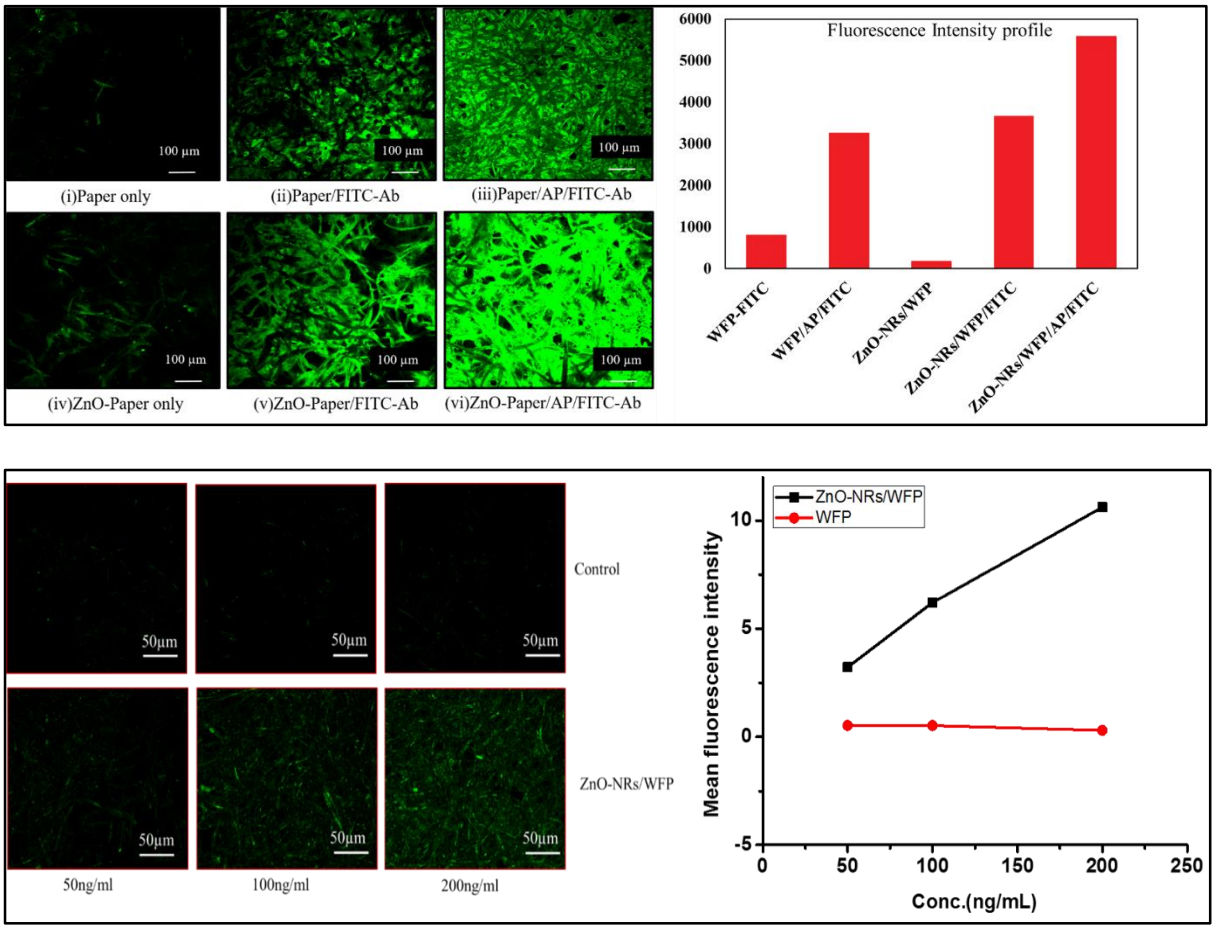

Figure 5-2: (A) Confocal microscopy images and fluorescence intensity profile of WFP, WFP/FITC-Ab, WFP/AP/FITC-Ab as control and ZnO-NRs/WFP, ZnO-NRs-WFP/FITC-Ab, ZnO-NRs-WFP/AP/FITC-Ab; (B) Images with low protein concentration on ZnO-NRs/WFP and WFP (control) and plot showing change in fluorescence intensity with concentration in both types of paper.

Figure 5-2B shows that with ZnO-NRs/WFP there is some level of fluorescence even at the lowest concentration used and that fluorescence increases with the concentration of the protein solution. Whereas, with the control WFP there is no significant fluorescence observed at any of the three protein concentrations studied. The contribution of ZnO-nanorods to increase the surface area available for biomolecules immobilization was very significant thanks to their high surface coverage on paper providing enhancing area by a factor of 6.5. Image analysis combined with basic calculations show that a 100 μm^2 (10 µm x 10 µm) section of paper, once treated, has a 90% surface coverage of hexagonal ZnO rods, consisting of 1000 rods 1 µm high and with a diagonal of 200 nm; this forest of rods provides an additional surface area of 650 μm^2 (Appendix A). Even at low concentration of antibodies, the ZnO-nanorods modified paper shows significant fluorescence in comparison with the unmodified paper, and the fluorescence intensity increases linearly with the increase in concentration of protein. However, fluorescence does not increase linearly with surface area as the 6.5x increase of surface area provided by the ZnO nanorods only provides a 2x factor increase in fluorescence (Appendix C). This might be due to some quenching or fluorescence saturation effect.

5.3.2. Paper-based ELISA for validation

To support the results from confocal microscopy and to show the activity as well as the efficiency of the bound protein on paper, we performed paper based ELISA(P-ELISA) on ZnO-NRs/WFP. A schematic of the P-ELISA methodology performed on the strips is illustrated in Figure 5-3.

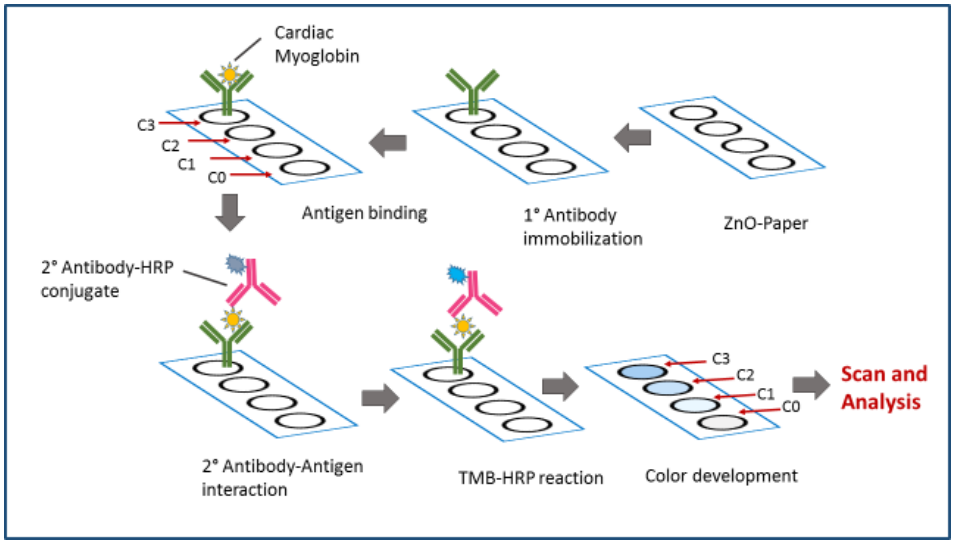

Figure 5-3: Schematic of Paper-ELISA representing the steps of the detection process. In this sandwich ELISA, identical circular regions with hydrophobic boundaries were marked on ZnO-NRs/WFP; the

primary antibodies were immobilized on ZnO paper for 10 minutes.; four different concentrations of antigen were allowed to bind for 10 minutes.; HRP-conjugated secondary antibodies were allowed to bind for 1 minute. followed by a quick wash with PBS and then TMB was added to react with the enzyme HRP for 30 minutes and produce colour. The strips were scanned and the colour intensity and spectra were analyzed using image J (version 1.45).

Upon completion of the ELISA, the colour intensity of each test region was determined by images analysis. Concentration versus relative intensity plots obtained for three separate sets of sandwich paper-ELISA are given in Figure 5-4A. ZnO-NRs/WFP can capture very low concentration of cardiac myoglobin (50 nM) very efficiently compared to paper (Figure 5-4B) due to the high available surface area contributed by ZnO-nanorods. The plot obtained from P-ELISA provided a rough quantitative estimation of bound target protein in terms of colour intensity (Figure 5-4B). An enhanced colour intensity was observed when the protein solution was flown through the ZnO-NRs/WFP as compare to the unmodified paper.

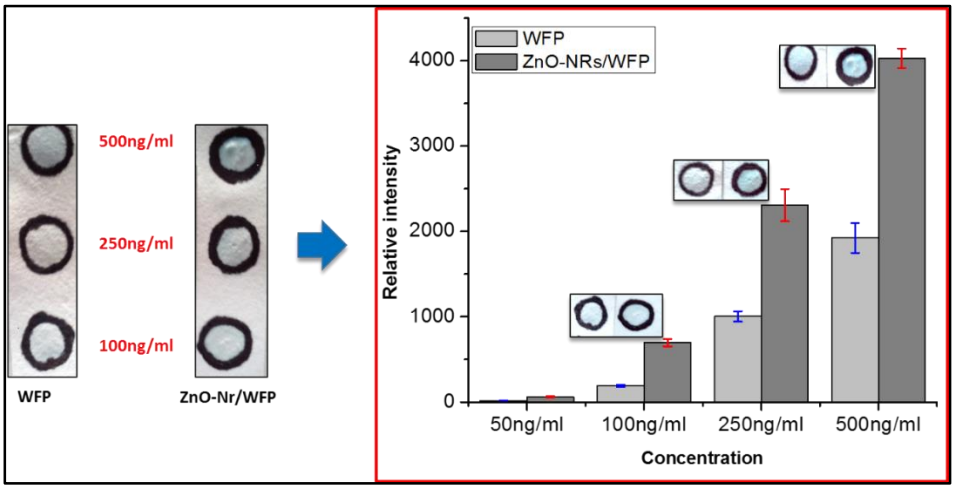

(A) **(B)**

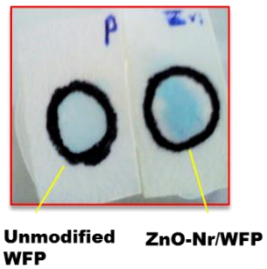

Figure 5-4: P-ELISA at different protein(myoglobin) concentration (A), plot showing colour intensity comparison for two types of paper using image J (B) and comparison with much diluted protein solution on unmodified WFP and ZnO-NRs/WFP(C).

To evaluate if the protein capture efficiency of ZnO-NRs/WFP is retained even with large volumes, we passed 1 mL of protein solution (0.5 ng/mL) through the paper and performed the ELISA assay. Figure 5-4C shows the difference in colour intensities of unmodified WFP and ZnO-NRs/WFP. The enhancement of protein capture by ZnO-nanorods modified paper is demonstrated by a more intense blue colour on ZnO-NRs/WFP. The ZnO-NRs/WFP was further tested as a protein pre-concentrator platform by elution of bound protein.

5.3.3. Measuring the eluted protein from ZnO-NRs functionalized paper

For a preconcentrator, beside concentrating the target protein, the ability to release the captured protein is equally important so that it can be pass through the sensing device.

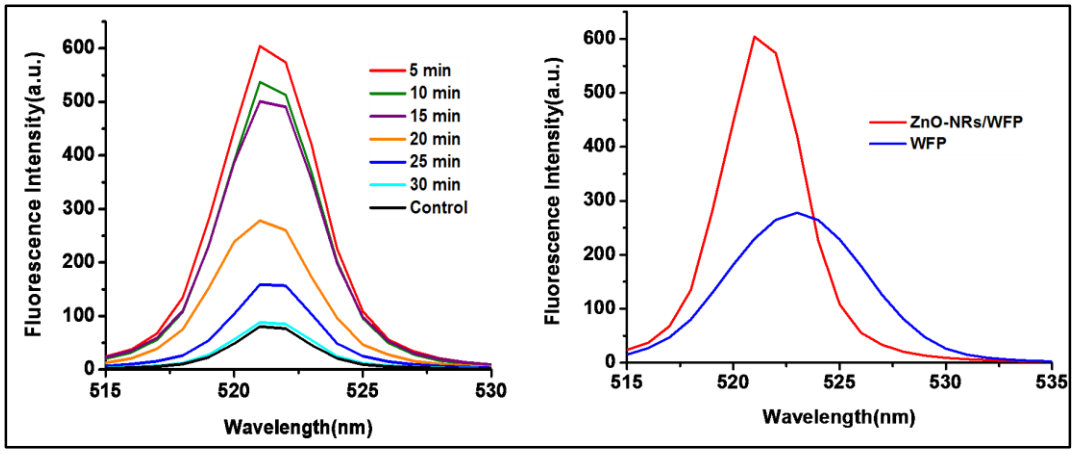

(A) **(B)**

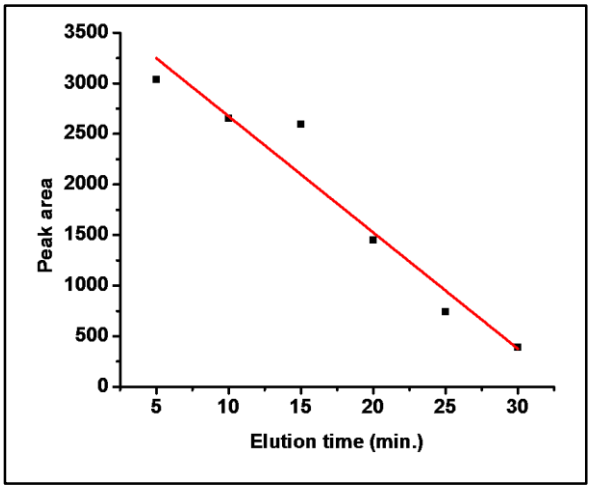

(C)

Figure 5-5: (A) Emission spectra for FITC-Ab after elution at different time (B) Comparison of fluorescence intensity of FITC-Ab with and without ZnO-nanorods on paper (C) Plot between area under the individual spectrum with respect to elution time.

A semi-quantitative estimation of eluted protein was performed by measuring fluorescence spectroscopy intensity. The absorbance of eluates with FITC tagged antibodies was recorded at 488nm and the corresponding emission at 520 nm. Fluorescence spectra of the protein eluates collected from ZnO-NRs/WFP at different time intervals are presented in Figure 5-5A. Standard deviation (SD) for Figure 5-5A for all the plots at different elution time was calculated for the wavelength range; (500 nm - 530 nm). The calculated value of mean and SD for different plots in Figure 5-5A is listed in Table 5-1:

Elution time	Mean Intensity (AU)	Standard Deviation
5 minutes	100.5	175.9
10 minutes	87.6	155.5
15 minutes	86.1	148.5
20 minutes	48.1	82.5
25 minutes	25.1	44.5
30 minutes	13.2	24.2

Table 5-1: Representation of mean intensity and standard deviation (SD) calculated for each elution time.

For plot for comparison of fluorescence intensity of eluted tagged protein (after elution for 30 minutes) from WFP and ZnO-NRs/WFP shown in Figure 5-5B, the value of calculated mean intensity and standard deviation is given in Table 5-2.

Elution Substrate (after 30 min)	Mean Intensity (AU)	Standard Deviation
WFP	72	96.3
ZnO-NRs/WFP	100.5	175.9

Table 5-2: Mean intensity and standard deviation calculated for eluate from both modified and unmodified Whatman filter paper after 30 min.

Most of the bound protein eluted from the substrate within 20 minutes. Emission spectra for the protein eluates obtained from ZnO nanorods paper and paper control are compared in Figure 5-5B. Protein elution was based on breaking antigen-antibody interaction using high pH=8.5 buffer. The pH shock created the breakage of protein-antibody interaction completely within 30 minutes, whereas maximum amount of bound protein was eluted in 15 minutes with passing elution buffer.

The fluorescence intensity of tagged protein was higher on ZnO-NRs/WFP which corroborates the results from P-ELISA and confocal microscopy. More than two-fold increase in emission intensity of the protein eluate in the case of ZnO-NRs/WFP compared to the control (unmodified WFP) sample indicates efficient protein pre-concentration by the ZnO nanorods. For further confirmation relative fluorescence units (RFU) were calculated using ELISA reader.

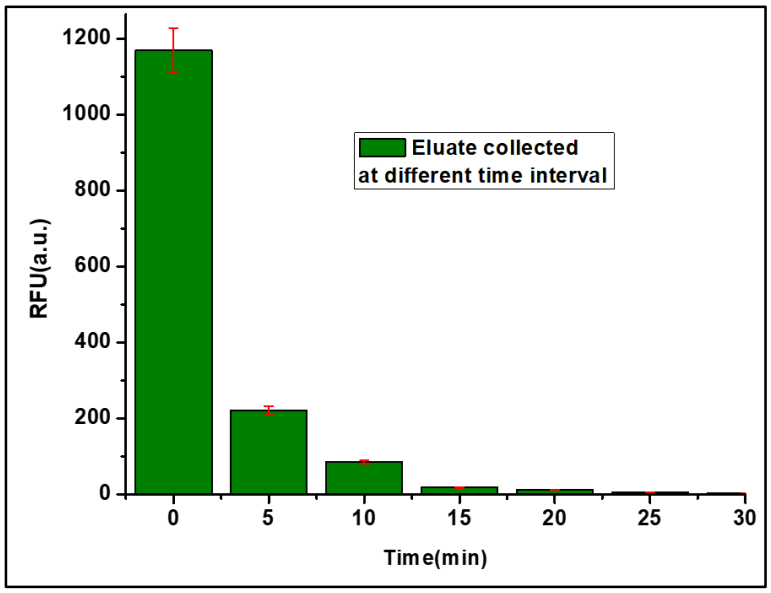

Figure 5-6: Plot showing mean RFUs after different time obtained by ELISA.

100 µL of eluate from each tube and positive (working concentration of FITC-antiHIgG) and negative control (working concentration of elution buffer) was put into separate wells of ELISA plate. Figure 5-6 shows the plot showing RFU present in eluate after 30 minutes of elution at different time interval. The readings were collected in three different set of eluates at same time interval. It is clear that there is decrease in RFU values in eluate in different tubes as the time increases. Maximum RFUs are present in eluate after 5 minutes and then 10 minutes in all the three sets this shows that most of the HIgG+FITC-antiHIgG complexes broke after 10 minutes of passing elution buffer. Post-elution, the fluorescence intensity of the tagged antibodies was higher with ZnO-NRs/WFP; this is likely due to the higher amount of captured protein with modified paper and subsequently the higher amount of eluted protein than with the untreated paper in same eluted volume. The desorption rate of proteins from biospecific binding is probably higher than that from protein physically adsorbed on paper through un-specific interactions, typically less sensitive to pH. This complements the results obtained from P-ELISA and confocal microscopy.

5.4. Summary and Conclusion

Novel ZnO nanorods functionalized paper was investigated as a preconcentrator unit for application in paper biotest and biodiagnostics devices. The efficiency of the ZnO nanorods treated paper as protein concentrator was successfully tested for myoglobin, a biomarker for heart disease. In a first step, a preconcentrator is required to capture high density of the target protein for the concentrating step; in the second, the paper unit must be able to elute the captured protein so that it can be pass through the sensing device for detection. ZnO-NRs/WFP chemisorbed with an antibody proved very efficient for both steps with myoglobin full release upon change of pH (8.5). Fluorescence spectroscopic study using fluorescent tagged molecules showed the bound protein to be released from ZnO-NRs/WFP without loose in activity. P-ELISA provides quantitative estimation of bound target protein i.e. cardiac myoglobin in terms of colour intensity. Using ZnO nanorods paper as preconcentrator, myoglobin could be detected at concentration as low as 50 ng/mL. ELISA results revealed a threefold enhancement in protein capture with ZnO-NR paper compared to the control paper. This ZnO-NRs/WFP platform can easily be integrated with µ-PAD or other biosensors based on antigen-antibody interaction. Future scope of the work involves the design and integration of the preconcentrator with sensing device and experimentation with mixture of different proteins and other biomarkers in biofluid samples including blood, plasma and serum.

Chapter 6[2]

6. Blood-Plasma Separation with ZnO-NRs/Paper

[2] This chapter draws on author's publication: S. Tiwari, et al., One dimensional zinc oxide nanostructures assisted paper-based blood-plasma separation, Vacuum (2017), 146, pp. 586-591.

6.1. Introduction

Blood is a complex colloidal system containing large numbers of small and large biological components like proteins, carbohydrates and minerals along with blood cells. In many diagnostic techniques, therefore, blood is widely used as a high potential sample. However, it is highly desirable to reduce the avoidable complexity of blood sampling by separating blood cells and to use plasma or serum sampling to achieve better results. The conventional blood-plasma separation involves centrifugation, which generally enables very efficient and fast results. But in case of point-of-care miniature devices it is necessary to have an integrated miniature blood-plasma separation system to reduce the number of sample preparation steps, which is also helpful in increasing its speed and ensuring accuracy [135].

Currently, a trend in engineering and product development can be observed which seeks to investigate and integrate frugal solutions for device design [136]. Frugal innovations often seek to increase affordability of high quality solutions by using modern technologies, reducing avoidable complexity and thus increasing resource-efficiency [137]. Substantially-reduced total cost of ownership and usage are being seen as increasingly necessary to ensure affordable healthcare for a growing world population. In recent past, several groups have reported remarkable research on developing various cost-effective miniaturized microfluidics-based continuous real time, on chip blood-plasma separation [138] and whole blood filtration devices including PDMS hybrid microsystem [139], in-situ fabricated porous filters [140], on-chip bead packed separator with microchannel [141]. In these systems, blood cells are separated from plasma via some driving forces like electroosmotic separation [142], forces generated by acoustic standing waves [143] and hydrophoretic filtration [144].

In addition, paper-based analytical devices (µPADs) are also gaining popularity for being simple, cost-effective, biocompatible and environment friendly. Several groups have utilized these advantages of paper to develop paper-based blood-plasma separator by creating 2-dimensional paper-based network [145], microfluidic channels on paper for integrated blood-plasma separation [146] and salt functionalization of paper to capture red blood cells [147]. Zinc oxide nanostructures; nanorods, nanowires, nanoporous ZnO film [148], nanocages [149], nanoplant-like structures[150], hybrid oxide nanopowders [151] have been potentially used in fabrication of sensors [125], [152]–[154] and other wide range of applications [155], [156], protein preconcentration [157] and cancer detection [158], [159] due their distinctive physical and chemical properties. There are many reports on modification of paper with nanoparticles

for sensor applications [8], [160], [161] but there are very few reports on paper-based blood-plasma separation using nanostructures.

Low cost paper based platforms are gaining very much appreciation in modern diagnostics and sensing. In most of the diagnostic system where we use blood as sample to be analysed there is need of separation of plasma from blood to get better results. Most of the blood plasma separation is done by various membrane based filter. In this study we propose a new method to capture red blood cells on paper. The papers used for this study were Whatman filter paper no.1, 2, 5 and glass fibre discs. All the four types of paper were subjected to modification by growing Zinc Oxide nanorods. The nanorods were grown by hydrothermal route by dipping the all strips in the solution of precursor after seed layer deposition. Confirmation of zinc oxide nanorods growth and their morphological characterization was done by scanning electron microscopy, X-ray diffraction and X-ray photon spectroscopy. The blood plasma separation experiments were done by cutting the papers in strips of identical dimension i.e. 5 mmx20 mm. 3 µL of blood was mixed with equal volume of antibody solution and pipetted on each strip. The antibody solution is mixed with dye to track the path of antibody eventually the separated plasma. After drying all the strips were scanned and the difference in the distance travelled by coloured solution of antibodies was measured. From the images and calculations, it was clear that all the four types of paper strips having the nanorods over them have shown more distance travelled and better separation than their control.

6.2. Materials and Methods

6.2.1. Materials

The different types of qualitative grade filter papers, viz. Glass fiber discs (GF/C. Pore size=1.2 µm), Whatman filter paper no. 1 (W1. Pore size=11 µm) no. 2 (W2. Pore size=8 µm) and no. 5 (W5. Pore size=2.4 µm), glass Petri dishes were procured from Sigma-Aldrich (Australia). Micro-centrifuge tubes of volume 1ml were purchased from Eppendorf GmbH (Germany). Precursors for Zinc Oxide nanorods (ZnO-NRs) synthesis, Zinc acetate dihydrate (98%), Zinc nitrate hexahydrate (98%) and hexamethylenetetramine (99%) were purchased from Sigma-Aldrich. These were analytical grade and used without further purification. For the synthesis process customized mini-autoclave was used by putting it inside oven. Blood samples with EDTA were provided by Australian Red Cross Blood Service (ARCB) and were kept at

appropriate storage conditions (4°C). Colored Antibodies solution (Anti-A with blue dye) was procured from ALBA biosciences, Edinburgh (UK) and used without any further purification. Phosphate buffer saline (PBS) was used for all the washing steps and was purchased in tablet form from Sigma-Aldrich and solution was prepared in MilliQ water and NaCl.

6.2.2. Preparation of ZnO-NRs/Paper hybrid surface

All four types of paper, viz. Whatman filter paper no. 1(W1), no. 2(W2), no. 5(W5), and Glass fiber discs, were subjected to conventional hydrothermal process for modifying them with ZnO nanorods by solution phase growth all over the paper fibers. All the four types of paper were cut into strips of dimensions 2 cm x 6 cm and subjected to hydrothermal synthesis of nanorods following the process discussed in chapter 3 in detail. The reaction was allowed to occur for 5 hours at 90°C by keeping the mini-vessel inside the oven. The growth of hexagonal nanorods took place along c-axis which was further confirmed by XRD analysis.

6.2.3. Morphological characterizations of ZnO-NRs/Paper

Variation in morphology and the growth pattern of nanorods with the four types of paper were investigated by scanning electron microscopy. For the morphological studies we excluded Glass Fibre paper (GF) as it was difficult to fix it on the stub for the examination. Therefore, only three types of paper W1, W2 and W5 were selected for the study. To study the crystallinity of the nanorods hybrid paper X-ray diffraction analysis was done with RigakuSmartLab Instrument (Japan) using $Cu_{K\alpha 1}$ at 40 kV/30 mA, over a range of 10°- 60° as discussed in chapter 3. For quantitative determination of Zinc and Oxygen in the form of percentage concentration within few microns of surface, X-ray photon spectroscopy was done using model PHI 5000 Versa Probe-II (USA). The percentage concentration of both elements could be directly co-related with the formation of nanostructures. Effect of nanorods on paper morphology has been investigated by observing scanning electron micrographs obtained by Magellan 400 FEGSEM (FEI) at Monash University, Melbourne.

6.2.4. Blood-plasma separation on the nanorods hybrid paper

The role of Zinc oxide nanorods on blood-plasma separation and behaviour of blood flow was investigated. Four different types of paper were selected as they provide wide range of pore size from fine, small, medium and large in form of GF/C, W5, W2, and W1, respectively. 5 mm x 20 mm strips were cut from all four types of ZnO-NRs/Paper along with control (strips

without ZnO-nanorods) were placed on cleaned glass petri dishes separately. Blood samples from B-group were used for all the studies, 3 µL of undiluted blood was taken in microcentrifuge tube. To track the plasma and observe the difference clearly 3 µL of blue coloured solution of Anti-A antibodies was mixed into the blood making final volume 6 µL. 3 µL of the blood+Anti-A mixture was taken in the pipette and the entire volume gently dropped at the one end of ZnO-NRs/W1 strip and control (W1) as well. Identical process was repeated with rest of the strips (W2, W5, GF/C) along their respective controls. Blood samples on the strips were allowed to dry for 10 minutes. An identical process was applied on another set of all the four type of strips with coloured antibodies solution only. Images of all the strips were captured for further analysis and the strips were stored at 4°C. Obtained results are presented and discussed in the following section.

6.3. Results and Discussion

6.3.1. Effect of ZnO nanorods on pore size of the paper

Figure 6-1 shows scanning electron micrographs of W2, at different magnification and imaging areas of interest. The average measured dimensions of nanorods are 1 µm length and 200 nm diameter. These rods grow all over the paper fibers in all direction, impacting the pore size of the paper significantly. From the micrographs it was observed that nanorods affected pores of papers either by clogging the pore (Figure 6-1A) or by reducing the pore size by making a layer of rods around them (Figure 6-1B).

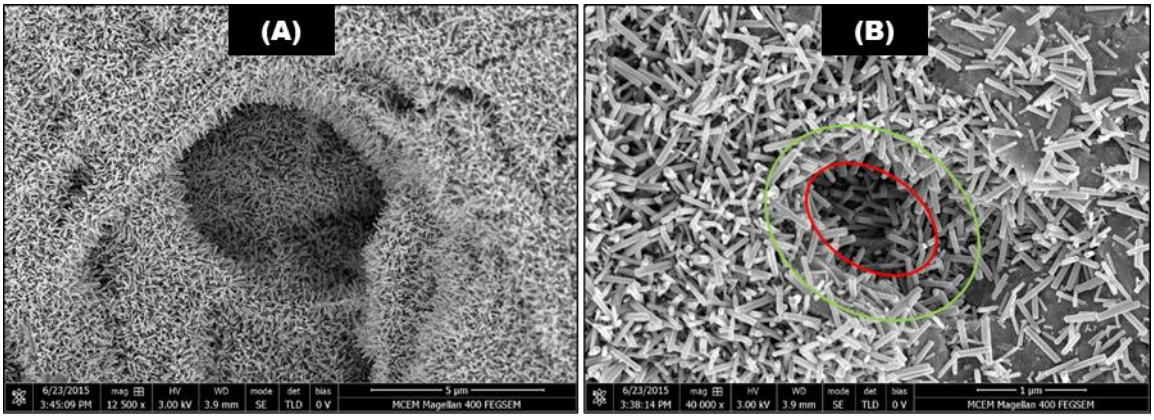

Figure 6-1: SEM micrographs showing two possible ways to affect pore size: (A) clogging of the pores, (B) reduction in pore size.

In both ways it can affect flow of the fluid (in our study, blood) through the paper. Based on these findings we further investigated the possibility of thus-modified papers as a potential blood-plasma separation system.

6.3.2. Effect of ZnO nanorods on blood-plasma separation

In order to investigate the opportunities of using ZnO-NRs/Paper as a potential blood-plasma separation module all four types of ZO-NRs hybrid paper (GF/C, W1, W2 and W5) were treated with blood samples. The scanned images obtained from the study are presented in Figure 6-3. Distance travelled by blood on paper strips with ZnO-NRs was found slightly less than the distance travelled on paper without the nanorods. Also, there was less spreading observed in case of the modified strips. Washburn's equation for capillary rise for porous medium could provide a good explanation of the phenomenon [162].

$$h^2 = \frac{r\gamma cos\theta}{2\eta} t$$

In the above equation; h is penetration height by the liquid at time t, r is capillary radius, θ is contact angle at solid liquid interface, γ is interfacial tension and η is viscosity of the liquid. In case of porous medium like paper capillary radius r is represented by average pore size of the porous medium. As the pore size shrinks, the penetration height of the liquid in the medium also decreases since they both share a direct proportionality as per the above equation.

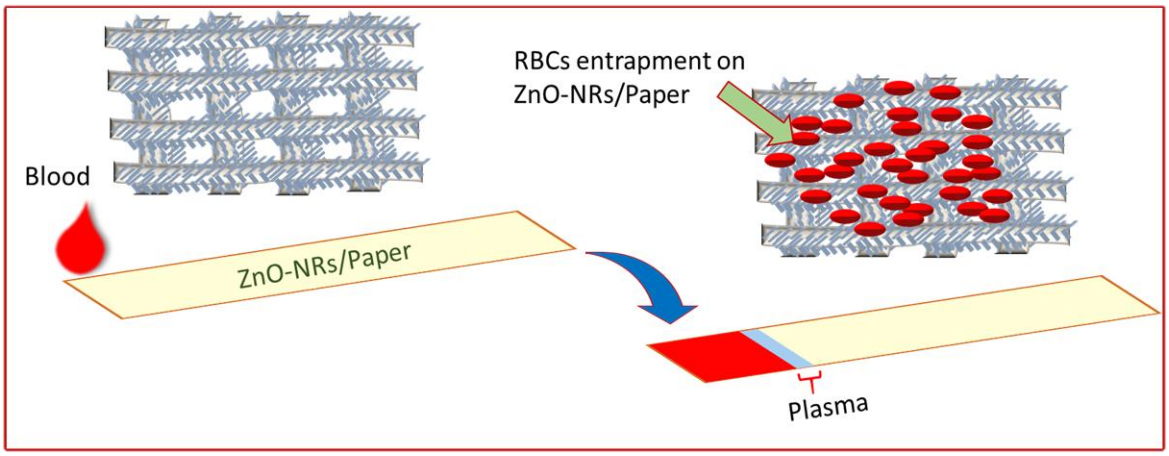

Figure 6-2: Schematic of ZnO-NRs/Paper based blood-plasma separation showing Zinc Oxide nanorods grown all over paper fibers; trapped RBCs in the nanorods mesh and separated plasma from blood on the paper strip.

In the ZnO-NRs/WFP, there are two types of porous media involved. One is the porous cellulose that is within the paper matrix and the second one is the ZnO nanorods which creates a porous medium with finite porosity and effective permeability and it could have significant role in flow of fluid(blood) through it. This can be explained by considering a steady, single-phase Stokesian fluid flow in random dual porous media with explicit account of a spatially disordered microstructure, in our study these are; ZnO nanorods. In phenomenological, deterministic continuum mechanics, such a flow is described by Darcy's law (1856). With the slow flow in a porous medium, also considered as incompressible and viscous, Darcy's law is governed by the equations:

$$\boldsymbol{U} = -\frac{\boldsymbol{K}}{\boldsymbol{\mu}}.\boldsymbol{\nabla p}$$

where U is the Darcy (volume averaged) velocity, ∇p is the applied pressure gradient driving the flow, μ is the fluid viscosity and K is the permeability, that depends on the microstructure of the porous medium. K is usually considered a material property, since it depends on the porous microstructure and thus it is also a scale dependent property [163], [164]. The another widely-used and well-founded semi-empirical expression that relates the permeability of a structure and its conductivity is the Katz-Thompson equation:

$$\boldsymbol{K} = \boldsymbol{c}\boldsymbol{l}_{\boldsymbol{c}}^{\boldsymbol{2}}\frac{\boldsymbol{\sigma}_{\boldsymbol{e}}}{\boldsymbol{\sigma}_{\boldsymbol{0}}}$$

Here, c is a constant related to the local pore geometry and lc is the size of the critical pore. The ratio of the effective conductivity σ_e of the porous medium (conductivity of porous media saturated with some fluid of conductivity σ_0) and its bulk conductivity σ_0 is called formation factor. The formation factor is a measure of the connectivity of the pore space. The better connected the pores are, the higher the formation factor is. Therefore, in case of paper with ZnO nanorods the effective conductivity increases as there is more available space for liquid to saturate the pores hence, there is significant increase in permeability K [165].

ZnO-nanorods form a dense mesh all over paper fibres. Red blood cells (RBCs) were trapped in the mesh and, as a result, the blood could not rise on the modified paper as high as on their control strips. A schematic of concept is shown in Figure 6-2. This hypothesis was also supported by the SEM micrographs (Figure 6-1) that show the clogging and reduction of pore size in ZnO-NRs/Paper. Figure 6-3 shows all four types of paper strips with and without modification with ZnO-nanorods. Strips having nanorods show clear separation of blue colored antibodies solution, whereas no blue color was observed on unmodified strips. This shows that

paper with the nanorods not only captured red blood cells effectively but also facilitated the separation of blood-plasma and other small proteins in the blood.

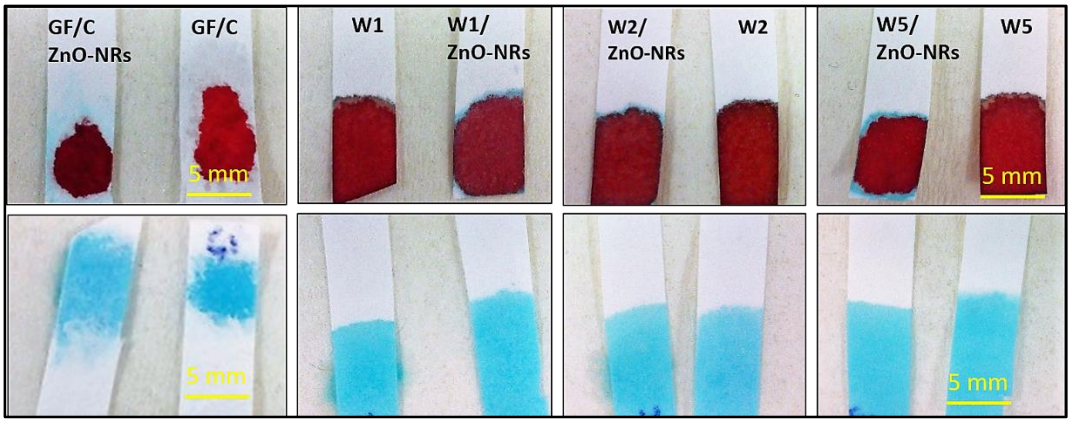

Figure 6-3: Different paper strips with their control showing blood flow and plasma separation (top panel) and blue colored Anti-A antibodies solution flow through the modified and unmodified paper strips (bottom panel).

Images obtained from the strips only with colored antibodies show that there is a remarkable difference in penetration length by the antibodies solution on modified and unmodified papers. But with the antibodies solution the length is more in case of the nanorods modified paper, in contrast with blood samples. Zinc oxide nanostructures possess very high hydrophilicity which could be the underlying phenomenon behind more penetration length with antibodies solution. Whereas in case of blood samples the viscosity and the size of RBCs (8 µm diameter and 2 µm thickness) played important role in their entrapment in the nanorods mesh leading to confine the spreading and penetration length. As regards the modified paper both W5 and W2 show similar patterns, but the effect was more evident with W5 where pore size is less (Figure 6-4 A, B). With unmodified W5 paper a slightly reddish layer of plasma was also observed, which could be due to the smaller pore size of W5 (2.4 µm). The layer was clear blue with the modified W5 paper which was earlier masked with viscous plasma and blood cells as shown in Figure 6-4C, D. The cell-free layer theory could possibly provide a better explanation for this as it describes blood flow behaviour and axial migration of blood cells in capillary tube leading clear cell-free zone near to wall of the capillaries [166]. The cell-free layer depends on several biophysical parameters such as viscosity of blood, flow rate, cell concentration, deformability, vessel diameter and cell aggregation [167]. These parameters play an important role in determining the behaviour of blood flow as well as in blood-plasma separation. The thickness of the cell-free layer increases with a corresponding decrease in the pore size; and

the pore size evidently decreased with the nanorods modified paper (Figure 1B). However, no cell-free layer could be observed with unmodified paper even with the least pore size (W5=2.4 µm).

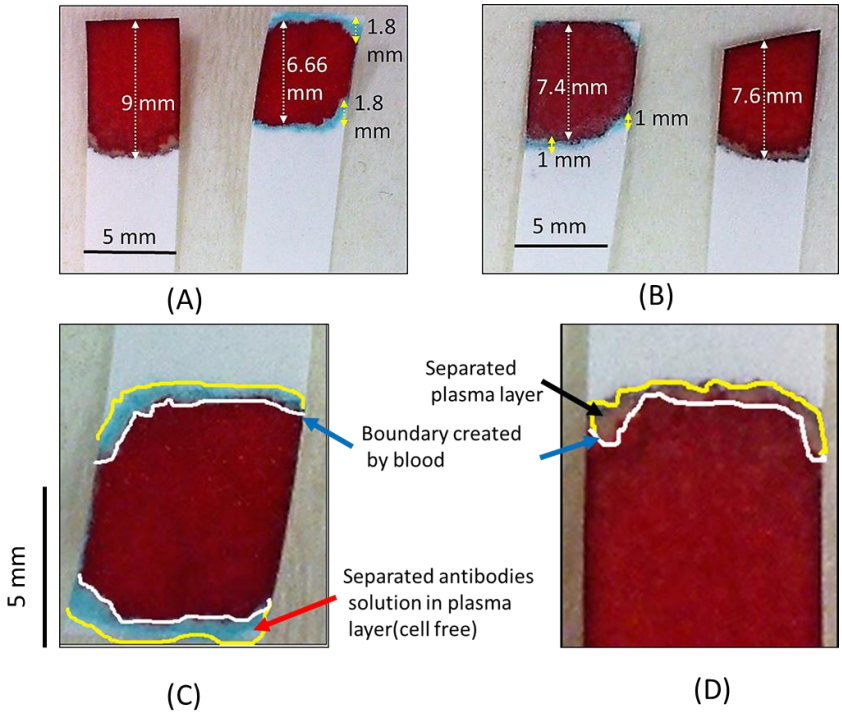

Figure 6-4: Comparison of blood-plasma separation with W5 (A); ZnO-NRs/W5 (right), unmodified (left) and W2 (B); ZnO-NRs/W2 (left), unmodified (right) showing distance travelled by blood and separated antibodies solution enlarged image of modified and unmodified W5 paper showing clear boundaries formation by blood cells, plasma and colored antibodies solution (cell-free layer).

Furthermore, elasticity of blood cells contributes to deformability due to which they can easily adapt their size and manage to pass through the passage of much lower diameters than the size of RBCs [168]. This hinders the separation even with filters with lesser pore size than the blood cells. Nanorods with length of only few microns and high surface coverage on the paper reduce the pore size significantly and, therefore, largely contribute towards formation of cell aggregates at the centre of the strips (Figure 6-4A, B, C). The aggregate formation on the strips is represented in the results as the distance travelled by the blood with and without ZnO-NRs. In all paper strips the travelled distance is significantly more in case of unmodified paper which supports the concept of cell aggregation with the nanorods.

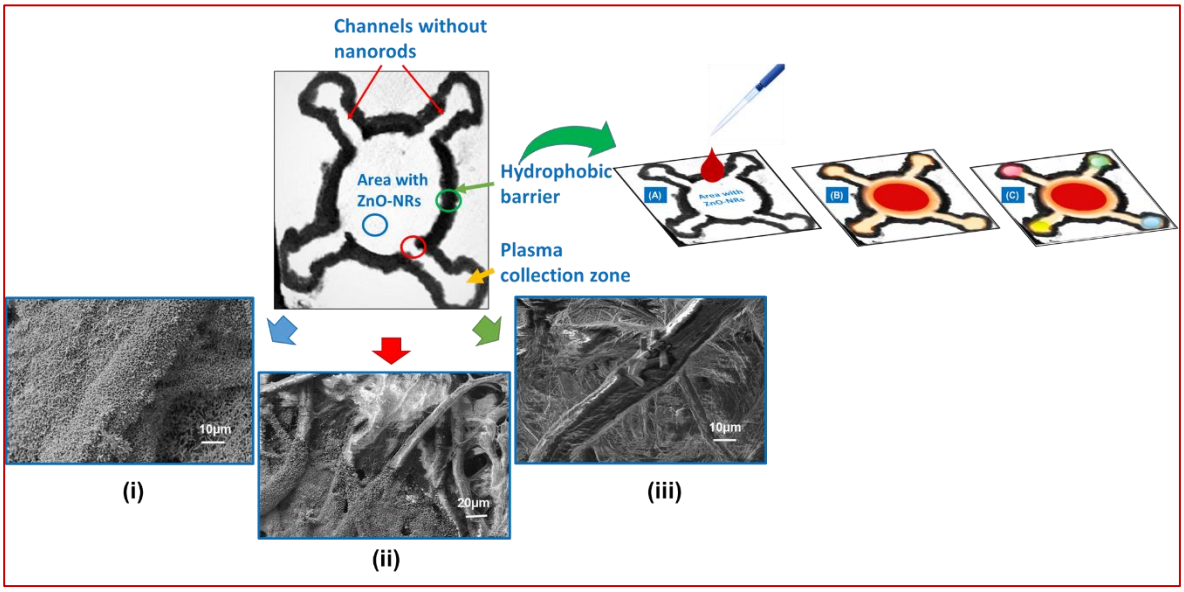

Figure 6-5: Left: ZnO-NRs/Paper based blood plasma separation substrate with selectively grown nanorods region by creating hydrophobic barriers with SEM images of the different regions showing; (i) dense nanorods forest region at the circular hydrophilic part (ii) at the boundary of channels and circular, nanorods zone (iii) on the hydrophobic barrier and on right: layout of red blood cells and plasma separation device with the concept of multiple analyte detection on single device.

On the basis of above findings, we came up with the nanorods modified paper based blood-plasma separation device. Figure 6-5 is a schematic of one of the possible µPAD device design for ZnO-NRs/Paper based blood-plasma separation. The device could serve as substrate for on-paper blood-plasma separation and multiple analyte sensing on a single device.

6.4. Study of antibodies and protein behaviour on paper

Whatman filter paper being highly absorptive could not be a suitable paper substrate to study the behaviour antibodies and proteins towards paper. Therefore, it is required to choose a paper with less absorptivity and porosity so that decreased availability of analyte could be minimized due to absorption. For this paper towel could provide better opportunities to investigate the protein behaviour on paper. The advantage of paper towel is that blood flows with ease on the paper as it is highly porous and less absorptive. The major objectives of the investigation were; (i) to test how far the antibodies run down the paper towelling, (ii) to test if protein from an added sample would elute independently from the agglutinated cells, (iii) to test that the agglutination of cells impede the movement of the antibody down the paper and (iv) to see if

all blood groups cells could be retained by mixing different antibodies. For the study, paper towel, blood from different groups; A (+-), B (+-), O (+-), antibodies(IgM) against different blood group antigens; Anti-A, Anti-B, Anti-D, crude Anti-A solution FP (finished product), anti-A with blue dye, anti-D FFMU (for further manufacturing use), PBS and image J software for analysis were used.

For fulfillment of our first objective i.e. to test how far the antibodies run down the paper towel, 10 µL of Antisera was dispensed on the end of a 5mm wide paper towel strip and were allowed to elute up the paper. 3 µL group A cells were dispensed in different points along the antisera pathway followed by washing with PBS (3x 100 µL) drop by drop over blotting paper. Similarly, to test if protein from an added sample would elute independently from the agglutinated cells, sample to be tested was made up using a mixture of 50% concentrated A negative cells and 50% anti-D FFMU by volume. Afterwards, O positive blood were pipetted at three different positions. O negative blood was used as control. For the third objective that is to test that the agglutination of cells impedes the movement of the antibody down the paper, anti-A was dispensed at one end and A cell were added. 1.5 µL of anti-D FFMU was dispensed at one end of paper and O positive cells were added at different position. Lastly, to see if all blood groups cells could be retained by mixing different antibodies, 25 µL of anti-A, B and D together with 40 µL of anti-H and c was mixed together to see if all blood groups could be retained by the second method. After each experiments the used strips were allowed to dry at room temperature and fixed on a thick paper sheet for imaging. The strips were scanned with desktop scanner and obtained images were analyzed with image J software.

6.4.1. Movement of antibodies on paper

It is clearly observed in the images and intensities plot shown in Figure 6-6A that the A cells were retained by the anti-A in all sections along the path of the antisera which implies that the antibodies travelled all the way with the solution with retaining their activity and much adsorption on paper. Paper does not hold much antibodies on its surface during the flow, as it can be seen in intensity profile in Figure 6-6A (right) that there is not much difference in intensities of colour in all the three position. Whereas, the O cells were not retained as expected.

6.4.2. Elution behaviour of added protein

The observation made from second experiment was as per our expectations; the A cells bound to the anti-A and did not elute up the strip of paper. O pos (positive) cells will not react with

the anti-A already on the paper, but will only be retained if the anti-D from the A neg (negative) sample has eluted up the paper. O pos cells did react with the anti-D so it has travelled down the paper. Although not enough time elapsed for the anti-D to elute to the end of the anti-A antisera.

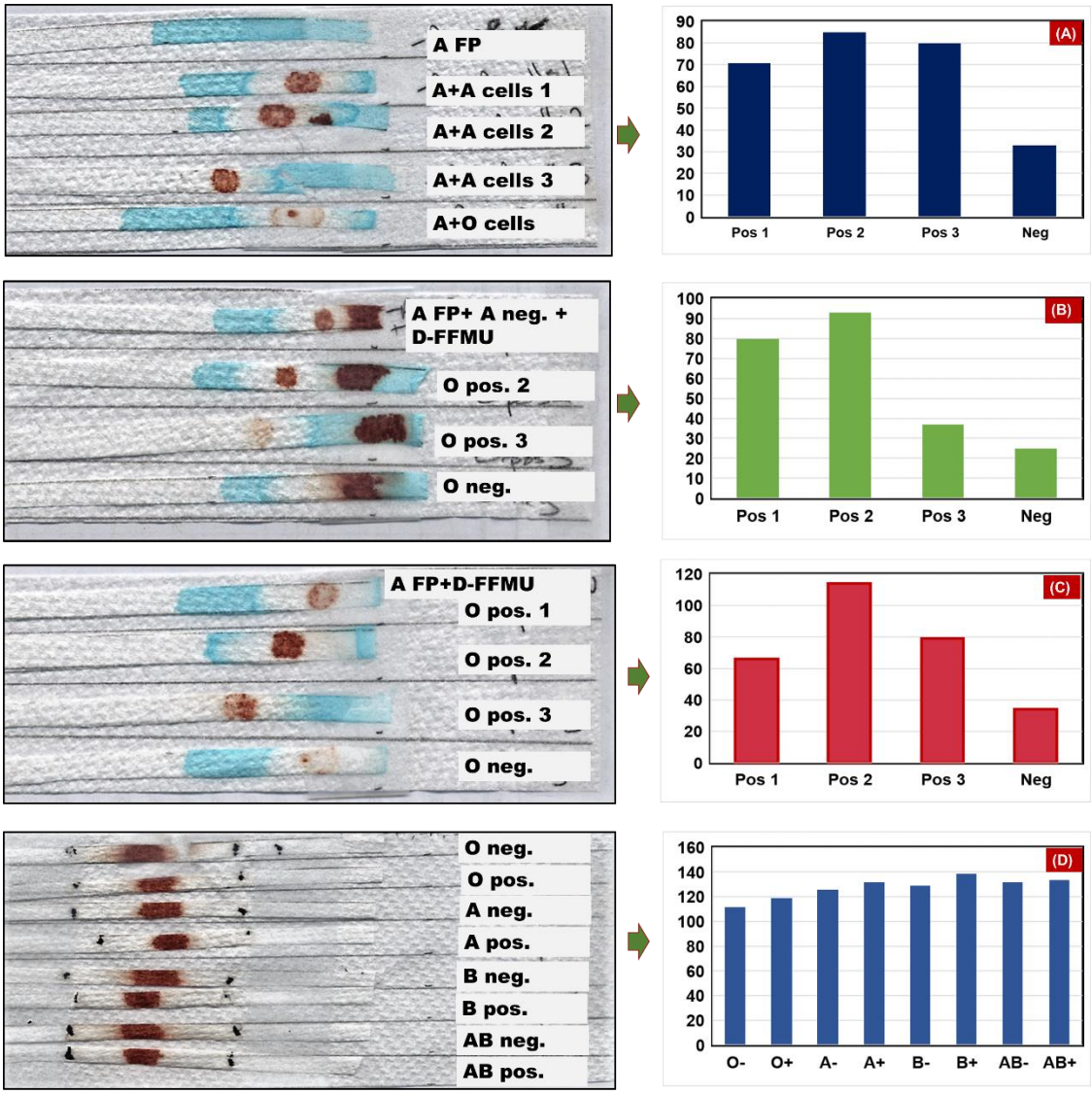

Figure 6-6: Scanned images and intensity plots of all the four set of experiments (A) to test how far the antibodies run down the paper towelling (B) to test if protein from an added sample would elute independently from the agglutinated cells (C) to test that the agglutination of cells impede the movement of the antibody down the paper (D) to see if all blood groups cells could be retained by mixing different antibodies.

The image J results show that the anti-D has definitely travelled from where the A neg cells agglutinated. The another significant observation was made regarding effect of agglutination of red blood cells on further elution of target protein in plasma. It was observed that

agglutination of RBCs does impede the further movement of added proteins and it would not independently elute in the fluid and move with the flow as shown in Figure 6-6B.

6.4.3. Effect of agglutination on antibodies movement

Figure 6-6C shows the result obtained from the strip where A cells were not added in the mixture of sample protein and Anti-A solution. By comparing the results with and without the addition of A cells the movement of the anti-D does appear to be impeded by the agglutination of the cells. The paper towel thus could also use as an efficient substrate for blood-plasma separation by implying blood cells agglutination using mixture of ABO antisera (Figure 6-6D). Mixture of antibodies against each blood group antigen is capable to holds their respective blood cells very efficiently thus separate blood cells from whole blood and leaving plasma having proteins of interest along with other biological constituents. Blood-plasma separation based on agglutination of RBCs could also affect the efficiency of further sensing of target protein present in separated plasma. The observations were based on preliminary results however; further testing is being carried forward in this direction by our research group.

6.5. Summary and Conclusion

The presented section is dedicated on investigation of a new, cost-effective and simple paper-based passive separation device which could be potentially used for blood-plasma separation with undiluted blood without use of any additional pumping device. To develop this, we exploit distinct properties of zinc oxide nanorods and paper, which have been proven favourable subsequently. The nanorods were successfully grown on different papers via hydrothermal route and characterized. Effect of nanorods on paper's pore size and blood transport behaviour has been investigated on different types of paper. Using the new platform, separation of plasma from whole undiluted blood has been successfully achieved with clear cell free region on paper strips. The nanorods-assisted, blood-plasma separation is also supported by various underlying theories. Our initial investigations on antibodies behaviour on paper studies could be very helpful for future studies, specially while dealing with real samples like; blood, plasma and serum. The obtained results offer a new insight towards development of a frugal blood-plasma separation device, and could be effectively used in the applications in microscale devices where few micro or nanolitres sample (plasma) is needed.

7. Conclusions and Future Perspectives

Novel ZnO nanorods functionalized paper was investigated as a preconcentrator unit for application in paper biotest and biodiagnostics devices. The efficiency of the ZnO nanorods treated paper as protein concentrator was successfully tested for myoglobin, a biomarker for heart disease. Hexagonal nanorods of high aspect ratio and very high packing density were grown on paper to provide the high surface area of binding sites required to chemisorb the antibody molecules and was used to selectively capture the target protein. In a first step, a preconcentrator is required to capture high density of the target protein for the concentrating step; in the second, the paper unit must be able to elute the captured protein so that it can be pass through the sensing device for detection. ZnO-NRs/WFP chemisorbed with an antibody proved very efficient for both steps with myoglobin full release upon change of pH (8.5). Fluorescence spectroscopic study using fluorescent tagged molecules showed the bound protein to be released from ZnO-NRs/WFP without loose in activity. P-ELISA provides quantitative estimation of bound target protein i.e. cardiac myoglobin in terms of colour intensity. Using ZnO nanorods paper as preconcentrator, myoglobin could be detected at concentration as low as 50 ng/mL. ELISA results revealed a threefold enhancement in protein capture with ZnO-NR paper compared to the control paper. This ZnO-NRs/WFP platform can easily be integrated with μ-PAD or other biosensors based on antigen-antibody interaction.

Surface Plasmon Resonance studies for validation of the preconcentration hypothesis proven an excellent tool. A new Zinc oxide nanorods modified sensing chip (ZnO-NRs/Au chip) was successfully fabricated and tested with cardiac myoglobin as target antigen. ZnO-NRs were hydrothermally synthesized and bare gold SPR chip was modified with the nanorods. Thus modified ZnO-NRs/Au chip was then biofunctionalized using 3-APTES and its surface morphology was examined using scanning electron microscopy. The chip was optimized to get maximum immobilization level using anti-Myoglobin antibodies(Mab) and protein binding experiments were performed with different concentrations of Myoglobin protein and compared with conventional SPR chip. The ZnO-NRs/Au chip showed 300% increase in protein capture than to conventional chip. To investigate the compatibility, reproducibility and stability of the modified chip with real samples, 12 different plasma samples were used. It was observed that ZnO-NRs/Au chip is excellent in terms of protein capture but it could also serve as potential sensing surface after ensuring specificity.

Blood-plasma separation study with ZnO-NRs/Paper have shown quite remarkable findings through red blood cells capture Whatman filter paper with no. 1, 2, 5 and glass fiber discs. All four paper types were subjected to modification with hydrothermally grown zinc oxide nanorods. Growth and morphologies of zinc oxide nanorods were confirmed by SEM, XRD and XPS studies. The blood plasma separation experiments were done by cutting the papers into identical strips with dimension of 5 x 20 mm^2. 3 µL of blood was mixed with equal volume of antibody solution and pipetted on each strip. The colored antibody solution was used to track the path of antibody, eventually the separated plasma. The dried strips were scanned and the difference in the distance travelled by colored solution of antibodies was measured. From the results, it is clear that all four paper strips covered with nanorods have shown more distance travelled and better separation than their control samples.

Further investigations on all-in-one ZnO-NRs/Paper based microfluidic device which could be potentially used for blood-plasma separation, protein preconcentration and sensor, could be a potential scope of the study. There is a huge scope of the work on design and integration of the preconcentrator with sensing device and test the performance with mixture of different proteins and other biomarkers in biofluid samples including blood, plasma and serum. Results showed that nanorods-assisted paper has the potential to enable low-cost and high-quality solutions ("affordable excellence") associated with frugal innovations in healthcare devices and may contribute to developing substantially affordable and very effective healthcare solutions to the society.

Appendix A

Nanorods on paper area and density calculation:

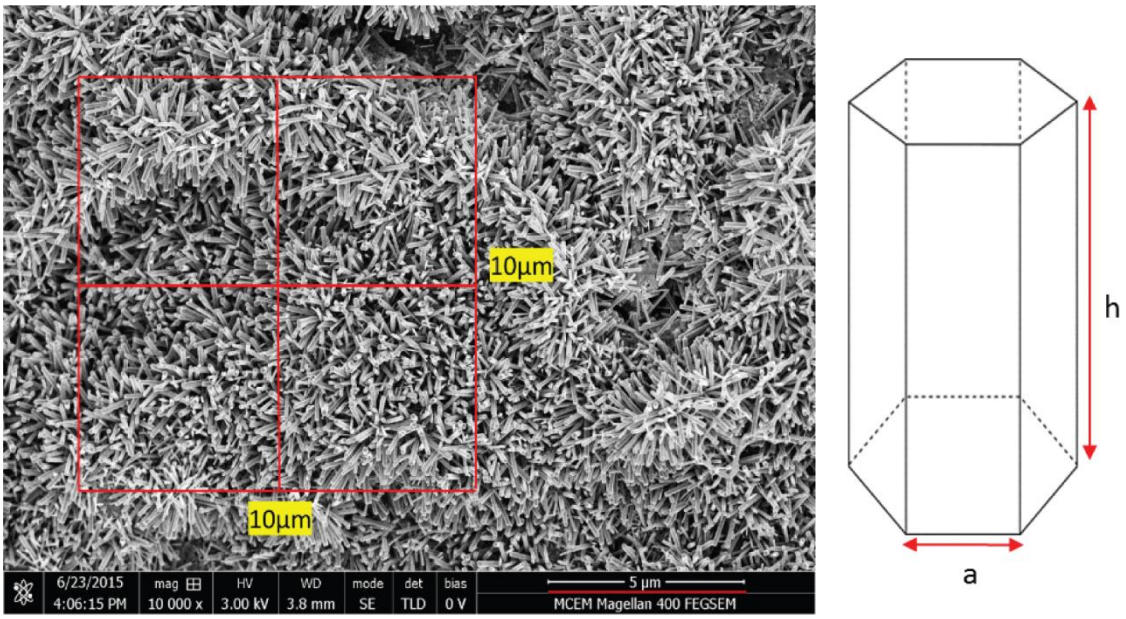

Figure: SEM image of ZnO-NRs/WFP and shape of individual rod obtained from SEM and used for calculations.

2.1 Surface area calculation:

Shape of nanorod is like hexagonal prism

Parameter calculated from SEM image:

No. of nanorods in 100 μm^2 is 1000

Height(h): 1 µm

Diagonal(D): 200 nm

Edge length(a): D/2= 100 nm

Area of a hexagonal prism= $3\sqrt{3}a^2 + 6ah$

Hence, area of one nanorod = 6.5×10^{-13} m^2 = 0.65 μm^2

Area of 1000 rods will be= 650 μm^2

2.2 Number of nanorods/m^2 calculation:

Approximate no. of nanorods in 100 μm^2 area is 1000 (from SEM image).

No. of rods/m^2 will be:

#rods in 10^{-4} m^2 is =1000, assuming uniform distribution

In 1 m^2 = $1000/10^{-4} = 10^7$ rods/m^2

So, density of rods= 10^7 rods/m^2

Surface coverage of paper by nanorods is about 90% as seen by SEM images.

Therefore, increase in surface area will be= density of rods x area of one rod

$$= 6.5 \times 10^{-13} \times 10^7$$

$$= 6.5 \times 10^{-6}\ m^2 \text{ or } 6.5 \times 10^6\ \mu m^2$$

$$= 7 \times 10^6\ \mu m^2$$

Appendix B

Calculation of target protein binding capacity of chip:

Binding capacity of chip surface was calculated by using expression:

$$R_{\max=} \frac{analyte\ MW}{ligand\ MW} x immobilized\ amount x\ valency\ of\ ligand$$

In our study:

Molecular weight of analyte myoglobin: 17,000 D

Molecular weight of ligand anti-myoglobin: 150,000 D

Putting these values in above expression we get:

For ZnO-NRs/Au chip surface :

$$R_{max} = \frac{17000}{150000} x\ 3200x2 = 725 \text{ RU}$$

For CM5 chip:

$$R_{max} = \frac{17000}{150000} x\ 2000x2 = 450 \text{ RU}$$

Appendix C

Fluorescence data obtained by ELISA reader

Sample	Time	RFU(set 1)	RFU(set 2)	RFU(set 3)	Mean values
Positive control	0	1170	-	-	1170
1	5 min	89.833	57.618	66.062	71.171
2	10 min	18.585	10.765	7.893	12.414
3	15 min	12.229	6.346	5.912	7.922
4	20 min	6.591	4.292	3.114	4.665
5	25 min	4.628	4.188	4.962	4.592
6	30 min	3.496	3.002	2.991	3.163
Blank	-	1.109	-	-	1.109

Relation with increase in fluorescence

Sample	Average Intensity
WFP	6440184
ZnO-NRs/WFP	22101495

Percent increase in fluorescence intensity=

$$\frac{FinalIntensity - InitialIntensity}{InitialIntensity} x100$$

Which gives,

= 22101495-6440184/6440184*100

> 200% increase in fluorescence.

8. References

[1] "WHO | Cardiovascular diseases (CVDs)," *WHO*, 2017.

[2] J. L. Martin-Ventura, L. M. Blanco-Colio, J. Tunon, B. Munoz-Garcia, J. Madrigal-Matute, J. A. Moreno, M. Vega de Ceniga, and J. Egido, "Biomarkers in cardiovascular medicine," *Rev. Esp. Cardiol.*, 2009.

[3] A. Qureshi, Y. Gurbuz, and J. H. Niazi, "Biosensors for cardiac biomarkers detection: A review," *Sensors Actuators, B Chem.*, vol. 171–172, pp. 62–76, 2012.

[4] S. Gupta, A. Venkatesh, S. Ray, and S. Srivastava, "Challenges and prospects for biomarker research: a current perspective from the developing world," *Biochim. Biophys. Acta*, vol. 1844, pp. 899–908, 2014.

[5] Z. Z. Hu, H. Huang, C. H. Wu, M. Jung, A. Dritschilo, A. T. Riegel, and A. Wellstein, "Omics-based molecular target and biomarker identification.," *Methods Mol. Biol.*, vol. 719, pp. 547–571, 2011.

[6] B. Derkus, "Applying the miniaturization technologies for biosensor design," *Biosens. Bioelectron.*, vol. 79, pp. 901–913, 2016.

[7] D. Chimene, D. L. Alge, and A. K. Gaharwar, "Two-Dimensional Nanomaterials for Biomedical Applications: Emerging Trends and Future Prospects.," *Adv. Mater.*, vol. 27, pp. 7261–7284, 2015.

[8] Y. H. Ngo, D. Li, G. P. Simon, and G. Garnier, "Gold Nanoparticle − Paper as a Three-Dimensional Surface Enhanced Raman Scattering Substrate," *Langmuir*, vol. 28, pp. 8782–8790, 2012.

[9] Y. H. Ngo, D. Li, G. P. Simon, and G. Garnier, "Paper surfaces functionalized by nanoparticles," *Adv. Colloid Interface Sci.*, vol. 163, no. 1, pp. 23–38, 2011.

[10] H. D. White, K. Thygesen, J. S. Alpert, and A. S. Jaffe, "Republished: Clinical implications of the Third Universal Definition of Myocardial Infarction," *Postgrad. Med. J.*, vol. 90, pp. 502–510, 2014.

[11] M. E. Reid, C. Lomas-Francis, and M. L. Olsson, *The Blood Group Antigen FactsBook*. Elsevier Science, 2012.

[12] M. Shen, H. Yang, V. Sivagnanam, and M. A. M. Gijs, "Microfluidic protein preconcentrator using a microchannel-integrated nafion strip: Experiment and modeling," *Anal. Chem.*, vol. 82, no. 24, pp. 9989–9997, 2010.

[13] and J. H. V. Liu, Y. A. Song, "Capillary-valve-based fabrication of ion-selective membrane junction for electrokinetic sample preconcentration in PDMS chip," *Energy Environ. Sci.*, vol. 10, pp. 1485–1490, 2010.

[14] H. Yang, M. Shen, V. Sivagnanam, and M. A. M. Gijs, "High-performance protein preconcentrator using microchannel-integrated nafion strip," *2011 16th Int. Solid-State Sensors, Actuators Microsystems Conf. TRANSDUCERS'11*, pp. 238–241, 2011.

[15] A. Sarkar and J. Han, "Non-linear and linear enhancement of enzymatic reaction kinetics

using a biomolecule concentrator," *Lab Chip*, vol. 11, no. 15, p. 2569, 2011.

[16] R. Kwak, S. J. Kim, and J. Han, "Continuous-Flow Biomolecule and Cell Concentrator by Ion Concentration Polarization," *Anal. Chem.*, vol. 83, no. 19, pp. 7348–7355, 2011.

[17] L. F. Cheow and J. Han, "Continuous signal enhancement for sensitive aptamer affinity probe electrophoresis assay using electrokinetic concentration," *Anal. Chem.*, vol. 83, no. 18, pp. 7086–7093, 2011.

[18] A. Kraytsberg and Y. Ein-Eli, "Review of Advanced Materials for Proton Exchange Membrane Fuel Cells," *Energy & Fuels*, vol. 28, no. 12, pp. 7303–7330, Dec. 2014.

[19] D. Hlushkou, R. Dhopeshwarkar, R. M. Crooks, and U. Tallarek, "The influence of membrane ion-permselectivity on electrokinetic concentration enrichment in membrane-based preconcentration units," *Lab Chip*, vol. 8, no. 7, p. 1153, 2008.

[20] Z. Li, Q. He, D. Ma, H. Chen, and S. A. Soper, "Thermoswitchable Electrokinetic Ion-Enrichment/Elution Based on a Poly(*N* -isopropylacrylamide) Hydrogel Plug in a Microchannel," *Anal. Chem.*, vol. 82, no. 24, pp. 10030–10036, Dec. 2010.

[21] P. N. Nge, W. Yang, J. V. Pagaduan, and A. T. Woolley, "Ion-permeable membrane for on-chip preconcentration and separation of cancer marker proteins," *Electrophoresis*, vol. 32, no. 10, pp. 1133–1140, 2011.

[22] S. Polarz and B. Smarsly, "Nanoporous Materials," *J. Nanosci. Nanotechnol.*, vol. 2, no. 6, pp. 581–612, 2002.

[23] G. Q. Lu and X. S. Zhao, "Nanoporous Materials — An Overview," *Nanoporous Mater. Sci. Eng.*, pp. 3–4, 2004.

[24] S. P. Adiga, C. Jin, L. A. Curtiss, N. A. Monteiro-Riviere, and R. J. Narayan, "Nanoporous membranes for medical and biological applications," *Wiley Interdisciplinary Reviews: Nanomedicine and Nanobiotechnology*. pp. 568–581, 2009.

[25] Y. MO and T. FEI, "Nanoporous Membrane for Biosensing Applications," *Nano Life*, vol. 02, no. 01, p. 1230003, 2012.

[26] H. Uehara, M. Kakiage, M. Sekiya, D. Sakuma, T. Yamonobe, N. Takano, A. Barraud, E. Meurville, and P. Ryser, "Size-selective diffusion in nanoporous but flexible membranes for glucose sensors," *ACS Nano*, vol. 3, no. 4, pp. 924–932, 2009.

[27] S. P. Adiga, L. a Curtiss, J. W. Elam, M. J. Pellin, C. Shih, C. Shih, S. Lin, Y. Su, S. D. Gittard, J. Zhang, and R. J. Narayan, "Nanoporous Materials for Biomedical Devices," *J. Miner.*, vol. 60, no. 3, pp. 26–32, 2008.

[28] R. A. Siegel and R. Langert, "A new Monte Carlo approach to diffusion in constricted porous geometries," *J. Colloid Interface Sci.*, vol. 109, no. 2, pp. 426–440, 1986.

[29] J. Cichelli and I. Zharov, "Chiral permselectivity in surface-modified nanoporous opal films," *J. Am. Chem. Soc.*, vol. 128, no. 25, pp. 8130–8131, 2006.

[30] W. Ye, Y. Xu, L. Zheng, Y. Zhang, M. Yang, and P. Sun, "A nanoporous alumina membrane based electrochemical biosensor for histamine determination with biofunctionalized magnetic nanoparticles concentration and signal amplification," *Sensors (Switzerland)*, vol. 16, no. 10, 2016.

[31] A. Mendelsohn and T. Desai, “Inorganic nanoporous membranes for immunoisolated cell-based drug delivery,” *Adv. Exp. Med. Biol.*, vol. 670, pp. 104–125, 2010.

[32] M. M. Gong, P. Zhang, B. D. Macdonald, and D. Sinton, “Nanoporous membranes enable concentration and transport in fully wet paper-based assays,” *Anal. Chem.*, vol. 86, no. 16, pp. 8090–8097, 2014.

[33] M. A. Shahbazi, B. Herranz, and H. A. Santos, “Nanostructured porous Si-based nanoparticles for targeted drug delivery.,” *Biomatter*, vol. 2, pp. 296–312, 2012.

[34] G. Jeon, S. Y. Yang, and J. K. Kim, “Functional nanoporous membranes for drug delivery,” *J. Mater. Chem.*, 2012.

[35] D. Li, Y. S. Lin, and V. V. Guliants, “Synthesis and characterization of ordered meso-macro-porous silica membranes on a porous alumina support,” *Tsinghua Sci. Technol.*, vol. 15, no. 4, pp. 377–384, 2010.

[36] R. S. Foote, J. Khandurina, S. C. Jacobson, and J. M. Ramsey, “Preconcentration of proteins on microfluidic devices using porous silica membranes,” *Anal. Chem*, vol. 77, no. 1, pp. 57–63, 2005.

[37] Y. Zeng and D. J. Harrison, “Self-assembled colloidal arrays as three-dimensional nanofluidic sieves for separation of biomolecules on microchips,” *Anal. Chem.*, vol. 79, no. 6, pp. 2289–2295, 2007.

[38] S. Zheng, E. Ross, M. A. Legg, and M. J. Wirth, “High-speed electroseparations inside silica colloidal crystals,” *J. Am. Chem. Soc.*, vol. 128, no. 28, pp. 9016–9017, 2006.

[39] Y.-C. Wang and J. Han, “Pre-binding dynamic range and sensitivity enhancement for immuno-sensors using nanofluidic preconcentrator,” *Lab Chip*, vol. 8, no. 3, p. 392, 2008.

[40] J. Han and J. Fu, “Biomolecule separation by steric hindrance using nanofluidic filters.,” *Conf. Proc. IEEE Eng. Med. Biol. Soc.*, vol. 4, pp. 2611–2614, 2004.

[41] S. Chung, J. H. Lee, M. W. Moon, J. Han, and R. D. Kamm, “Non-lithographic wrinkle nanochannels for protein preconcentration,” *Adv. Mater.*, vol. 20, no. 16, pp. 3011–3016, 2008.

[42] Y. C. Wang, C. H. Tsau, T. P. Burg, S. Manalis, and J. Han, “Efficient biomolecule pre-concentration by nanofilter-triggered electrokinetic trapping,” *Micro Total Anal. Syst. - Proc. MicroTAS 2005 Conf. 9th Int. Conf. Miniaturized Syst. Chem. Life Sci.*, vol. 1, pp. 238–240, 2005.

[43] J. H. Lee, Y. Song, S. R. Tannenbaum, and J. Han, “Increase of Reaction Rate and Sensitivity of Low-Abundance Enzyme Assay Using Micro/ Nanofluidic Preconcentration Chip,” *Lab Chip*, vol. 80, no. 9, pp. 6592–6598, 2008.

[44] L. F. Cheow, S. H. Ko, S. J. Kim, K. H. Kang, and J. Han, “Increasing the sensitivity of enzyme-linked immunosorbent assay using multiplexed electrokinetic concentrator,” *Anal. Chem.*, vol. 82, no. 8, pp. 3383–3388, 2010.

[45] C. H. Chen, A. Sarkar, Y. A. Song, M. A. Miller, S. J. Kim, L. G. Griffith, D. A. Lauffenburger, and J. Han, “Enhancing protease activity assay in droplet-based microfluidics using a biomolecule concentrator,” *J. Am. Chem. Soc.*, vol. 133, no. 27, pp. 10368–10371, 2011.

[46] J. Zhang, K. O. Voss, D. F. Shaw, K. P. Roos, D. F. Lewis, J. Yan, R. Jiang, H. Ren, J. Y. Hou, Y. Fang, X. Puyang, H. Ahmadzadeh, and N. J. Dovichi, "A multiple-capillary electrophoresis system for small-scale DNA sequencing and analysis.," *Nucleic Acids Res.*, vol. 27, p. e36, 1999.

[47] X. C. Huang, M. a Quesada, and R. a Mathies, "DNA sequencing using capillary array electrophoresis.," *Anal. Chem.*, vol. 64, pp. 2149–2154, 1992.

[48] C. A. Emrich, H. Tian, I. L. Medintz, and R. A. Mathies, "Microfabricated 384-lane capillary array electrophoresis bioanalyzer for ultrahigh-throughput genetic analysis," *Anal. Chem.*, vol. 74, pp. 5076–5083, 2002.

[49] J. H. Lee, Y.-A. Song, and J. Han, "Multiplexed proteomic sample preconcentration device using surface-patterned ion-selective membrane," *Lab Chip*, vol. 8, no. 4, p. 596, 2008.

[50] S. H. Ko, S. J. Kim, L. F. Cheow, L. D. Li, K. H. Kang, and J. Han, "Massively parallel concentration device for multiplexed immunoassays," *Lab Chip*, vol. 11, no. 7, p. 1351, 2011.

[51] P. Sabounchi, A. M. Morales, and B. A. Simmons, "Integrated microfluidic sample precon- centrator and impedance detection platform for pathogen monitoring," *October*, no. Figure 1, pp. 1051–1053.

[52] Y.-H. Choi, M. Kim, D.-H. Kang, J. Sim, J. Kim, and Y.-J. Kim, "An electrodynamic preconcentrator integrated thermoelectric biosensor chip for continuous monitoring of biochemical process," *J. Micromechanics Microengineering*, vol. 22, no. 4, p. 045022, 2012.

[53] V. Krivitsky, L. C. Hsiung, A. Lichtenstein, B. Brudnik, R. Kantaev, R. Elnathan, A. Pevzner, A. Khatchtourints, and F. Patolsky, "Si nanowires forest-based on-chip biomolecular filtering, separation and preconcentration devices: Nanowires do it all," *Nano Lett.*, vol. 12, no. 9, pp. 4748–4756, 2012.

[54] H. Gordon, "The beginnings of chromatography How paper chromatography," no. November, pp. 243–244, 1977.

[55] T. Review, "Paper Based Nanobiosensors for Diagnostics," pp. 450–457, 2013.

[56] A. H. Free, E. C. Adams, M. L. Kercher, H. M. Free, and M. H. Cook, "Simple specific test for urine glucose.," *Clin. Chem.*, vol. 3, no. 3, pp. 163–168, 1957.

[57] E. W. Nery and L. T. Kubota, "Sensing approaches on paper-based devices: A review," *Anal. Bioanal. Chem.*, vol. 405, no. 24, pp. 7573–7595, 2013.

[58] A. M. López-marzo and A. Merkoçi, "Lab on a Chip engineering design and the convergence of," *Lab Chip*, vol. 16, pp. 3150–3176, 2016.

[59] M. J. Benotti, R. A. Trenholm, B. J. Vanderford, J. C. Holady, B. D. Stanford, and S. A. Snyder, "Pharmaceuticals and endocrine disrupting compounds in U.S. drinking water," *Environ. Sci. Technol.*, 2009.

[60] J. Cortez and C. Pasquini, "Ring-oven based preconcentration technique for microanalysis: Simultaneous determination of Na, Fe, and Cu in fuel ethanol by laser induced breakdown spectroscopy," *Anal. Chem.*, vol. 85, no. 3, pp. 1547–1554, 2013.

[61] A. Abbas, A. Brimer, J. M. Slocik, L. Tian, R. R. Naik, and S. Singamaneni, "Multifunctional analytical platform on a paper strip: Separation, preconcentration, and subattomolar detection," *Anal. Chem.*, vol. 85, no. 8, pp. 3977–3983, 2013.

[62] S. Hong, R. Kwak, and W. Kim, "Paper-Based Flow Fractionation System Applicable to Preconcentration and Field-Flow Separation," *Anal. Chem.*, 2016.

[63] K. Lee, Y. K. Yoo, S. Il Han, J. Lee, D. Lee, C. Kim, and J. H. Lee, "Folding-paper-based preconcentrator for low dispersion of preconcentration plug," *Micro Nano Syst. Lett.*, vol. 5, no. 1, p. 11, 2017.

[64] S. Y. Son, H. Lee, and S. J. Kim, "Paper-based ion concentration polarization device for selective preconcentration of muc1 and lamp-2 genes," *Micro Nano Syst. Lett.*, vol. 5, no. 1, p. 8, 2017.

[65] C. Wu, O. Adeyiga, J. Lin, and D. Di Carlo, "Research highlights: increasing paper possibilities.," *Lab Chip*, pp. 3258–3261, 2014.

[66] L. H. Hung, H. L. Wang, and R. J. Yang, "A portable sample concentrator on paper-based microfluidic devices," *Microfluid. Nanofluidics*, vol. 20, no. 5, pp. 1–9, 2016.

[67] M. M. Gong, R. Nosrati, M. C. San Gabriel, A. Zini, and D. Sinton, "Direct DNA Analysis with Paper-Based Ion Concentration Polarization," *J. Am. Chem. Soc.*, vol. 137, no. 43, pp. 13913–13919, 2015.

[68] S. Il Han, K. S. Hwang, R. Kwak, J. Lee, S. Il, K. Seon, R. Kwak, and J. Hoon, "Microfluidic Paper-based Biomolecule Preconcentrator Based on Ion Concentration Polarization," *Lab Chip*, vol. 16, p. 2016, 2016.

[69] B. Y. Moghadam, K. T. Connelly, and J. D. Posner, "Isotachophoretic Preconcenetration on Paper-Based Micro fl uidic Devices," *Anal Chem*, vol. 86, pp. 5829–5837, 2014.

[70] R. J. Yang, H. H. Pu, and H. L. Wang, "Ion concentration polarization on paper-based microfluidic devices and its application to preconcentrate dilute sample solutions," *Biomicrofluidics*, 2015.

[71] S. Alila, A. M. Ferraria, A. M. Botelho do Rego, and S. Boufi, "Controlled surface modification of cellulose fibers by amino derivatives using N,N′-carbonyldiimidazole as activator," *Carbohydr. Polym.*, vol. 77, no. 3, pp. 553–562, 2009.

[72] Y. Deslandes, G. Pleizier, E. Poiré, S. Sapieha, M. R. Wertheimer, and E. Sacher, "The Surface Modification of Pure Cellulose Paper Induced by Low-Pressure Nitrogen Plasma Treatment," *Plasmas Polym.*, vol. 3, no. 2, pp. 61–76, 1998.

[73] S. Utsel, "Surface Modification of Cellulose-based Materials for Tailoring of Interfacial Interactions," 2012.

[74] S. Vaswani, J. Koskinen, and D. W. Hess, "Surface modification of paper and cellulose by plasma-assisted deposition of fluorocarbon films," *Surf. Coatings Technol.*, vol. 195, no. 2–3, pp. 121–129, 2005.

[75] J. Trejo-O'Reilly, J. Cavaille, and a Gandini, "The surface chemical modification of cellulosic fibres in view of their use in composite materials," *Cellulose*, vol. 4, no. 4, pp. 305–320, 1997.

[76] X. Zhang and J. Huang, "Functional surface modification of natural cellulose substances

for colorimetric detection and adsorption of Hg2+ in aqueous media," *Chem. Commun.*, vol. 46, no. 33, p. 6042, 2010.

[77] P. Peng, L. Summers, A. Rodriguez, and G. Garnier, "Colloids engineering and filtration to enhance the sensitivity of paper-based biosensors," *Colloids Surfaces B Biointerfaces*, vol. 88, no. 1, pp. 271–278, 2011.

[78] Y. H. Ngo, D. Li, G. P. Simon, and G. Garnier, "Effect of cationic polyacrylamides on the aggregation and SERS performance of gold nanoparticles-treated paper," *J. Colloid Interface Sci.*, vol. 392, no. 1, pp. 237–246, 2013.

[79] H. Mcliesh, S. Sharman, and G. Garnier, "Colloids and Surfaces B : Biointerfaces Effect of cationic polyelectrolytes on the performance of paper diagnostics for blood typing," *Colloids Surfaces B Biointerfaces*, vol. 133, pp. 189–197, 2015.

[80] M. S. Khan, D. Fon, X. Li, J. Tian, J. Forsythe, G. Garnier, and W. Shen, "Biosurface engineering through ink jet printing," *Colloids Surfaces B Biointerfaces*, vol. 75, no. 2, pp. 441–447, 2010.

[81] Y. H. Ngo, D. Li, G. P. Simon, and G. Garnier, "Gold nanoparticle-paper as a three-dimensional surface enhanced Raman scattering substrate.," *Langmuir*, vol. 28, no. 23, pp. 8782–90, 2012.

[82] J. X. Wang, X. W. Sun, A. Wei, Y. Lei, X. P. Cai, C. M. Li, and Z. L. Dong, "Zinc oxide nanocomb biosensor for glucose detection," *Appl. Phys. Lett.*, vol. 88, no. 23, 2006.

[83] S. A. Kumar and S. Chen, "Nanostructured Zinc Oxide Particles in Chemically Modified Electrodes for Biosensor Applications," *Anal. Lett.*, vol. 41, no. December 2013, pp. 141–158, 2008.

[84] B. S. Kang, H.-T. Wang, L.-C. Tien, F. Ren, B. P. Gila, D. P. Norton, C. R. Abernathy, J. Lin, and S. J. Pearton, "Wide Bandgap Semiconductor Nanorod and Thin Film Gas Sensors," *Sensors*, 2006.

[85] S. J. Pearton, F. Ren, Y. L. Wang, B. H. Chu, K. H. Chen, C. Y. Chang, W. Lim, J. Lin, and D. P. Norton, "Recent advances in wide bandgap semiconductor biological and gas sensors," *Progress in Materials Science*. 2010.

[86] X. Zhu, I. Yuri, X. Gan, I. Suzuki, and G. Li, "Electrochemical study of the effect of nano-zinc oxide on microperoxidase and its application to more sensitive hydrogen peroxide biosensor preparation," *Biosens. Bioelectron.*, vol. 22, no. 8, pp. 1600–1604, 2007.

[87] S. V Costa, A. S. Gonçalves, M. a Zaguete, T. Mazon, and A. F. Nogueira, "ZnO nanostructures directly grown on paper and bacterial cellulose substrates without any surface modification layer.," *Chem. Commun. (Camb).*, vol. 49, no. 73, pp. 8096–8, 2013.

[88] Z. Fan, Z. Fan, and J. G. Lu, "Zinc Oxide Nanostructures : Synthesis and Properties Zinc Oxide Nanostructures : Synthesis and Properties," no. July 2015, 2005.

[89] S. Xu and Z. L. Wang, "One-dimensional ZnO nanostructures: Solution growth and functional properties," *Nano Res.*, vol. 4, no. 11, pp. 1013–1098, 2011.

[90] L. Spanhel, "Colloidal ZnO nanostructures and functional coatings: A survey," *J. Sol-Gel Sci. Technol.*, 2006.

[91] X. Ma, H. Zhang, Y. Ji, J. Xu, and D. Yang, "Sequential occurrence of ZnO nanopaticles, nanorods, and nanotips during hydrothermal process in a dilute aqueous solution," *Mater. Lett.*, 2005.

[92] H. Y. Xu, H. Wang, Y. C. Zhang, S. Wang, M. K. Zhu, and H. Yan, "Asymmetric twinning crystals of zinc oxide formed in a hydrothermal process," *Cryst. Res. Technol.*, 2003.

[93] S. Danwittayakul and J. Dutta, "Controlled growth of zinc oxide microrods by hydrothermal process on porous ceramic supports for catalytic application," *J. Alloys Compd.*, 2014.

[94] S. Shingubara, "Fabrication of nanomaterials using porous alumina templates," *Journal of Nanoparticle Research*. 2003.

[95] M. A. Mahmood and J. Dutta, "Spray Pyrolized Pre-coating Layers for Controlled Growth of Zinc Oxide Nanorods by Hydrothermal Process," *Nanosci. Nanotechnology-Asia*, 2011.

[96] M. Krunks and E. Mellikov, "Zinc oxide thin films by the spray pyrolysis method," *Thin Solid Films*, 1995.

[97] J.-H. Lee, I.-C. Leu, Y.-W. Chung, and M.-H. Hon, "Fabrication of ordered ZnO hierarchical structures controlled via surface charge in the electrophoretic deposition process," *Nanotechnology*, 2006.

[98] C. Growth, Z. O. Nanowires, and V. Transport, "Catalytic Growth of Zinc Oxide Nanowires," *Adv. Mater.*, 2001.

[99] C. C. Tang, S. S. Fan, M. L. D. La Chapelle, and P. Li, "Silica-assisted catalytic growth of oxide and nitride nanowires," *Chem. Phys. Lett.*, 2001.

[100] Z. L. Wang, "Nanobelts, nanowires, and nanodiskettes of semiconducting oxides - From materials to nanodevices," *Adv. Mater.*, 2003.

[101] S. H. Dalal, D. L. Baptista, K. B. K. Teo, R. G. Lacerda, D. a Jefferson, and W. I. Milne, "Controllable growth of vertically aligned zinc oxide nanowires using vapour deposition," *Nanotechnology*, 2006.

[102] P. S. Venkatesh and K. Jeganathan, "Investigations on the growth and characterization of vertically aligned zinc oxide nanowires by radio frequency magnetron sputtering," *J. Solid State Chem.* , 2013.

[103] S.-T. Ho, C.-Y. Wang, H.-L. Liu, and H.-N. Lin, "Catalyst-free selective-area growth of vertically aligned zinc oxide nanowires," *Chem. Phys. Lett.*, 2008.

[104] S. Hindley, a C. Jones, S. Ashraf, J. Bacsa, a Steiner, P. R. Chalker, P. Beahan, P. a Williams, and R. Odedra, "Metal organic chemical vapour deposition of vertically aligned ZnO nanowires using oxygen donor adducts.," *J. Nanosci. Nanotechnol.*, 2011.

[105] C. Jagadish and S. Pearton, *Zinc Oxide Bulk, Thin Films and Nanostructures*. 2006.

[106] Z. W. Li and W. Gao, "Growth of zinc oxide thin films and nanostructures by wet oxidation," *Thin Solid Films*, 2007.

[107] S. Baruah and J. Dutta, "Hydrothermal growth of ZnO nanostructures," *Sci. Technol.*

Adv. Mater., vol. 10, no. 1, p. 013001, Jan. 2009.

[108] H. Gullapalli, V. S. M. Vemuru, A. Kumar, A. Botello-Mendez, R. Vajtai, M. Terrones, S. Nagarajaiah, and P. M. Ajayan, "Flexible piezoelectric zno-paper nanocomposite strain sensor," *Small*, vol. 6, no. 15, pp. 1641–1646, 2010.

[109] A. Manekkathodi, M. Y. Lu, C. W. Wang, and L. J. Chen, "Direct growth of aligned zinc oxide nanorods on paper substrates for low-cost flexible electronics," *Adv. Mater.*, vol. 22, no. 36, pp. 4059–4063, 2010.

[110] I. Udom, M. K. Ram, E. K. Stefanakos, A. F. Hepp, and D. Y. Goswami, "One dimensional-ZnO nanostructures: Synthesis, properties and environmental applications," *Mater. Sci. Semicond. Process.*, vol. 16, no. 6, pp. 2070–2083, 2013.

[111] Z. Ibupoto, K. Khun, M. Eriksson, M. AlSalhi, M. Atif, A. Ansari, and M. Willander, "Hydrothermal Growth of Vertically Aligned ZnO Nanorods Using a Biocomposite Seed Layer of ZnO Nanoparticles," *Materials (Basel).*, vol. 6, no. 8, pp. 3584–3597, 2013.

[112] K. H. Kim, K. Utashiro, Y. Abe, and M. Kawamura, "Growth of zinc oxide nanorods using various seed layer annealing temperatures and substrate materials," *Int. J. Electrochem. Sci.*, vol. 9, no. 4, pp. 2080–2089, 2014.

[113] P. E. Scopelliti, A. Borgonovo, M. Indrieri, L. Giorgetti, G. Bongiorno, R. Carbone, A. Podest??, and P. Milani, "The effect of surface nanometre-scale morphology on protein adsorption," *PLoS One*, vol. 5, no. 7, pp. 1–9, 2010.

[114] F. Kong and Y. F. Hu, "Biomolecule immobilization techniques for bioactive paper fabrication," pp. 7–13, 2012.

[115] M. Ben Haddada, J. Blanchard, S. Casale, J. Krafft, and A. Vallée, "Optimizing the immobilization of gold nanoparticles on functionalized silicon surfaces : amine- vs thiol-terminated silane," pp. 335–341, 2013.

[116] R. D. Munje, M. Jacobs, S. Muthukumar, B. Quadri, N. R. Shanmugam, and S. Prasad, "A novel approach for electrical tuning of nano-textured zinc oxide surfaces for ultra-sensitive troponin-T detection," *Anal. Methods*, vol. 7, no. 24, pp. 10136–10144, 2015.

[117] P. S. Katsamba, S. Park, and I. A. Laird-offringa, "Kinetic studies of RNA – protein interactions using surface plasmon resonance," vol. 26, pp. 95–104, 2002.

[118] B. Nguyen, F. A. Tanious, and W. D. Wilson, "Biosensor-surface plasmon resonance : Quantitative analysis of small molecule – nucleic acid interactions," vol. 42, pp. 150–161, 2007.

[119] Y. Arima, R. Ishii, I. Hirata, and H. Iwata, "High-Throughput Study of Protein – Surface Interactions Using a Surface Plasmon Resonance Imaging Apparatus," 2012.

[120] G. E. Healthcare and L. Sciences, "Biacore ™ Assay Handbook."

[121] A. Wei, L. Pan, and W. Huang, "Recent progress in the ZnO nanostructure-based sensors," *Mater. Sci. Eng. B*, vol. 176, no. 18, pp. 1409–1421, 2011.

[122] C. Lin, C. Chang, N. Chiu, D. S. Lin, Y. Chu-su, Y. Liang, and C. Lin, "High-sensitivity detection of carbohydrate antigen 15-3 using a gold / zinc oxide thin film surface plasmon resonance-based biosensor High-Sensitivity Detection of Carbohydrate

Antigen 15-3 Using a Gold / Zinc Oxide Thin Film Surface Plasmon Resonance-Bas," no. April 2017, 2010.

[123] R. Nuryadi and R. Dewi, "ZnO / Au-based surface plasmon resonance for CO 2 gas sensing application," *Appl. Phys. A*, vol. 122, no. 1, pp. 1–6, 2016.

[124] W. Feng, N. Chiu, H. Lu, H. Shih, D. Yang, and C. Lin, "Surface Plasmon Resonance Biochip Based on ZnO Thin Film for Nitric Oxide Sensing," no. 1, pp. 5757–5760, 2008.

[125] R. Tabassum, S. K. Mishra, and B. D. Gupta, "sulphide gas sensor utilizing Cu – ZnO thin films," pp. 11868–11874, 2013.

[126] P. Dextras, K. R. Payer, T. P. Burg, W. Shen, Y. C. Wang, J. Han, and S. R. Manalis, "Fabrication and characterization of an integrated microsystem for protein preconcentration and sensing," *J. Microelectromechanical Syst.*, vol. 20, no. 1, pp. 221–230, 2011.

[127] H. L. Jeong, S. Chung, J. K. Sung, and J. Han, "Poly(dimethylsiloxane)-based protein preconcentration using a nanogap generated by junction gap breakdown," *Anal. Chem.*, vol. 79, no. 17, pp. 6868–6873, 2007.

[128] J. Astorga-Wells and H. Swerdlow, "Fluidic preconcentrator device for capillary electrophoresis of proteins," *Anal. Chem.*, 2003.

[129] Q. Wang, B. Yue, and M. L. Lee, "Mobility-based selective on-line preconcentration of proteins in capillary electrophoresis by controlling electroosmotic flow," in *Journal of Chromatography A*, 2004.

[130] Y. Cong, F. Svec, and J. M. J. Fréchet, "Towards stationary phases for chromatography on a microchip: Molded porous polymer monoliths prepared in capillaries by photoinitiated in situ polymerization as separation media for electrochromatography," *Electrophoresis*, 2000.

[131] P. Lescuyer, D. F. Hochstrasser, and J.-C. Sanchez, "Comprehensive proteome analysis by chromatographic protein prefractionation," *Electrophoresis*, 2004.

[132] J. Khandurina, S. C. Jacobson, L. C. Waters, R. S. Foote, and J. M. Ramsey, "Microfabricated porous membrane structure for sample concentration and electrophoretic analysis," *Anal. Chem.*, 1999.

[133] C. Yu, M. H. Davey, F. Svec, and J. M. J. Fréchet, "Monolithic porous polymer for on-chip solid-phase extraction and preconcentration prepared by photoinitiated in situ polymerization within a microfluidic device," *Anal. Chem.*, 2001.

[134] A. Layek, S. De, R. Thorat, and A. Chowdhury, "Spectrally resolved photoluminescence imaging of ZnO nanocrystals at single-particle levels," *J. Phys. Chem. Lett.*, vol. 2, no. 11, pp. 1241–1247, 2011.

[135] W. S. Mielczarek, E. A. Obaje, T. T. Bachmann, and M. Kersaudy-Kerhoas, "Microfluidic blood plasma separation for medical diagnostics: is it worth it?," *Lab Chip*, vol. 16, no. 18, pp. 3441–3448, 2016.

[136] R. Tiwari, L. Fischer, and K. Kalogerakis, "Frugal Innovation: An Assessment of Scholarly Discourse, Trends and Potential Societal Implications," in *Lead Market India: Key Elements and Corporate Perspectives for Frugal Innovations*, Heidelberg: Springer, 2017, pp. 13–35.

[137] R. Tiwari and C. Herstatt, “Frugal Innovation: A Global Networks’ Perspective,” *Die Unternehmung Swiss J. Bus. Res. Pract.*, 2012.

[138] J. D. Zahn, “A microfluidic device for continuous , real time blood plasma separation,” pp. 871–880, 2006.

[139] S. Thorslund, O. Klett, F. Nikolajeff, K. Markides, and J. Bergquist, “A hybrid poly (dimethylsiloxane) microsystem for on-chip whole blood filtration optimized for steroid screening,” pp. 73–79, 2006.

[140] J. Moorthy, D. J. Beebe, R. January, and A. April, “In situ fabricated porous filters for microsystems,” 2003.

[141] J. S. Shim, A. W. Browne, and C. H. Ahn, “An on-chip whole blood / plasma separator with bead-packed microchannel on COC polymer,” pp. 949–957, 2010.

[142] H. Jiang, X. Weng, C. H. Chon, X. Wu, and D. Li, “A microfluidic chip for blood plasma separation using electro-osmotic.”

[143] F. Petersson, A. Nilsson, C. Holm, and H. Jo, “Continuous separation of lipid particles from erythrocytes by means of laminar flow and acoustic standing wave forces,” pp. 20–22, 2005.

[144] S. Choi, S. Song, C. Choi, and J. Park, “Continuous blood cell separation by hydrophoretic filtration,” *Lab Chip*, vol. 7, pp. 1532–1538, 2007.

[145] S. Kar, T. K. Maiti, and S. Chakraborty, “Capillarity-driven blood plasma separation on paper-based devices,” *Analyst*, vol. 140, no. 19, pp. 6473–6476, 2015.

[146] D. A. Links, “Lab on a Chip Integrated separation of blood plasma from whole blood for microfluidic paper-based analytical devices,” pp. 274–280, 2012.

[147] A. Nilghaz and W. Shen, “Low-cost blood plasma separation method using salt functionalized paper,” *RSC Adv.*, vol. 5, pp. 53172–53179, 2015.

[148] M. Fakhar-E-Alam, S. M. U. Ali, Z. H. Ibupoto, K. Kimleang, M. Atif, M. Kashif, F. K. Loong, U. Hashim, and M. Willander, “Sensitivity of A-549 human lung cancer cells to nanoporous zinc oxide conjugated with Photofrin,” *Lasers Med. Sci.*, vol. 27, no. 3, pp. 607–614, 2012.

[149] M. Snure and A. Tiwari, “Synthesis, characterization, and green luminescence in ZnO nanocages,” *J. Nanosci. Nanotechnol.*, 2007.

[150] A. Tiwari and M. Snure, “Synthesis and characterization of ZnO nano-plant-like electrodes.,” *J. Nanosci. Nanotechnol.*, 2008.

[151] M. Snure and A. Tiwari, “Band-gap engineering of Zn[sub 1−x]Ga[sub x]O nanopowders: Synthesis, structural and optical characterizations,” *J. Appl. Phys.*, vol. 104, no. 7, p. 073707, 2008.

[152] R. Wahab, F. Khan, Y. B. Yang, I. H. Hwang, H.-S. Shin, J. Ahmad, S. Dwivedi, S. T. Khan, M. A. Siddiqui, Q. Saquib, J. Musarrat, A. A. Al-Khedhairy, Y. K. Mishra, and B. A. Ali, “Zinc oxide quantum dots: Multifunctional candidates for arresting C2C12 cancer cells and their role towards caspase 3 and 7 genes,” *RSC Adv.*, vol. 6, no. 31, pp. 26111–26120, 2016.

[153] Z. Zhao, W. Lei, X. Zhang, B. Wang, and H. Jiang, “ZnO-based amperometric enzyme biosensors,” *Sensors*, vol. 10, no. 2, pp. 1216–1231, 2010.

[154] K. Tian, S. Alex, G. Siegel, and A. Tiwari, “Enzymatic glucose sensor based on Au nanoparticle and plant-like ZnO film modified electrode,” *Mater. Sci. Eng. C*, vol. 46, no. January, pp. 548–552, 2015.

[155] Y. K. Mishra, R. Adelung, C. Röhl, D. Shukla, F. Spors, and V. Tiwari, “Virostatic potential of micro-nano filopodia-like ZnO structures against herpes simplex virus-1,” *Antiviral Res.*, vol. 92, no. 2, pp. 305–312, 2011.

[156] R. Wahab, F. Khan, Y. K. Mishra, J. Musarrat, and A. A. Al-Khedhairy, “Antibacterial studies and statistical design set data of quasi zinc oxide nanostructures,” *RSC Adv.*, vol. 6, no. 38, pp. 32328–32339, 2016.

[157] S. Tiwari, M. Vinchurkar, V. R. Rao, and G. Garnier, “Zinc oxide nanorods functionalized paper for protein preconcentration in biodiagnostics,” *Nat. Publ. Gr.*, no. January, pp. 1–10, 2017.

[158] R. Wahab, N. Kaushik, F. Khan, N. K. Kaushik, E. H. Choi, J. Musarrat, and A. A. Al-Khedhairy, “Self-Styled ZnO Nanostructures Promotes the Cancer Cell Damage and Supresses the Epithelial Phenotype of Glioblastoma,” *Sci. Rep.*, vol. 6, no. November 2015, p. 19950, 2016.

[159] T. E. Antoine, S. R. Hadigal, A. M. Yakoub, Y. K. Mishra, P. Bhattacharya, C. Haddad, T. Valyi-Nagy, R. Adelung, B. S. Prabhakar, and D. Shukla, “Intravaginal Zinc Oxide Tetrapod Nanoparticles as Novel Immunoprotective Agents against Genital Herpes,” *J. Immunol.*, vol. 196, no. 11, pp. 4566–4575, 2016.

[160] X. Li, C. Zhao, and X. Liu, “A paper-based microfluidic biosensor integrating zinc oxide nanowires for electrochemical glucose detection,” *Microsystems Nanoeng.*, vol. 1, p. 15014, 2015.

[161] C. M. Silveira, T. Monteiro, and M. G. Almeida, “Biosensing with Paper-Based Miniaturized Printed Electrodes – A Modern Trend,” pp. 1–17, 2016.

[162] T. Dang-vu, “Characterization of porous materials by capillary rise method,” *Physicochem. Probl. Miner. Process.*, vol. 39, pp. 47–65, 2005.

[163] A. Y. Beliaev and S. M. Kozlov, “Darcy equation for random porous media,” *Commun. Pure Appl. Math.*, vol. 49, no. 1, pp. 1–34, 1996.

[164] X. Du and M. Ostoja-Starzewski, “On the size of representative volume element for Darcy law in random media,” *Proc. R. Soc. A Math. Phys. Eng. Sci.*, vol. 462, no. 2074, pp. 2949–2963, 2006.

[165] F. Wirner, “Flow and Transport of Colloidal Suspensions in Porous Media,” 2015.

[166] D. A. Fedosov, B. Caswell, A. S. Popel, and G. E. M. Karniadakis, “Blood Flow and Cell-Free Layer in Microvessels,” *Microcirculation*, 2010.

[167] S. Tripathi, Y. V. B. Varun Kumar, A. Prabhakar, S. S. Joshi, and A. Agrawal, “Passive blood plasma separation at the microscale: a review of design principles and microdevices,” *J. Micromechanics Microengineering*, vol. 25, no. 8, p. 083001, 2015.

[168] J. Zhang, P. C. Johnson, and A. S. Popel, “Effects of erythrocyte deformability and

aggregation on the cell free layer and apparent viscosity of microscopic blood flows," *Microvasc. Res.*, vol. 77, no. 3, pp. 265–272, 2009.

Research Outcomes

In Journals

Sadhana Tiwari, Madhuri Vinchurkar, V. Ramgopal Rao and Gil Garnier. "Zinc oxide nanorods functionalized paper for protein preconcentration in biodiagnostics". Scientific Reports 7 (43905), 1-10, 2017. DOI: 10.1038/srep43905.

Sadhana Tiwari, Gil Garnier and V. Ramgopal Rao. “One Dimensional Zinc Oxide nanostructures assisted paper-based blood-plasma Separation”. Vacuum, Elsevier. https://doi.org/10.1016/j.vacuum.2017.06.043.

In Conferences

Sadhana Dwivedi, Madhuri Vinchurkar, Gil Garnier and V. Ramgopal Rao. Oral contribution entitled, 'Paper based ZnO nanorods platform for preconcentration of cardiac biomarkers'. 7th Biennial Australian Colloid and Interface Symposium 2015, Hobart, Tasmania. 1-5 February 2015.

Sadhana Tiwari, Gil Garnier and V. Ramgopal Rao. “One Dimensional Zinc Oxide Nanostructures for Paper Based Biodiagnostics. Oral contribution and paper submission to EMRS Fall-2017, Warsaw, Poland. 18-20 September 2017.

Manuscripts in preparation

Sadhana Tiwari, V. Ramgopal Rao and Gil Garnier. “Enhanced binding of cardiac myoglobin on ZnO-nanorods modified surface plasmon resonance substrate”.

Sadhana Tiwari, Madhuri Vinchurkar, Gil Garnier and V. Ramgopal Rao. “Emerging trends in Preconcentrator for Biodiagnostics: Paper as Frugal Solution”.